INSIDE TRACK with THE DESICH SMART CENTER'S MATT APANIUS p32

SCREENING UPDATES IN RF/MW CAE p37

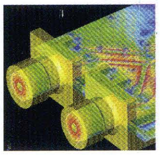

PHASED ARRAY FOCUSES ON 4G p50

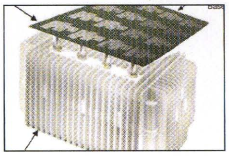

MicroWaves&RF

NOVEMBER 2012 TRUSTED ENGINEERING RESOURCE FOR 50 YEARS www.MWRF.com

SOFTWARE ISSUE

Transceiver ICs Target Wireless Infrastructure

A PENTON PUBLICATION Periodicals Postage Paid • USPS 100 Approved Poly

Phase Locked And Crystal Oscillators

Features:

- Band Coverage from VHF through Ka-Band
- Proven Performance in Various Applications
- Single and Dual Loop Models available with Internal and External Reference
- Small Modular Assemblies from 2.25" x 2.25" x 0.6"
- High Power and Low Harmonic Options available

3 YEAR WARRANTY

ISO 9001 Registered · ANAB ACCREDITED · AS9100 Registered · RoHS compliant Available

Model	Frequency Range	Type	Typical Phase Noise 10	100	1K	10K	100K	1M	Output Frequency	Output Power (dBm, Min.)
XTO-05	5-130 MHz	Ovenized Crystal	-95	-120	-140	-155	-160	-	100 MHz	11
PLD	30-130 MHz	P.L. Crystal	-95	-115	-140	-155	-155	-	100 MHz	13
PLD-1C	130-1000 MHz	P.L. Mult. Crystal	-80	-100	-120	-130	-135	-	560 MHz	13
BCO	100-16.5 GHz	P.L. Single Loop	-65	-75	-80	-90	-115	-	16.35 GHz	13
VFS	1-14 GHz	Multiple Freq. Dual Loop	-60	-75	-110	-115	-115	-	12.5 GHz	13
DLCRO	.8-26 GHz	P.L. CRO Dual Loop	-60	-85	-110	-115	-115	-138	10 GHz	13
PLDRO	2-40 GHz	P.L. DRO Single/Dual	-60	-80	-110	-115	-120	-145	10 GHz	13
CP	.8-3.2 GHz	P.L. CRO Single Loop	-80	-110	-120	-130	-130	-140	2 GHz	13
CPM	4-15 GHz	P.L. Mult. Single Loop	-60	-90	-105	-110	-115	-130	12 GHz	13
ETCO	.1-24 GHz	Voltage Tuned CRO	-	-	-70	-100	-120	-130	2-4 GHz*	13

* Octave band.

For additional information or technical support, please contact our Sales Department at (631) 439-9220 or e-mail components@miteq.com

MITEQ

100 Davids Drive, Hauppauge, NY 11788
(631) 436-7400 FAX: (631) 436-7430

www.miteq.com

LIMITERS, DIODE DETECTORS & THRESHOLD DETECTORS

Offering a full line of RF & Microwave Limiter and Detector Products to 40GHz

- Amplifiers
- Attenuators - Variable
- DLVA & ERDLVA & SDLVA's
- DTO's
- Filters
- Form, Fit & Function Products
- Hybrids, Dividers & Couplers
- IFM's & Frequency Discriminators
- Integrated MIC/MMIC Modules
- I/Q Vector Modulators
- Limiters & Detectors
- Log Amplifiers
- Pulse & Bi-Phase Modulators
- Phase Shifters
- Rack & Chassis Mount Products
- Receiver Front Ends
- Single Sideband Modulators
- SMT & QFN Products
- Solid-State Switches
- Switch Matrices
- Switch Filter Banks
- Threshold Detectors
- USB Products

Limiters & Limiter Detectors

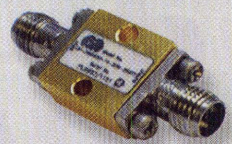
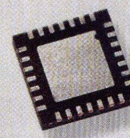

- DC to 40 GHz in Narrow, Wide & Octave Bands
- QFN/Surface Mount, Connectorized and Coaxial models
- High Power Limiters, 400 Watt Peak & 50 Watt CW
- Hermetic Sealing and MIL-STD-883 Screening Available
- Example:

◆ **LM-26G40G-14-20W-292FF**

Frequency Range: 26.5 -40.0GHz, 4.0dB Insertion Loss, 2.0:1 VSWR, 20 Watts Peak RF Input, 40% Duty Cycle, +14dBm Leakage, 250nS Recovery Time. Size: 0.5" x 0.5" x 0.22"

High Speed, Diode Detectors

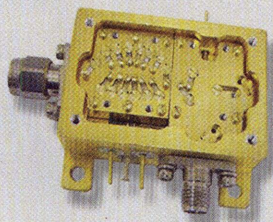

- DC to 40 GHz in Narrow, Wide & Octave Bands
- QFN/Surface Mount, Connectorized and Coaxial models
- Tunnel Diode and Zero Bias Schottky Diode Detectors
- Positive or Negative Output Available
- Filter Detectors, Directional Detectors & Detector Amplifiers Available
- Hermetic Sealing and MIL-STD-883 Screening Available
- Example:

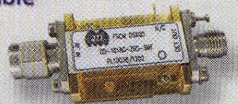

◆ **DD-50-218-10PF-1-N**

Frequency Range: 2.0-18.0 GHz, 3.5:1 VSWR, Frequency Flatness ±1.5dB Typical, Speed: 5nS, +17dBm Max RF Input, Voltage Sensitivity 700mV/mW Typical. Size: 0.5" x 0.5" x 0.22"

High Speed, Threshold Detectors

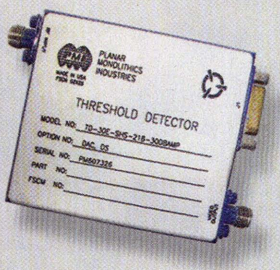

- DC to 40 GHz in Narrow, Wide & Octave Bands
- High Dynamic Ranges, -75dBm to +10dBm Available
- Surface Mount, Connectorized & USB Models Available
- Fixed, Adjustable and Digitally Controlled Threshold Levels
- TTL and ECL Detected Output Available
- Hermetic Sealing and MIL-STD-883 Screening Available
- Example:

◆ **TD-30T-SHS-218-30DBAMP-DAC-DS**

Frequency Range: 2.0-18.0 GHz, Propagation Delay From 50% Monitor Logic Output on Leading Edge for an Input of -45 dBm: 15nS Typ., Propagation Delay From 50% RF Input to 50% Logic Output When Input -45 dBm: 30nS Typ., Minimum Signal Level: -45dBm, 8 Bit Digital Control on Threshold Level. Size: 2.50" x 2.00" x 0.50"

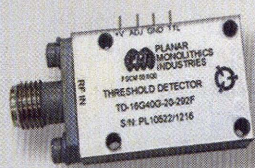

PMI

PLANAR MONOLITHICS INDUSTRIES, INC.

7311-F Grove Road, Frederick, Maryland 21704 USA
Tel: 301-662-5019 | Fax: 301-662-1731
Email: sales@pmi-rf.com | www.pmi-rf.com

ISO9001:2008 Certified


DON'T LET THE SAME OLD SUPPLIER SOLUTION RAIN ON YOUR DEVELOPMENT PARADE.
WE'VE GOT YOU COVERED!
narda Defense Technology Solutions
High dynamic range front-end assembly
L3

AWR A National Instruments Company™

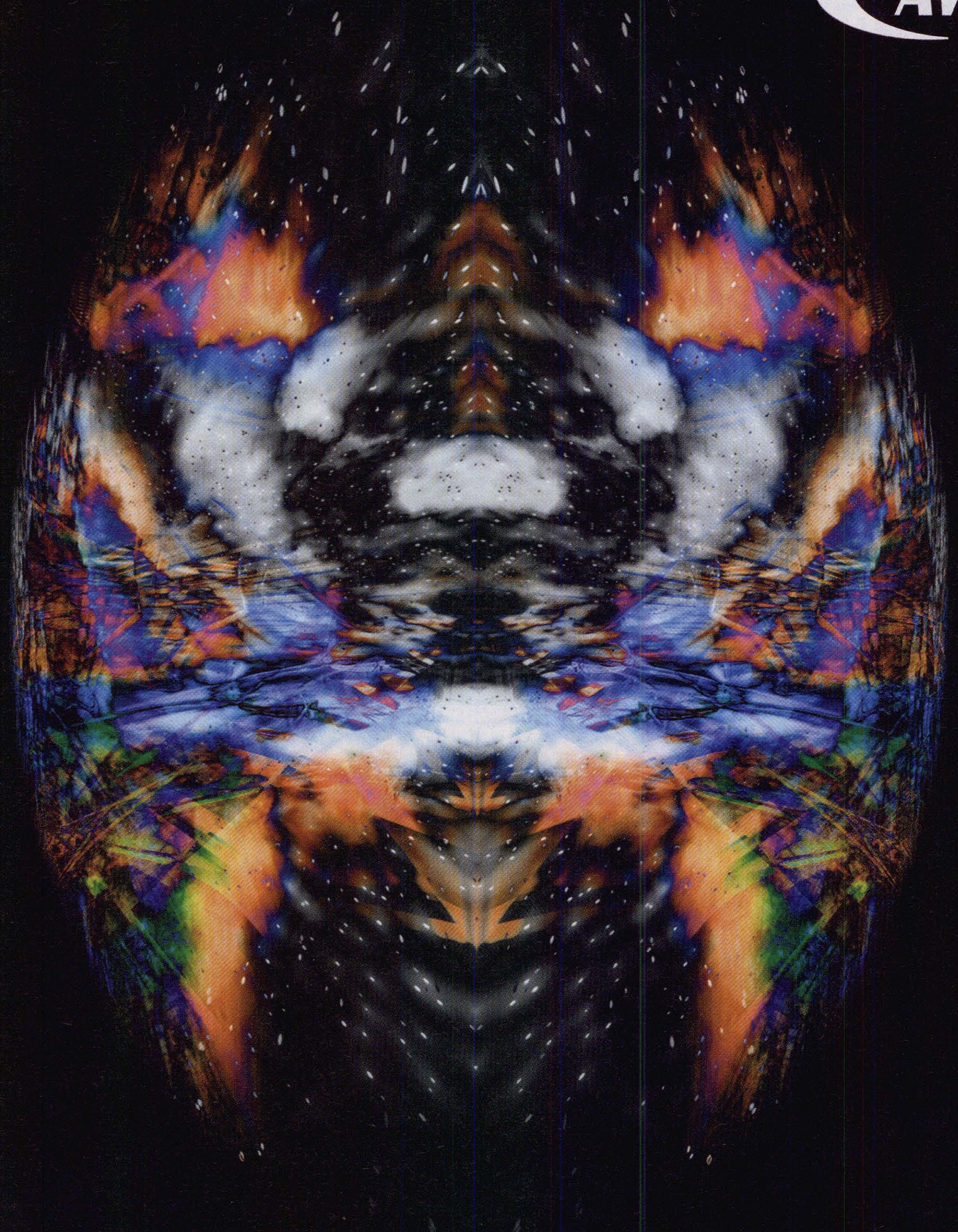

EM speed that will turbocharge your design creativity.

Stop waiting and wishing for an EM tool that keeps pace with your own creative ideas. AXIEM is capable of solving big problems fast — typically 10x faster than current alternatives for designs of 10K unknowns or more. And now that it handles antennas, too, your creativity will know no bounds. For the most accurate EM results in minutes rather than hours, go with AXIEM. Grab a test copy today at awrcorp.com/AXIEM.

Stop waiting and start designing™

AXIEM®
3D PLANAR EM

NOVEMBER | 2012
Volume 51, Issue 11

CONTENTS

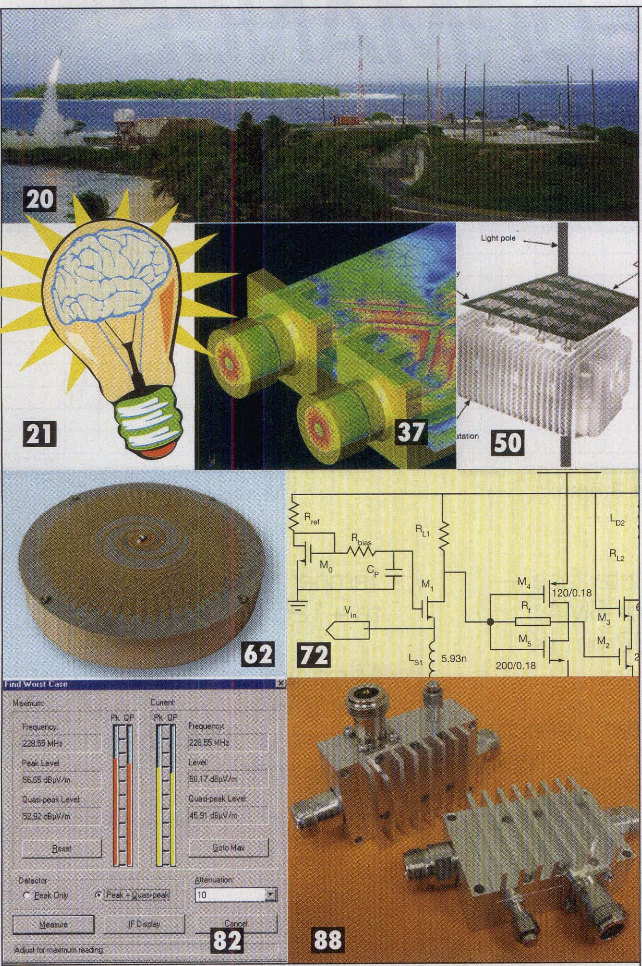

Penton
Design Engineering & Sourcing Group

Introducing the World's First Vector Signal Transceiver

VSA + VSG + User-Programmable FPGA = RF Redefined

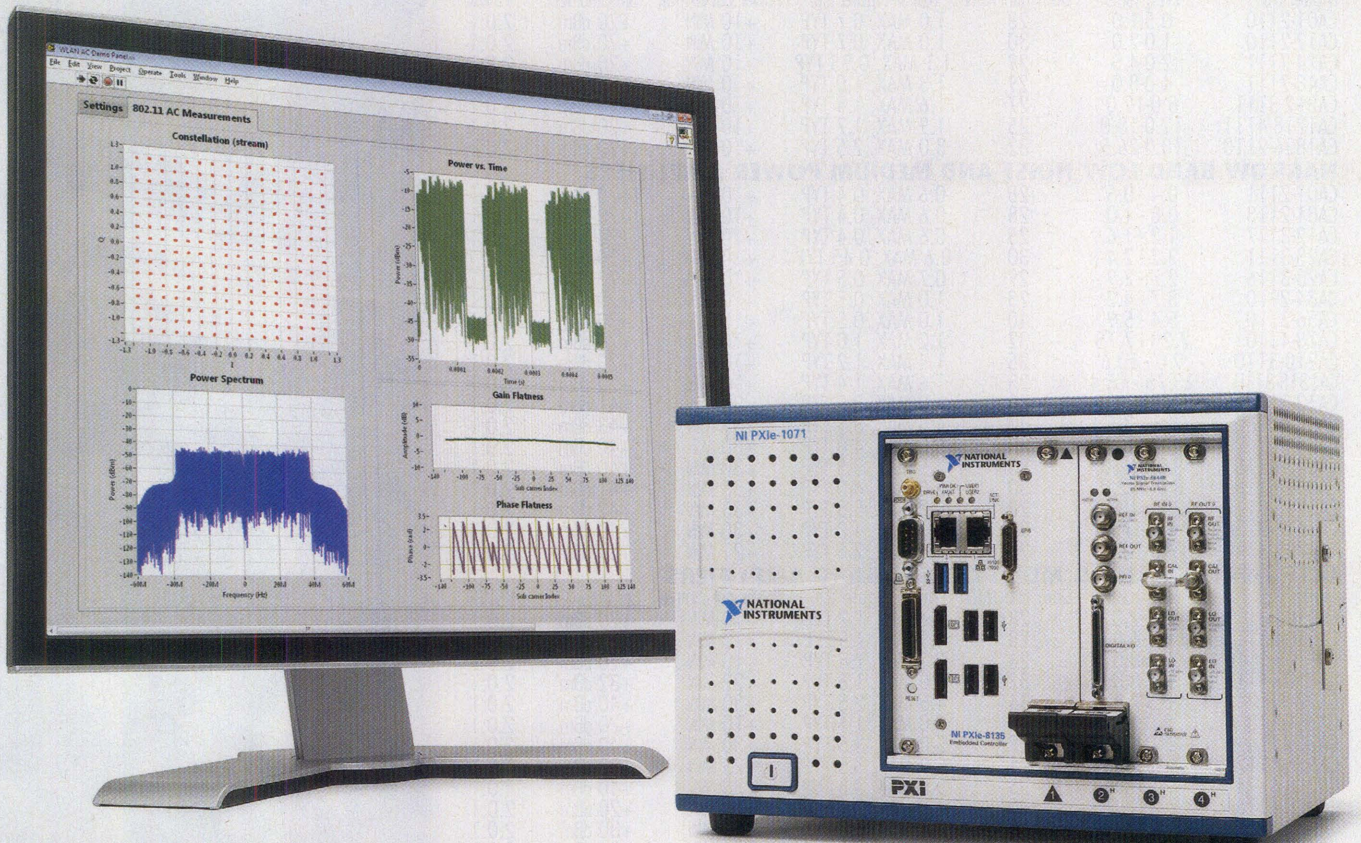

Combining a vector signal analyzer and a vector signal generator with a user-programmable FPGA for real-time signal processing and control, this vector signal transceiver is a fraction of the size and cost of a traditional solution. More importantly, the NI PXIe-5644R is the first software-designed instrument. With NI LabVIEW system design software, you can modify its software and firmware to create an instrument that meets your exact needs.

WIRELESS TECHNOLOGIES

National Instruments supports a broad range of wireless standards including:

802.11a/b/g/n/ac	LTE
CDMA2000/EV-DO	GSM/EDGE
WCDMA/HSPA/HSPA+	Bluetooth

>> Learn more at ni.com/vst

800 813 5078

NATIONAL INSTRUMENTS™

RF Amplifiers and Sub-Assemblies for Every Application

Delivery from Stock to 2 Weeks ARO from the catalog or built to your specifications!

- Competitive Pricing & Fast Delivery
- Military Reliability & Qualification
- Various Options: Temperature Compensation, Input Limiter Protection, Detectors/TTL & More
- Unconditionally Stable (100% tested)

ISO 9001:2000 and AS9100B CERTIFIED

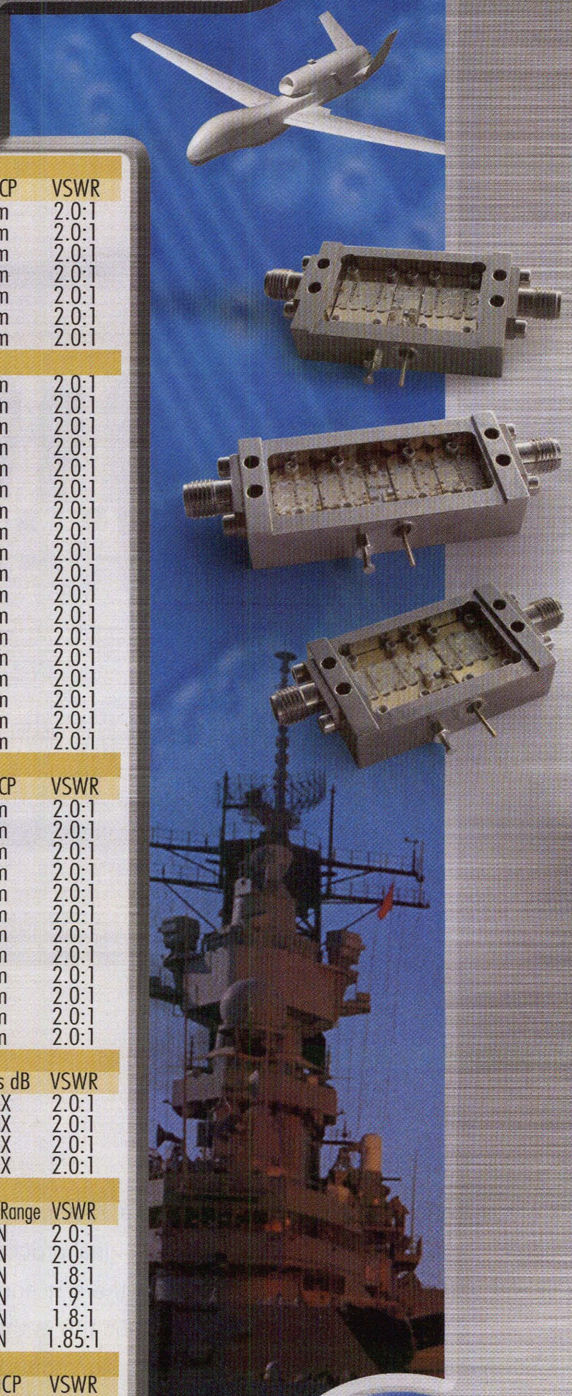

OCTAVE BAND LOW NOISE AMPLIFIERS

Model No.	Freq (GHz)	Gain (dB) MIN	Noise Figure (dB)	Power-out @ P1-dB	3rd Order ICP	VSWR
CA01-2110	0.5-1.0	28	1.0 MAX, 0.7 TYP	+10 MIN	+20 dBm	2.0:1
CA12-2110	1.0-2.0	30	1.0 MAX, 0.7 TYP	+10 MIN	+20 dBm	2.0:1
CA24-2111	2.0-4.0	29	1.1 MAX, 0.95 TYP	+10 MIN	+20 dBm	2.0:1
CA48-2111	4.0-8.0	29	1.3 MAX, 1.0 TYP	+10 MIN	+20 dBm	2.0:1
CA812-3111	8.0-12.0	27	1.6 MAX, 1.4 TYP	+10 MIN	+20 dBm	2.0:1
CA1218-4111	12.0-18.0	25	1.9 MAX, 1.7 TYP	+10 MIN	+20 dBm	2.0:1
CA1826-2110	18.0-26.5	32	3.0 MAX, 2.5 TYP	+10 MIN	+20 dBm	2.0:1

NARROW BAND LOW NOISE AND MEDIUM POWER AMPLIFIERS

Model No.	Freq (GHz)	Gain (dB) MIN	Noise Figure (dB)	Power-out @ P1-dB	3rd Order ICP	VSWR
CA01-2111	0.4 - 0.5	28	0.6 MAX, 0.4 TYP	+10 MIN	+20 dBm	2.0:1
CA01-2113	0.8 - 1.0	28	0.6 MAX, 0.4 TYP	+10 MIN	+20 dBm	2.0:1
CA12-3117	1.2 - 1.6	25	0.6 MAX, 0.4 TYP	+10 MIN	+20 dBm	2.0:1
CA23-3111	2.2 - 2.4	30	0.6 MAX, 0.45 TYP	+10 MIN	+20 dBm	2.0:1
CA23-3116	2.7 - 2.9	29	0.7 MAX, 0.5 TYP	+10 MIN	+20 dBm	2.0:1
CA34-2110	3.7 - 4.2	28	1.0 MAX, 0.5 TYP	+10 MIN	+20 dBm	2.0:1
CA56-3110	5.4 - 5.9	40	1.0 MAX, 0.5 TYP	+10 MIN	+20 dBm	2.0:1
CA78-4110	7.25 - 7.75	32	1.2 MAX, 1.0 TYP	+10 MIN	+20 dBm	2.0:1
CA910-3110	9.0 - 10.6	25	1.4 MAX, 1.2 TYP	+10 MIN	+20 dBm	2.0:1
CA1315-3110	13.75 - 15.4	25	1.6 MAX, 1.4 TYP	+10 MIN	+20 dBm	2.0:1
CA12-3114	1.35 - 1.85	30	4.0 MAX, 3.0 TYP	+33 MIN	+41 dBm	2.0:1
CA34-6116	3.1 - 3.5	40	4.5 MAX, 3.5 TYP	+35 MIN	+43 dBm	2.0:1
CA56-5114	5.9 - 6.4	30	5.0 MAX, 4.0 TYP	+30 MIN	+40 dBm	2.0:1
CA812-6115	8.0 - 12.0	30	4.5 MAX, 3.5 TYP	+30 MIN	+40 dBm	2.0:1
CA812-6116	8.0 - 12.0	30	5.0 MAX, 4.0 TYP	+33 MIN	+41 dBm	2.0:1
CA1213-7110	12.2 - 13.25	28	6.0 MAX, 5.5 TYP	+33 MIN	+42 dBm	2.0:1
CA1415-7110	14.0 - 15.0	30	5.0 MAX, 4.0 TYP	+30 MIN	+40 dBm	2.0:1
CA1722-4110	17.0 - 22.0	25	3.5 MAX, 2.8 TYP	+21 MIN	+31 dBm	2.0:1

ULTRA-BROADBAND & MULTI-OCTAVE BAND AMPLIFIERS

Model No.	Freq (GHz)	Gain (dB) MIN	Noise Figure (dB)	Power-out @ P1-dB	3rd Order ICP	VSWR
CA0102-3111	0.1-2.0	28	1.6 Max, 1.2 TYP	+10 MIN	+20 dBm	2.0:1
CA0106-3111	0.1-6.0	28	1.9 Max, 1.5 TYP	+10 MIN	+20 dBm	2.0:1
CA0108-3110	0.1-8.0	26	2.2 Max, 1.8 TYP	+10 MIN	+20 dBm	2.0:1
CA0108-4112	0.1-8.0	32	3.0 MAX, 1.8 TYP	+22 MIN	+32 dBm	2.0:1
CA02-3112	0.5-2.0	36	4.5 MAX, 2.5 TYP	+30 MIN	+40 dBm	2.0:1
CA26-3110	2.0-6.0	26	2.0 MAX, 1.5 TYP	+10 MIN	+20 dBm	2.0:1
CA26-4114	2.0-6.0	22	5.0 MAX, 3.5 TYP	+30 MIN	+40 dBm	2.0:1
CA618-4112	6.0-18.0	25	5.0 MAX, 3.5 TYP	+23 MIN	+33 dBm	2.0:1
CA618-6114	6.0-18.0	35	5.0 MAX, 3.5 TYP	+30 MIN	+40 dBm	2.0:1
CA218-4116	2.0-18.0	30	3.5 MAX, 2.8 TYP	+10 MIN	+20 dBm	2.0:1
CA218-4110	2.0-18.0	30	5.0 MAX, 3.5 TYP	+20 MIN	+30 dBm	2.0:1
CA218-4112	2.0-18.0	29	5.0 MAX, 3.5 TYP	+24 MIN	+34 dBm	2.0:1

LIMITING AMPLIFIERS

Model No.	Freq (GHz)	Input Dynamic Range	Output Power Range Psat	Power Flatness dB	VSWR
CLA24-4001	2.0 - 4.0	-28 to +10 dBm	+7 to +11 dBm	+/- 1.5 MAX	2.0:1
CLA26-8001	2.0 - 6.0	-50 to +20 dBm	+14 to +18 dBm	+/- 1.5 MAX	2.0:1
CLA712-5001	7.0 - 12.4	-21 to +10 dBm	+14 to +19 dBm	+/- 1.5 MAX	2.0:1
CLA618-1201	6.0 - 18.0	-50 to +20 dBm	+14 to +19 dBm	+/- 1.5 MAX	2.0:1

AMPLIFIERS WITH INTEGRATED GAIN ATTENUATION

Model No.	Freq (GHz)	Gain (dB) MIN	Noise Figure (dB)	Power-out @ P1-dB	Gain Attenuation Range	VSWR
CA001-2511A	0.025-0.150	21	5.0 MAX, 3.5 TYP	+12 MIN	30 dB MIN	2.0:1
CA05-3110A	0.5-5.5	23	2.5 MAX, 1.5 TYP	+18 MIN	20 dB MIN	2.0:1
CA56-3110A	5.85-6.425	28	2.5 MAX, 1.5 TYP	+16 MIN	22 dB MIN	1.8:1
CA612-4110A	6.0-12.0	24	2.5 MAX, 1.5 TYP	+12 MIN	15 dB MIN	1.9:1
CA1315-4110A	13.75-15.4	25	2.2 MAX, 1.6 TYP	+16 MIN	20 dB MIN	1.8:1
CA1518-4110A	15.0-18.0	30	3.0 MAX, 2.0 TYP	+18 MIN	20 dB MIN	1.85:1

LOW FREQUENCY AMPLIFIERS

Model No.	Freq (GHz)	Gain (dB) MIN	Noise Figure dB	Power-out @ P1-dB	3rd Order ICP	VSWR
CA001-2110	0.01-0.10	18	4.0 MAX, 2.2 TYP	+10 MIN	+20 dBm	2.0:1
CA001-2211	0.04-0.15	24	3.5 MAX, 2.2 TYP	+13 MIN	+23 dBm	2.0:1
CA001-2215	0.04-0.15	23	4.0 MAX, 2.2 TYP	+23 MIN	+33 dBm	2.0:1
CA001-3113	0.01-1.0	28	4.0 MAX, 2.8 TYP	+17 MIN	+27 dBm	2.0:1
CA002-3114	0.01-2.0	27	4.0 MAX, 2.8 TYP	+20 MIN	+30 dBm	2.0:1
CA003-3116	0.01-3.0	18	4.0 MAX, 2.8 TYP	+25 MIN	+35 dBm	2.0:1
CA004-3112	0.01-4.0	32	4.0 MAX, 2.8 TYP	+15 MIN	+25 dBm	2.0:1

CIAO Wireless can easily modify any of its standard models to meet your "exact" requirements at the Catalog Pricing.

Visit our web site at www.ciaowireless.com for our complete product offering.

Ciao wireless

Ciao Wireless, Inc. 4000 Via Pescador, Camarillo, CA 93012

Tel (805) 389-3224 Fax (805) 389-3629 sales@ciaowireless.com

Optimize Signal/Spectrum Analyzer Throughput For High-Volume Manufacturing Test

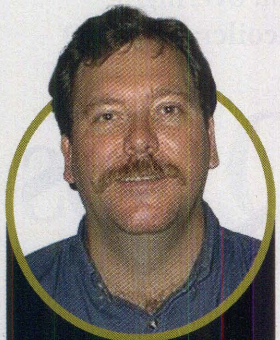

BOB NELSON

TO OBTAIN THE HIGHEST THROUGHPUT for the analyzers used in manufacturing test, one should create a test plan that accounts for speed, repeatability, and dynamic range. In this web-exclusive article, Agilent Technologies' Bob Nelson provides you with the blueprint.

To read the article in its entirety, go to http://mwrf.com/contributors/optimize-signalspectrum-analyzer-throughput-high-volume-manufacturing-test.

ALSO, BE SURE CHECK OUT THESE OTHER RECENT ARTICLES IN OUR CONTRIBUTED TECHNICAL EXPERT SERIES.

Visit www.mwrf.com/community/contributors.

KANG CHEN

DAVID A. HALL

MEET THE CHALLENGES OF TESTING EIGHT-ANTENNA LTE

KANG CHEN—Senior Applications Specialist, Spirent Communications

FIND OUT WHY PXI IS BEING USED FOR RF INSTRUMENTS

DAVID A. HALL—Senior Product Marketing Manager, RF and Communications, National Instruments

REVISIT IMS2012

The 2012 installment of the RF/microwave industry's flagship event, the *International Microwave Symposium,* has come and gone. Luckily for you, it needn't live on just in memory. Visit www.mwrf.com to check out our show coverage, as well as www.engineering tv.com to view exclusive videos from the show floor.

engineering tv

IMS2012 MONTRÉAL

NEWS UPDATES Sent To Your Desktop

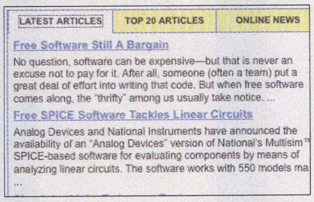
LATEST ARTICLES | TOP 20 ARTICLES | ONLINE NEWS

Free Software Still A Bargain

No question, software can be expensive—but that is never an excuse not to pay for it. After all, someone (often a team) put a great deal of effort into writing that code. But when free software comes along, the "thrifty" among us usually take notice. ...

Free SPICE Software Tackles Linear Circuits

Analog Devices and National Instruments have announced the availability of an "Analog Devices" version of National's Multisim™ SPICE-based software for evaluating components by means of analyzing linear circuits. The software works with 550 models ma ...

Don't believe everything you read, unless it's in the latest issue of *Microwaves & RF UPDATE.* The industry's longest-running weekly e-mail newsletter, it combines insightful commentary with the latest product and industry business news. It is sent directly to your computer desktop each week, and often contains the little things that engineers love, such as links to free white papers and even design software. If you're not already reading it, subscriptions are free, and available from the *Microwaves & RF* website at www.mwrf.com.

MWRF.com has archives of print and online articles dating back to October 2002. Visit mwrf.com today and click the "Back Issues" link. And while you're taking a look around the site, click on "Product Directory" to gain access to our complete directory of products and suppliers.

TIP 1 For an inductor with the absolute maximum Q, pick one of these air core "Springs". They have flat tops for easy mounting and exceptional current ratings.

TIP 2 If you prefer conventional chip inductors, you'll get the highest Q with our new ceramic body 0402HP and 0603HP families. These tiny wirewound coils handle up to 2 times more current than the nearest competitor.

This new web tool finds inductors with the highest Q at your operating frequency

TIP 3 Need to find coils with the best Q at your L and frequency? Our **Highest Q Finder** web tool tells you in just seconds. Click again to plot the L, Q, Z and ESR of up to 4 parts simultaneously.

TIP 4 When it's time to build your prototypes, be sure to ask us for evaluation samples. They're always free and we can get them to you overnight.

To get started, visit **www.coilcraft.com/Q**

Here are some high Q tips

Q-Tips® is a registered trademark of Chesebrough-Ponds, Inc.

Coilcraft®

WWW.COILCRAFT.COM

coilcraftdirect.com
No min order. Next day delivery.

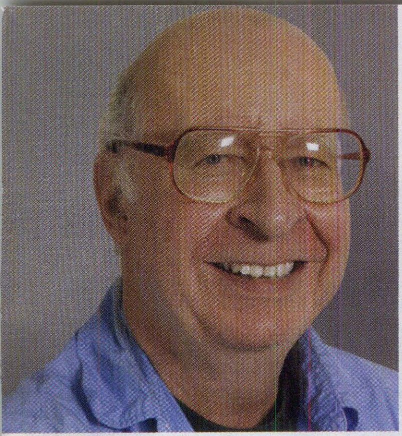

From the Editor

Lean Less On That Computer

COMPUTER-AIDED ENGINEERING (CAE) has been a part of this industry in some shape or form since the 1960s, growing from a curiosity into a crutch. Naturally, as computers have gotten better, the software that goes with them has also improved, and many RF/microwave-related CAE software tools represent the cumulative knowledge of many years of design experience from some of the top minds in this industry. There is an easy tendency to load the software and let it do all the design work, trusting completely in the results.

More often than not, this can save a great deal of trial-and-error effort as part of the design procedure, and yield typically excellent results. But it may not bring about that moment of insight or inspiration that many engineers have experienced as part of their on-the-job learning process—that moment when everything looked so clear that even a child could do it. Sometimes, attaining that special moment is worth suffering through the trials and tribulations of designing, prototyping, and testing.

Of course, in an issue devoted to design and simulation software, it may seem odd to criticize such software here, and that is not the intention. The strides that computers and engineering software programs have made over these past 30 years have been marvelous to behold. In particular, compute-intensive software, such as electromagnetic (EM) simulation tools working with Maxwell's equations, has benefitted from expanded memory and computing power over the years, whether these programs are working on planar or three-dimensional (3D) circuit problems.

Those working in this industry long enough will remember some of the early software tools as being little more than calculators. The development of SPICE software at the University of California at Berkeley in the 1970s and '80s—along with the creation of commercial RF/microwave design tools by Les Besser (see *Microwaves & RF*, November 2011, p. 52) and others during that timeframe—set the stage for what would become a healthy market for linear and nonlinear circuit and EM simulation tools, leveraging each new improvement in computer microprocessor capability with new sets of functions and easier-to-use graphical user interfaces (GUIs).

Modern software design and simulation tools truly are the accumulated knowledge of many design engineers who came before—not just their wisdom and insights into designing couplers, filters, amplifiers, and other circuits, but files with models that have proven successful and test results from actual circuits to fortify the software. So why not count on these software design tools completely? Because this industry has been built by folks willing to take chances, by design engineers who didn't always follow what came before, but chased their own creative thought processes to develop out-of-the-ordinary solutions to a design problem. A proven efficiency enhancer, CAE software is a tremendous benefit to this industry. But it never hurts to walk away from the computer and try thinking "out of the box" now and then, just to see what wild ideas come. MWRF

Jack Browne

Technical Contributor

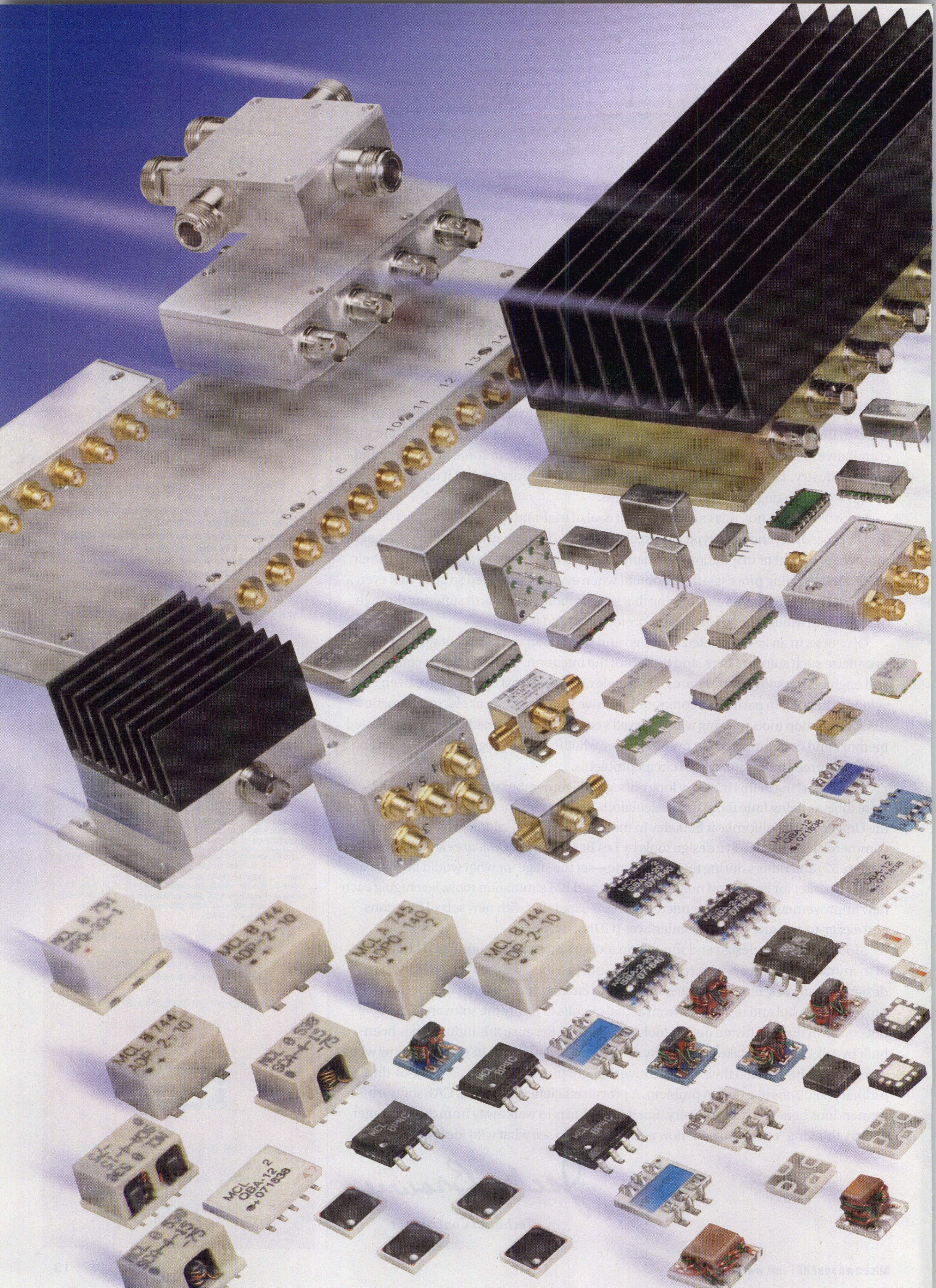
MCL B 744
ADP-2-10
MCL A 745
ADPQ-140
MCL B 744
ADP-2-10
MCL B 744
ADP-2-10
MCL
QBA-12
071836
MCL
BPNC
MCL
BPNC
MCL
BPNC

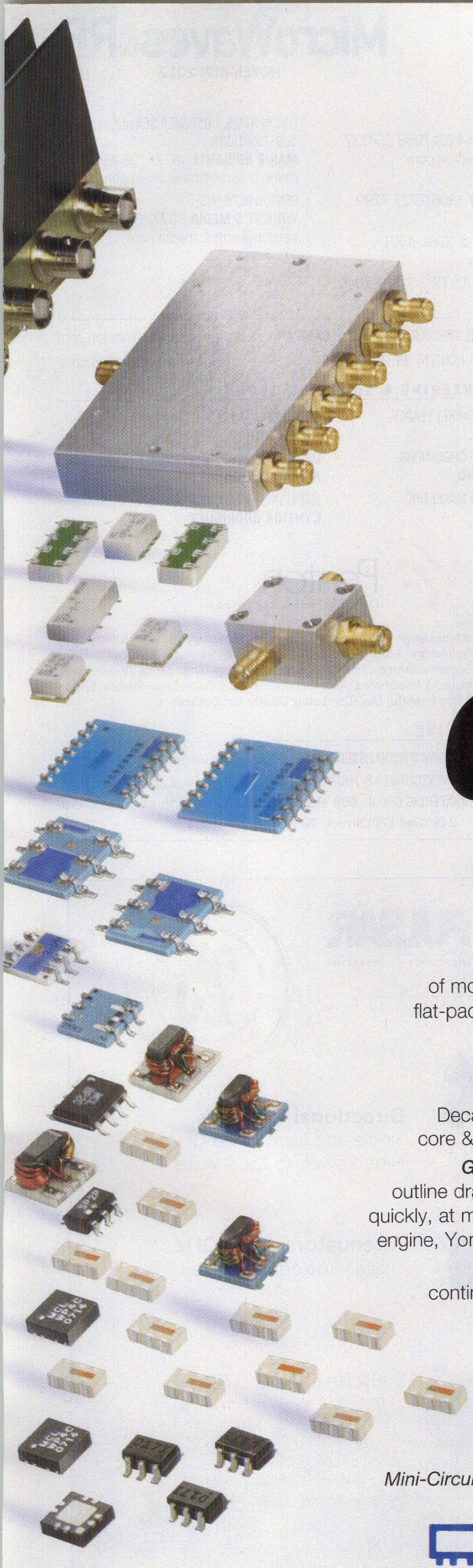

EDITORIAL

EDITOR IN CHIEF: **NANCY K. FRIEDRICH** (212) 204-4373 nancy.friedrich@penton.com

TECHNICAL CONTRIBUTOR: **JACK BROWNE** (212) 204-4377 jack.browne@penton.com

MANAGING EDITOR: **JEREMY COHEN** (212) 204-4243 jeremy.cohen@penton.com

GROUP DESIGN DIRECTOR: **ANTHONY VITOLO** tony.vitolo@penton.com

ART DEPARTMENT

CREATIVE DIRECTOR: **DIMITRIOS BASTAS** dimitrios.bastas@penton.com
SENIOR ARTIST: **JAMES MILLER** james.miller@penton.com
INTERN: **KAMIL WIERCISZEWSKI**

PRODUCTION

GROUP PRODUCTION DIRECTOR: **JUSTIN MARCINIAK** justin.marciniak@penton.com
AD PRODUCTION COORDINATOR: **KARA WALBY** kara.walby@penton.com
CLASSIFIED PRODUCTION COORDINATOR: **LINDA SARGENT** linda.sargent@penton.com

AUDIENCE MARKETING

AUDIENCE MARKETING MANAGER: **BRENDA ROODE** brenda.roode@penton.com
ONLINE MARKETING SPECIALIST: **RYAN MALEC** ryan.malec@penton.com

Free Subscription • Status of Subscription • Address Change • Missing Back Issues
(866)-505-7173 microwaves&rf@halldata.com

SALES & MARKETING

BRAND DIRECTOR, e/DESIGN:
TRACY SMITH (913) 967-1324
Tracy.Smith@penton.com

Northwest/Northern CA/ Western Canada
REGIONAL SALES REPRESENTATIVE:
JAMIE ALLEN (415) 608-1959
Jamie.Allen@penton.com

South
REGIONAL SALES REPRESENTATIVE:
BILL YARBOROUGH (713) 636-3809
Bill.Yarborough@penton.com

BRAND CHAMPION:
DAVID MADONIA (212) 204-4331
Dave.Madonia@penton.com

EUROPEAN SALES:
MARK DURHAM 44 (0) 7958 564137
mark.durham@penton.com

Taiwan, R.O.C
CHARLES C.Y. LIU (866)2727 7799

Japan
HIRO MORITA 81-3-3261-4591

Korea
JO YOUNG SANG (011)82-2-739-7840

LIST RENTALS, CUSTOMER SERVICE-SUBSCRIPTIONS:
MARIE BRIGANTI (877) 796-6947
marie.briganti@meritdirect.com

PENTON REPRINTS:
WRIGHT'S MEDIA (877) 652-5295
penton@wrightsmedia.com

ONLINE

ONLINE DEVELOPMENT DIRECTOR: **STEPHANIE CAMPANA** stephanie.campana@penton.com
DIRECTOR OF DIGITAL CONTENT: **PETRA ANDRE** petra.andre@penton.com

DESIGN ENGINEERING & SOURCING GROUP

VICE PRESIDENT & MARKET LEADER:
BILL BAUMANN

GROUP DIRECTOR OF OPERATIONS:
CHRISTINA CAVANO

GROUP DIRECTOR OF MARKETING:
JANE COOPER

RESEARCH MANAGER:
JULIE RITCHIE

MARKETING & EVENTS SPECIALIST:
ADRIAN PIAZZA

MARKETING COMMUNICATIONS SPECIALIST:
CYNTHIA RODRIGUEZ

Penton
Design Engineering & Sourcing Group

Electronic Design • Machine Design • Microwaves & RF • Source ESB • Energy Efficiency & Technology
Power Electronics Technology • Global Purchasing • Defense Electronics • Medical Design •
Mobile DevDesign • Electronic Design China • Motion System Design • Engineering TV • Electronic
Design Europe • Hydraulics & Pneumatics • Auto Electronics • Fluid Power Expo • Medical Silicon
Medical Prototyping • One Powerful Day • Combating Counterfeit Conference

PENTON MEDIA, INC.

CHIEF EXECUTIVE OFFICER: **DAVID KIESELSTEIN** david.kieselstein@penton.com
CHIEF FINANCIAL OFFICER/EXECUTIVE VP: **NICOLA ALLAIS** nicola.allais@penton.com
SENIOR VP, DESIGN ENGINEERING GROUP: **BOB MacARTHUR** bob.macarthur@penton.com
249 West 17th Street, New York, NY 10011

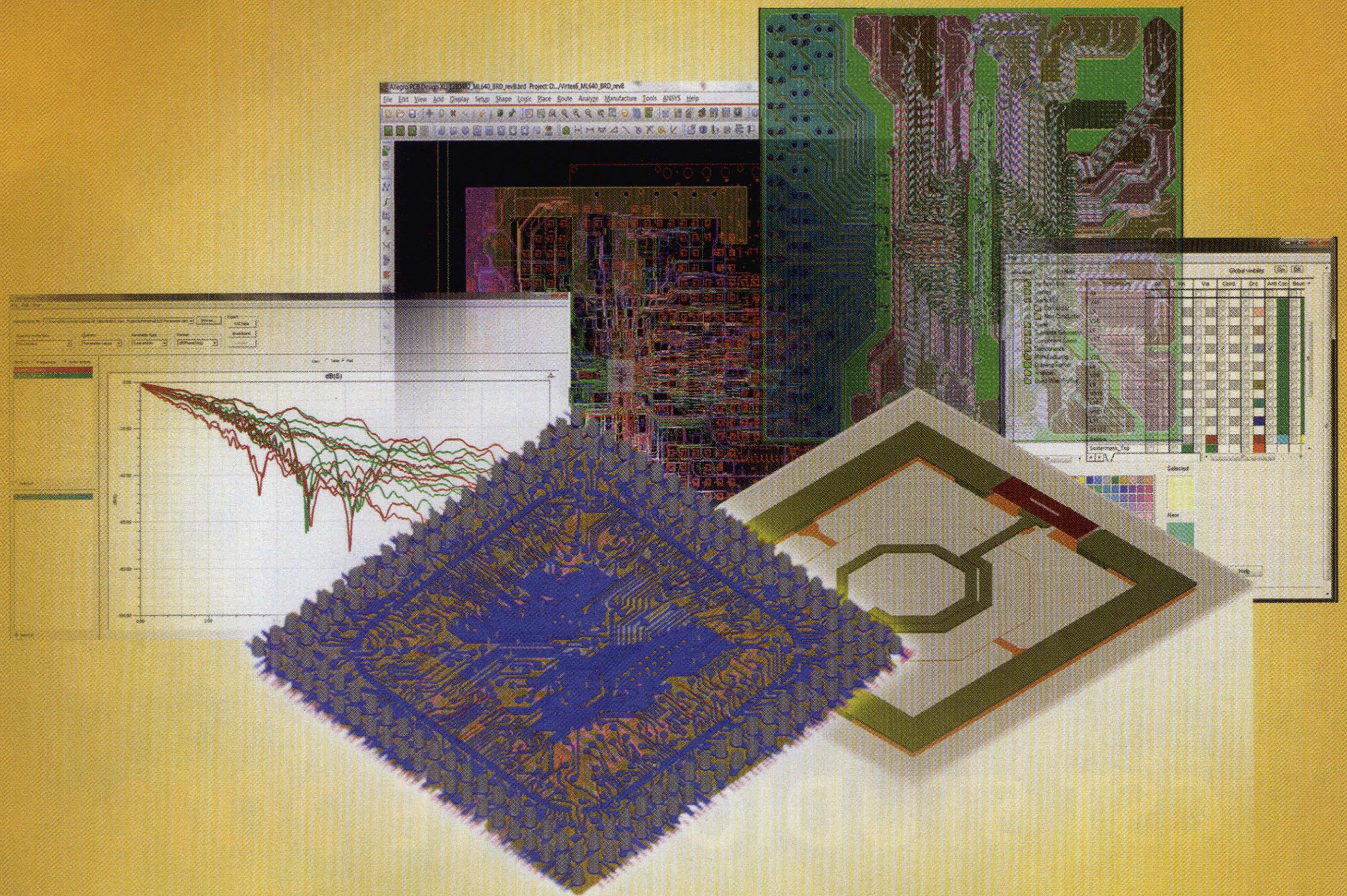

PICKING PRODUCTS

I have read your "Product Features" over the years with great interest, and have often wondered what strategy is used in selecting the products for review. They do not appear to always come from advertisers appearing in your magazine, as one might expect. In fact, many are for products and companies that one probably would never see in an advertisement in this or other trade magazines, or hear about outside of a trade show. How do you come to pick the products for review? And how come there is never a summary of the type of equipment contained in your magazine test laboratory for these reviews?

AN INTERESTED OBSERVER

EDITOR'S NOTE

As you have observed, there is little or no link between the products selected for extended reviews in each issue and the companies choosing to advertise in each issue. Of course, advertisers are welcome to submit new products for these extended reviews. But even when non-advertising companies submit new products for a Product Feature, each product is considered based on its own merits, its pure performance, its price/performance ratio, and the segment of the industry that it serves. For example, a breakthrough product that may only benefit five people in the industry is less likely to be the topic of a Product Feature than a product that can be used potentially by thousands.

Companies in this industry tend to alert our editors of new product developments and expected introductions. Many products are not "groundbreaking," but may simply be additions or extensions to an existing product line. However, when something comes along that does break a barrier (such as price, performance, size, etc.), the enthusiasm of the inventor is obvious and honest. This magazine has established a long record of trying to present new product developments as honestly and straightforwardly as possible. As for the test laboratory, the costs of maintaining such a lab are prohibitive. From time to time, test-equipment manufacturers have been kind enough to provide "loaners" for testing other products (or with the loaner itself being the subject of a review), but the magazine currently is without an active test laboratory.

JACK BROWNE
TECHNICAL CONTRIBUTOR

Microwaves & RF welcomes mail from its readers. The magazine reserves the right to edit letters appearing in "Feedback." Address letters to:

Nancy Friedrich
Editor-In-Chief
nancy.friedrich@penton.com

Jack.Browne
Technical Contributor
jack.browne@penton.com

Three-Pronged Missile-Defense Test Engages Multiple Targets

A THAAD interceptor is launched from Meck Island on its way to intercept a ballistic-missile target during MDA's flight test last month. (Photo courtesy of Lockheed Martin)

MUCH PROGRESS HAS BEEN MADE IN MISSILE-DEFENSE TECHNOLOGIES IN RECENT YEARS. Ideally, these various systems will work together seamlessly to protect the US and its allies. To demonstrate such interoperability, Lockheed Martin (www.lockheedmartin.com) recently performed a test involving its Aegis Ballistic Missile Defense System, Patriot Advanced Capability-3 (PAC-3) Missile, and Terminal High-Altitude Area Defense (THAAD) weapon system. This marked the first such test and successful engagement of all three systems.

Working together, the systems detected, tracked, engaged, and negated two ballistic-missile targets and one cruise-missile-like target. Known as Flight Test Integrated-01 (FTI-01), these different sensors and weapons systems were integrated through the Command and Control, Battle Management, and Communications (C2BMC) system developed by Lockheed Martin.

This live-fire flight test was conducted by the Missile Defense Agency (MDA) at the Ronald Reagan Ballistic Missile Defense Test Site (RTS), located on the Kwajalein Atoll in the South Pacific **(see photo)**. The test began with an Extended Long Range Air Launch Target (E-LRALT) missile, which was airdropped over the ocean area north of Wake Island from a US Air Force C-17 aircraft (staged from Joint Base Pearl Harbor-Hickam, HI). The AN/TPY-2 X-band radar, which is located with the THAAD system on Meck Island, tracked the E-LRALT. A THAAD interceptor then successfully intercepted the Medium-Range Ballistic Missile. The THAAD system was operated by soldiers from the 32nd Army Air and Missile Defense Command (AAMDC).

> **The systems detected, tracked, engaged, and negated two ballistic-missile targets and one cruise-missile-like target.**

Another short-range ballistic missile was launched from a mobile launch platform located in the ocean area northeast of Kwajalein Atoll. The PATRIOT system, which was manned by soldiers of the 94th AAMDC, detected, tracked, and intercepted the target with a PAC-3 interceptor. A second PAC-3 interceptor also intercepted a low-flying cruise missile target over water.

For its part, the USS FITZGERALD (DDG 62) successfully engaged a low-flying cruise missile over water. The Aegis system also tracked and launched an SM-3 Block 1A interceptor against a Short-Range Ballistic Missile (SRBM). Despite indication of a nominal flight of the SM-3 Block 1A interceptor, however, there was no indication of an SRBM intercept.

The FTI-01 exercise was a combined developmental and operational test involving soldiers, sailors, and airmen from the multiple combatant commands that operated the systems. The test provided them with a unique opportunity to refine operating procedures. As part of the Kwajalein Range Service (KRS) joint venture, Lockheed Martin employees directed and controlled the radar, telemetry, and optics systems for this test at the newly established RTS Operations Center in Huntsville, AL. Program officials continue to evaluate system performance based upon telemetry and other data obtained during the test.

Control Lights From Afar

ONE OF THE ADVANTAGES of smart homes is that aspects like heat or air conditioning can be controlled remotely. While this suggests images of someone controlling their utilities from afar, lighting is increasingly being adjusted remotely from both inside and outside the house. Using a smartphone, for example, a user can turn off their hallway and bathroom lights from bed. The rise in such usages will lead to the emergence of RF-embedded light bulbs in 2013, predicts IMS Research (www.imsresearch.com).

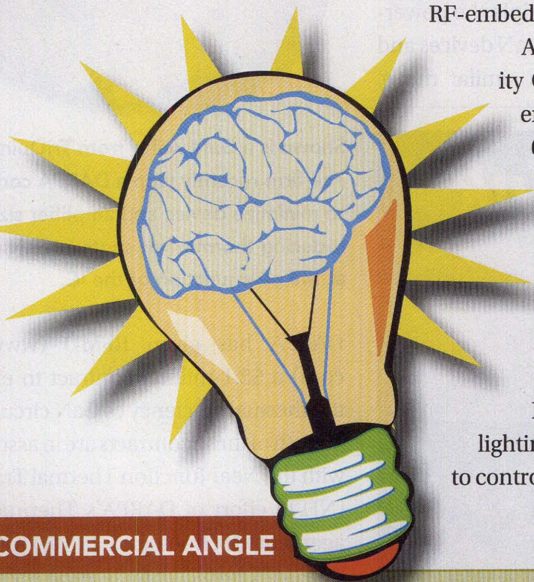

According to the organization's recently published report, "Connectivity Opportunities in Lighting Controls – 2012 Edition," shipments of RF-embedded light bulbs and their associated remote controllers will top 600,000 in 2013. That number is predicted to rise to 11.7 million in 2017. Several large manufacturers are planning to release new wireless-lighting products using a range of technologies.

Currently, most RF-embedded lightbulb systems, such as Insteon's (www.insteon.net), use a proprietary technology or a proprietary IEEE 802.15.4 software stack. Greenwave Reality (www.greenwavereality.com) is currently showcasing NXP's (www.nxp.com) JenNet-IP protocol. According to NXP, that protocol is being made an open one.

Meanwhile, the ZigBee Alliance (www.zigbee.org) recently launched a lighting-specific profile. Called "ZigBee Light Link," it is designed specifically to control both the color and light level of light-emitting-diode (LED) light bulbs. Several tier-1 lighting manufacturers, such as Osram and Philips, have already had devices certified using this protocol. IMS Research predicts that ZigBee will emerge as the main wireless technology for these systems.

Most systems are expected to offer remote access via an application or cloud-based service. While this feature is available on current residential lighting-control systems, the cost can be too high for many. The RF-embedded light bulbs will be sold at a more consumer-friendly price, leading to higher residential adoption.

THE COMMERCIAL ANGLE

ACCORDING TO IMS RESEARCH (www.imsresearch.com), the market for lighting-control devices in commercial buildings will double from 2010 to 2017. From 29.6 million, shipments of devices are expected to reach 61.6 million. Driving much of the adoption in commercial buildings is the need to reduce energy consumption in accordance with energy legislation. According to the US Department of Energy, lighting accounts for 25.5% of a typical commercial building's energy usage.

Most of these systems' components will be connected ballasts that contain a connectivity technology, such as DALI or ZigBee. It is expected that a standard for both ballasts and sensors will be released in 2013. This will drive the adoption of DALI, as lighting controls from different manufacturers may then become widely interoperable. For wireless communication, IEEE 802.15.4 technology is widely used. Because of the closed nature of the lighting-control industry, however, proprietary systems are used in most cases.

KU-Band Satellite Will Cover Asia

MANY INDUSTRIES are eying opportunities in Indonesia and Northeast and Southeast Asia, thanks to the rapid economic growth of those areas. For example, satellite operator SES SA (www.ses.com) has contracted Boeing (www.boeing.com) for a new satellite to expand direct-to-home broadcasting and other communications services to those markets **(see photo)**. This satellite also will provide maritime communications for vessels in the Indian Ocean.

Dubbed SES-9, this Ku-band 702 high-power (HP) satellite will be built in Boeing's El Segundo, CA Satellite Development Center. It is designed to operate for 15 years in geosynchronous orbit with a 12.7-kW payload and 57 high-power Ku-band transponders (equivalent to 81 36-MHz transponders). Boeing introduced the 702 satellite design more than 15 years ago and has evolved the design since then. This satellite's xenon-ion propulsion and chemical bi-propellant systems are uniquely designed to reduce launch weight while allowing for maximum payload capacity.

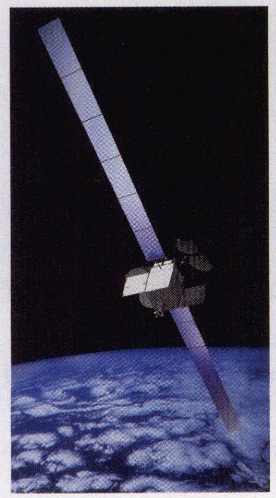

The Ku-band 702 high-power satellite will provide broadcasting services to thriving Asian markets.

The spacecraft, which will be co-located with SES' existing SES-7 and NSS-11 satellites, will be positioned at 108.2 deg. east longitude. It will provide incremental additional as well as replacement communications capacity. This is the 11th spacecraft that SES SA has ordered from Boeing and the contract includes an option for another.

DARPA GaN Contracts Go Head To Head

TO REACH ITS CURRENT STATE of success and industry acclaim, gallium-nitride (GaN) technology had to overcome a number of performance challenges. Now, the technology may reach further heights. Some GaN research and development efforts are currently underway with backing from the Defense Advanced Research Projects Agency (DARPA). TriQuint Semiconductor, Inc. (www.triquint.com) has received a $2.7-million contract from DARPA to triple the power-handling performance of GaN devices and circuits (**see figure**). In a similar move, DARPA has given RFMD (www.rfmd.com) a $2.1-million contract to enhance the thermal efficiency of GaN circuits.

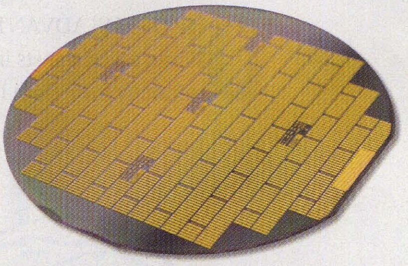

Shown is a GaN wafer from TriQuint. The firm recently won a DARPA contract to minimize device and amplifier sizes by reducing thermal hot spots in GaN circuits at the near junction of the IC.

Both of these contracts are in association with the Near Junction Thermal Transport (NJTT) effort of DARPA's Thermal Management Technologies (TMT) program. The NJTT initiative focuses on thermal resistance at the "near junction" of the transistor die as well as the device substrate material. These areas can be responsible for more than 50% of operational temperature increases. NJTT is expected to lay the groundwork for monolithic-microwave-integrated-circuit (MMIC) performance enhancements like reduced size, weight, and power consumption while increasing reliability and output power.

For TriQuint, this effort will build on both the firm's GaN-on-silicon-carbide (SiC) technology and RF integrated circuits (RF ICs). By combining its GaN-on-SiC process technology with diamond substrates and new thermal-handling processes, TriQuint seeks to significantly reduce heat build-up. In doing so, it hopes to enable GaN devices that can generate more power. Among TriQuint's partners in this program are the University of Bristol (known for thermal testing, modeling, and micro Raman thermography) and diamond-substrate specialist Group4 Labs. In addition, Lockheed Martin will evaluate the results of the program for its projected impact on future defense systems.

For its part, RFMD hopes to improve both power density and power-handling capability by combining thermally enhanced diamond substrates with its GaN-

TINY TOUGHEST MIXERS UNDER THE SUN

Rugged, tiny ceramic SIM mixers *from $4.95 ea. qty. 1000* offer unprecedented wide band, high frequency performance while maintaining low conversion loss, high isolation, and high IP3.


0.2" x 0.18"

Over 21 models IN STOCK are available to operate from an LO level of your choice, +7, +10, +13, and +17 dBm. So regardless of the specific frequency band of your applications, narrow or wide band, there is a tiny SIM *RoHS* compliant mixer to select from 100 kHz to 20 GHz. Built to operate in tough environments, including high ESD levels, the SIM mixers are competitively priced for military, industrial, and commercial applications. Visit our website to view comprehensive performance data, performance curves, data sheets, pcb layouts, and environmental specifications. And, you can even order direct from our web store and have it in your hands as early as tomorrow!

Mini-Circuits...we're redefining what VALUE is all about!

U.S. Patent # 7,027,795 *RoHS compliant*

Mini-Circuits®
ISO 9001 ISO 14001 AS 9100

P.O. Box 350166, Brooklyn, New York 11235-0003 (718) 934-4500 Fax (718) 332-4661

Yoni2® ***The Design Engineers Search Engine*** *finds the model you need, Instantly* • For detailed performance specs & shopping online see **minicircuits.com**

U.S. Patents
7739260, 7761442

IF/RF MICROWAVE COMPONENTS

428 rev H

on-SiC technology. RFMD's partners in the program include the Georgia Institute of Technology (known for thermal testing, modeling, and micro Raman thermography), Stanford University (a leader in thermal measurement of the interface layers within a transistor die), Group4 Labs, and Boeing. Boeing plans to evaluate the resulting technology to assess its projected impact on future defense systems.

According to DARPA, varied NJTT approaches may be implemented to reduce the near-junction thermal barrier. These include the use of high-thermal-conductivity diamond substrates, which will replace lower-conductivity materials like SiC, Si, and sapphire. In addition, low-conductivity epitaxial and transition layers at the interface of the GaN active layers and the substrate can be removed by etching or other techniques. DARPA also points to the introduction of liquid cooling in the near-junction region as well as the use of metrology and modeling—both to address the challenges of measurement verification at this scale and quantify the thermal and electrical performance of the GaN devices.

PEOPLE

MICROSEMI CORP.—Amr El-Ashmawi has joined the company as Worldwide Vice President of Strategic Marketing, a newly created role. El-Ashmawi comes to Microsemi from Altera, where he held several senior leadership roles within the defense, security, and high-performance computing areas.

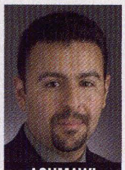
ASHMAWI

EXALT COMMUNICATIONS—Greg Gum has been named Senior Vice President of Marketing and Business Development. Prior to joining Exalt, Gum served as Senior Vice President, Chief Marketing and Business Development Officer at Telco Systems.

CTIA–THE WIRELESS ASSOCIATION—Maurice B. Tose has been re-elected to the nonprofit organization's board of directors. Tose is Chief Executive Officer, President, and Chairman of the Board for TeleCommunication Systems, Inc. (TCS).

LOCKHEED MARTIN—Rick Edwards and Dale Bennett have been named Executive Vice Presidents of the company's new business areas. Edwards will head up the Missiles and Fire Control (MFC) business while Bennett will lead the Mission Systems and Training (MST) business. As three-decade veterans of Lockheed Martin, both executives have served in roles of increasing responsibility.

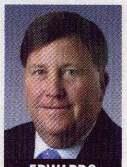
EDWARDS


BENNET

RFMD—Has appointed Alan Hallberg Corporate Vice President and Chief Marketing Officer. Hallberg most recently served as Vice President, Global Brand Communications at Lenovo, following earlier stints at Cisco and Apple.

HOLOGRAPHIC RADAR Cuts Wind-Farm Clutter

TO MEET THE RISING DEMAND FOR GREEN ENERGY, wind farms should be growing and expanding. Unfortunately, such growth has been limited because of the interference that wind turbines have on local air-traffic-control (ATC) radars. Although many proposals have sought to mitigate this interference, no reliable, zero-degradation solution currently exists. In hopes of providing a better answer, Saab Sensis Corp. (www.saabsensis.com) and Aveillant (www.aveillant.com), a Cambridge Consultants spinout, are demonstrating an end-to-end, wind-farm radar-clutter-removal solution. This solution can be integrated with operational ATC systems.

The goal of this program is to show that seamless, clutter-free ATC surveillance data from non-cooperating targets can be produced using Aveillant's 3D Holographic Radar and existing Primary Surveillance Radar (PSR). Aveillant's Holographic Radar clearly distinguishes between moving objects with differing behaviors and 3D trajectories. Unlike the current generation of ATC radars, which scan a narrow beam using the familiar rotating antenna, the Holographic Radar looks in all directions at once. In addition, the solution continuously measures the dynamic characteristics of each target. As a result, it sees both wind turbines and aircraft and can tell the difference between the two.

Saab Sensis' fusion technology combines primary-plot-extracted data from the local airport PSR with either the co-mounted Secondary Surveillance Radar (SSR; when operating in combiner mode) or with a remote asynchronous SSR site (when operating in Assignor mode). In the demonstration, for example, it is using both the 3D Holographic Radar and data provided by NATS from Glasgow International Airport's PSR. Consequently, the fusion technology will generate a combined output in the common ASTERIX ATM format.

A secondary demonstration will incorporate Saab Sensis' Wide Area Multilateration (WAM) data with PSR and Holographic Radar data to illustrate the ability to use both cooperative and non-cooperative surveillance sources. WAM uses a distributed system of non-rotating sensors, which triangulate an aircraft's position based on transponder signals—either passively or through interrogation, providing a once-per-second update rate.

DEVELOP SOFTWARE For Radios In Space

Opportunities to perform research and technology demonstrations on the International Space Station are now being offered to academia, industry, and government agencies. Using the newly installed Space Communications and Navigation (SCaN) testbed, researchers can develop software according to the Space Telecommunications Radio Standard (STRS) architecture for radios—and, in the process, reconfigure how radios communicate in space.

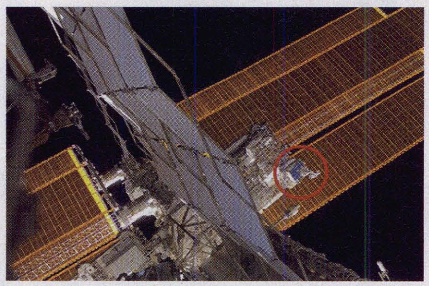

Shown is the SCaN testbed installed on the International Space Station. (Courtesy of NASA)

The SCaN Testbed is a communications, navigation, and networking demonstration platform based on the STRS **(see figure)**. The experimental platform will operate for at least three years. Participating developers will provide software components to the STRS repository while enabling future hardware platforms to use common, reusable software modules.

Those experimenters will gain the opportunity to create the latest communications, navigation, and networking technologies both in laboratory and space environments. These new concepts will be explored for future missions. The SCaN Testbed Cooperative Agreement Notice is available online at www.nasa.gov. NASA expects initial demonstrations to take place by early 2014.

KUDOS

TECOM—Has been awarded a Customer Service Award by AAI Unmanned Aircraft Systems for the second consecutive year. TECOM's Multi-Direction Antenna System and Tactical Unmanned Aerial Vehicle products are used in support of ongoing UAV operations overseas.

LOCKHEED MARTIN—Stephanie C. Hill, President of the Information Systems & Global Solutions (IS&GS) -Civil product line, was honored for career achievement in industry during the 17th annual Women of Color Science, Technology, Engineering, and Math (STEM) conference. The conference was held last month in Dallas, TX. Hill was one of 37 Lockheed Martin employees recognized. In addition, Lockheed Martin Mission Systems and Sensors (Syracuse, NY) and Lockheed Martin Space Systems (Sunnyvale, CA) each received the National Defense Industrial Association's (NDIA's) Top 5 DoD Program Award for 2012.

CONTRACTS

Avago Technologies—Multiple products based on the company's film-bulk-acoustic-resonator (FBAR) filter technology are supporting operation in 15 different frequency bands. The technology has proven applicable to smartphones required to operate on numerous frequency bands worldwide. At the same time, it supports high-speed Long Term Evolution (LTE) voice and data transmissions.

LOCKHEED MARTIN wins SBIR contract

RAYTHEON CO. Awarded Army Radio Contract

KOR Electronics—Has received a five-year, sole-source basic ordering agreement (BOA) from the US Navy. This BOA supports R&D, production, engineering services, and ongoing support associated with KOR Electronics' Digital RF Memory (DRFM) radar jammers. It is valued at up to $58 million.

Harris Corp.—Has announced a $24-million contract with the Regional Municipality of Durham, Ontario, Canada. Harris will design, deploy, and maintain a Project 25 (P25) Phase 2 simulcast radio system, to be utilized by public-safety and public-works agencies in the region.

Raytheon Co.—Has been awarded $51 million by the US Army to build and modernize airborne radios. This initiative includes Phase 3 of the Mobile User Objective Service/Cryptographic Modernization (MUOS/CM) Upgrade Program, which is intended to increase satellite capacity for soldiers.

Lockheed Martin—Has been awarded an $82-million contract by the US Air Force to begin initial work on the fifth and sixth geosynchronous (GEO) satellites in the Space-Based Infrared System (SBIRS) missile-warning constellation. The SBIRS program features a mix of GEO satellites, hosted payloads in highly elliptical earth (HEO) orbit, and associated ground hardware and software.

FRESH STARTS

I.F. Engineering—Has opened a new manufacturing and engineering development facility in Dudley, MA. The 20,000-sq.-ft building replaces the company's previous facility in Fabyan, CT.

Rakon—Has begun sampling oscillators utilizing microelectromechanical-systems (MEMS) technology to select customers. The company plans to ramp up volume production this quarter.

Anritsu—Has been chosen by UK-based Underwriters Laboratories (UL) as its provider of Long Term Evolution (LTE) telecom equipment. Consequently, Anritsu has become the first commercial, independent LTE-conformance test facility in the UK.

NuWaves Engineering—Has added authorized resellers in Southeast Asia, the Middle East, and Europe. MEDs Technologies will represent NuWaves in several Asian countries including Indonesia, Malaysia, Thailand, and Singapore. Mel Sivan Technologies will represent the company in Israel. Finally, two European companies join NuWaves' reseller network: Tech-Inter (France) and Medeos Srl (Italy).

California Eastern Laboratories (CEL)—Has signed EFO Ltd. as its sales representative for Russia. Based in St. Petersburg, EFO will represent CEL's MeshConnect line of IEEE 802.15.4/ZigBee wireless solutions.

RFE—Has been approved as a member of the Xilinx Alliance Program, a worldwide ecosystem of companies collaborating with Xilinx on product development. In addition, RFEL is now a member of the Altera Design Service Network (DSN), a listing of Altera-qualified field-programmable-gate-array (FPGA) designers.

Lockheed Martin—Is splitting its Electronic Systems business area into two new entities: the Missiles and Fire Control (MFC) and Mission Systems and Training (MST) business areas. The MFC business (16,000 employees) will be headquartered in Dallas, TX while the MST business (19,000 employees) will be based out of Washington, DC.

Teseq—Has acquired Instruments for Industry (IFI), a designer and manufacturer of solid-state and traveling-wave-tube (TWT) amplifiers. Teseq will incorporate IFI's Ronkonkoma, NY location as a fourth competency center, joining Luterbach, Switzerland; Berlin, Germany; and Ryde, Isle of Wight, UK.

TeleCommunication Systems (TCS)—Has been issued 12 patents by the US Patent and Trademark Office (USPTO) during the third quarter of 2012. These patents pertain to developments in wireless data, navigation, public safety, messaging, mobile location, and secure communications.

Pasternack Enterprises—Has released an online, interactive version of its 2012B RF catalog. Optimized for usage on all mobile devices, this new version features page-turning animation, multiple viewing options, and zoom capabilities.

AWT Global (AWTG)—Recently began operation in Parsippany, NJ. A subsidiary of the Korean design and manufacturing firm, AceWavetech, AWRG now has sole responsibility for worldwide sales, marketing, and support of AceWavetech products, systems, and services. More offices are planned to open in the US, Europe, the Middle East, and Asia.

Modelithics—Through a partnership with KEMET Corp., Modelithics is providing scalable global models of KEMET's CBR series capacitors.

ON Semiconductor—Has joined the multi-partner, industrial research and development program at imec, a nanoelectronics research center. ON Semiconductor will collaborate on imec's broad-scale research program to develop next-generation gallium-nitride-on-silicon (GaN-on-Si) technology on 200-mm wafers. It also will work to reduce the cost and improve the performance of GaN devices. Last year, imec's research program successfully produced 200-mm GaN-on-Si wafers, bringing processing within reach for standard, high-productivity 200-mm fabs.

Global Semiconductor Alliance (GSA)—Has formed a Technology Steering Committee (TSC), which is tasked with encouraging the advancement and adoption of leading technology and practices for GSA constituents. Chaired by Dr. Naveed Sherwani, President and Chief Executive Officer of Open-Silicon, Inc., the committee will meet quarterly.

2 W, 5 W, and 20 W

PRECISION ATTENUATORS

NOW up to 26 GHz from $29.95 ea. (1-49) RoHS compliant

For rugged, reliable, and repeatable attenuation when accuracy is key, our customers have come to rely on Mini-Circuits Fixed Precision Attenuators, rated at 2W or 5W for DC-18 GHz signals. And now we've gone even further, with a new series of **2 W models up to 26 GHz,** and a new series of **20 W models from DC-18 GHz!** They feature stainless steel construction, precision attenuation from 1 to 50 dB, and SMA or N-type connectors for 50 Ω systems.

Inherent accuracy, and finely-graded attenuation levels, make our "BW" family invaluable on the bench or in the field. They're a ready solution for extending the range of test instrumentation or meeting circuit- and system-level requirements, such as better matching for high-VSWR components, reducing power to maximize sensitive applications, or protecting valuable circuitry. Just go to minicircuits.com—they're on the shelf and ready to ship today, at the low prices you've come to expect!

See minicircuits.com for specifications, performance data, and surprisingly low prices!
Mini-Circuits...we're redefining what VALUE is all about!

Mini-Circuits®
ISO 9001 ISO 14001 AS9100

P.O. Box 350166, Brooklyn, New York 11235-0003 (718) 934-4500 Fax (718) 332-4661

Yoni2® **The Design Engineers Search Engine** *finds the model you need, Instantly* • For detailed performance specs & shopping online see **minicircuits.com**

U.S. Patents 7739260, 7761442

IF/RF MICROWAVE COMPONENTS

331 rev S

Inside Track with Matt Apanius,

DIRECTOR, THE RICHARD DESICH SMART COMMERCIALIZATION CENTER FOR MICROSYSTEMS

Interview by NANCY FRIEDRICH

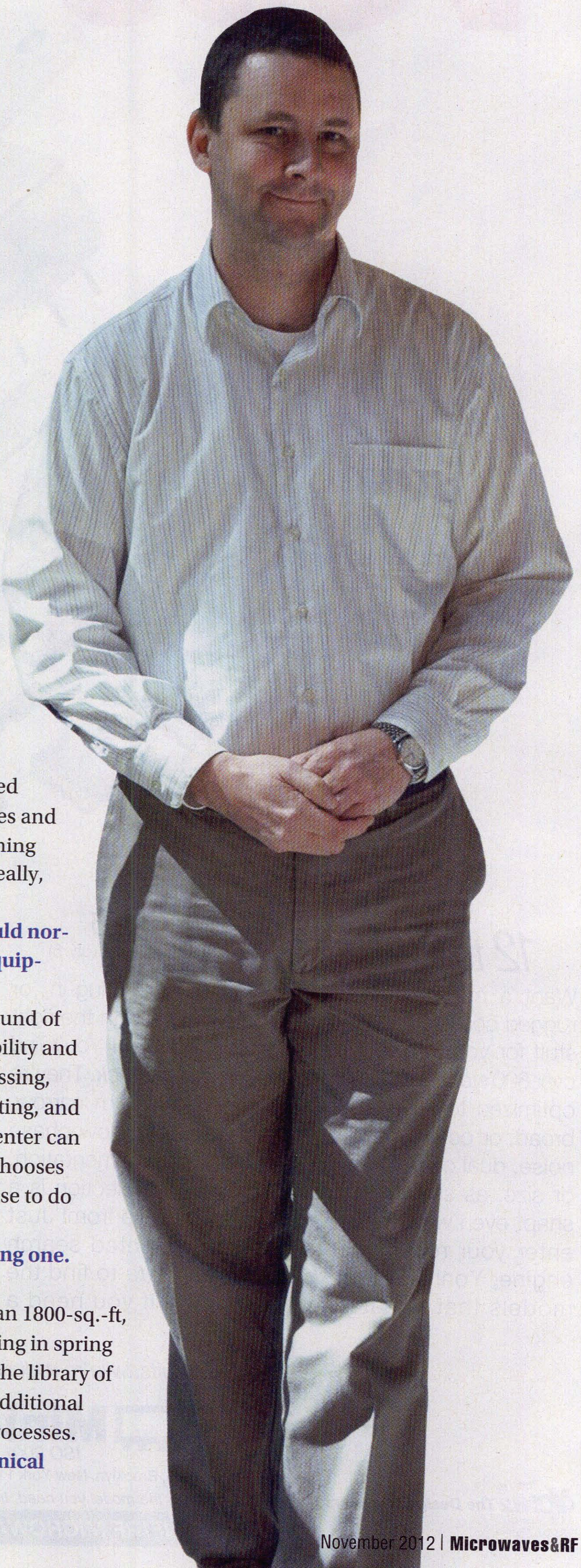

NF: The Desich SMART Center is a microsystems packaging lab focusing on commercialization. Which part of the design process does it target?

MA: We are focused on back-end-of-line processes—processes that will become a development bottleneck for commercialization if not addressed properly. The package interface determines how well the device will perform in the environment of its intended application. By providing package, assembly, and testing processes and expertise, the Desich SMART Center assists customers in overcoming these challenges earlier in the product-development process—ideally, before finalizing the design.

NF: The center contains about $5 million of equipment that would normally be found on a manufacturing floor. Please describe the equipment and capabilities offered by the center.

MA: We have established a great starting point with the current round of equipment investments by carefully balancing the needs for flexibility and manufacturability. The capabilities include back-end wafer processing, package assembly, performance testing, accelerated reliability testing, and package design. Development work done at the Desich SMART Center can seamlessly transition into manufacturing, whether the customer chooses to use a semiconductor assembly and test house or bring it in-house to do the manufacturing themselves.

NF: A new facility is currently being built in addition to the existing one. What capabilities and equipment will it offer?

MA: Since September 2011, we have been running projects out of an 1800-sq.-ft, class 10,000 cleanroom. The new 47,000-sq.-ft facility will be opening in spring 2013. It will have class 100 and class 1000 cleanrooms, expanding the library of existing process modules. The new process modules will include additional advanced packaging techniques and new wafer-level packaging processes.

NF: For a small company looking to develop microelectromechanical

systems (MEMS) devices, the Desich SMART Center can help them compete with larger companies in terms of available resources. How do those firms go about partnering with the center?

MA: As a development foundry, the Desich SMART Center offers access and services to companies that do not have the resources for the capital-intensive infrastructure required for MEMS packaging, assembly, and testing. Fabless companies have emerged over the years and have been successful in bringing new products to the market. Relying on outsourced manufacturers for development is challenging because it is disruptive to the manufacturer's operations. In addition, the management of intellectual property can be complicated. The Desich SMART Center's engagement model offers full access to capabilities required for back-end-of-line process development. At the same time, it protects the customer's intellectual property and, with partnerships, assists with the transfer to manufacturing.

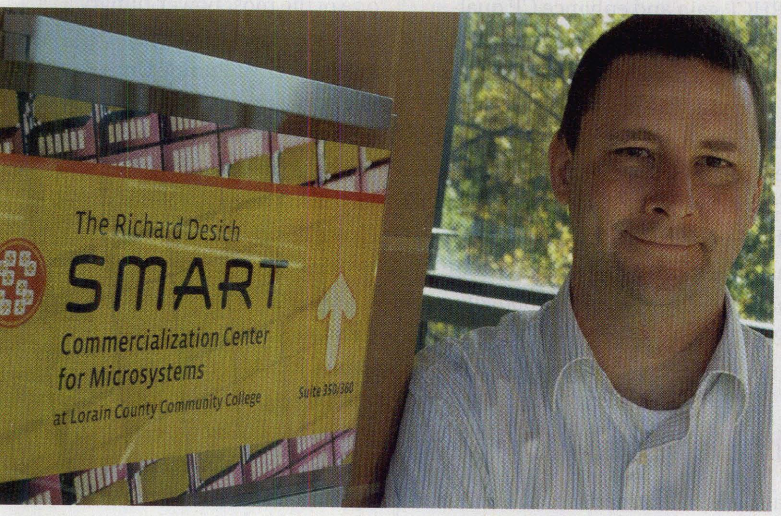

NF: How does the center solve the issues that designers are having with current approaches?

MA: The semiconductor supply chain is fragmented and the manufacturing models are driven by high volumes. These two characteristics can make it very difficult for a company interested in developing and launching a new MEMS product. In this case, additional resources are necessary to either manage the suppliers or build a prototype lab. This ultimately detracts from what the company is trying to accomplish—creating a new product.

The Desich SMART Center offers MEMS packaging and testing services in one location, reducing project costs and accelerating time to market. For example, a customer can have their device packaged, performance tested, and evaluated for reliability—all at the Desich SMART Center. Therefore, the customer can very quickly understand how the device performs within the constraints of a given package design and its manufacturing process.

NF: Can you share with us some examples of projects that have been completed with the center's help?

MA: Absolutely. We've supported the development of a low-temperature wafer-bond process for capping a MEMS micro valve. We have developed a package assembly process for a customer that is developing high-temperature integrated circuits (ICs). And we currently provide them with on-demand prototypes for their customers. We've also developed manufacturing specifications for several customers that have unique assembly processes for micro-actuators and sensors. In addition, we conduct third-party calibration and testing for MEMS devices.

NF: Do you feel that the center's location (15 miles outside of Cleveland in Elyria, OH) hampers its success at all?

MA: Not at all. In many ways, the location is ideal. Ohio is the third-largest manufacturing state in the US next to California and Texas. Many of our early customers have been regional companies that already manufacture products. They are looking for ways to leverage MEMS and sensors to differentiate their products from their competitors. We also have the benefit of being close to universities that are conducting world-class research in MEMS and microelectronics, advanced materials, and advanced manufacturing. They include Case Western Reserve University, the University of Akron, Carnegie Mellon University, the Ohio State University, and the University of Michigan.

NF: The Desich Smart Commercialization Center for Microsystems is a very unique model in that it has a relationship with a community college. Please describe that relationship and how the center came into being.

MA: The Desich SMART Center was launched in partnership with Lorain County Community College (also located in Elyria). As an institution of higher learning, the college has made great strides in rejuvenating a community that has suffered through a severe economic downturn. In serving its mission, the college has made significant commitments to resources that support the development of technology and new products. These include a technology business incubator called GLIDE, a pre-seed funding opportunity for technology startups known as the Innovation Fund, and now a technology facility that leverages capital equipment assets for MEMS and sensor technology development—the Desich SMART Center.

NF: Do you see a chance for the US to reinvigorate its manufacturing efforts with semiconductor development? How does the SMART Center contribute to these efforts?

MA: The opportunity for US manufacturing and MEMS can be realized with low- to mid-range-volume, high-performance products. For MEMS applications, the package is part of the system design. A robust system design delivers maximum performance. The Desich SMART Center is well-positioned to help companies quickly develop their products so that they can get them to market. I would like to think that we can have a positive impact on US manufacturing. There is no way to predict the magnitude of the potential. But at a minimum, we are taking a step in the right direction. MWRF

X-BAND ANTENNA ARRAYS Enrich RHCP

X-BAND ANTENNAS ARE often used for dense satellite-communications payloads. They handle the data transmission of high-resolution captured and detected images from a satellite to a ground station. Instead of a conventional microstrip line antenna, however, a substrate-integrated-waveguide (SIW) -based antenna array has been proposed and analyzed in several configurations at Korea Aerospace University. The arrays were fabricated as multilayer printed-circuit boards (PCBs) for right-handed circular polarization (RHCP) by a team of researchers comprising Eun-Young Jung, Jae W. Lee, Taek K. Lee, and Woo-Kyung Lee.

Specifically, the researchers proposed, designed, and investigated arrays based on a single element using two types of array antennas centered on SIW-based design. To increase the transmission efficiency between the satellite and ground system while enhancing antenna gain, for example, they introduced the design procedure, simulation, and measured data of SIW-based 2x2 and 2x4 array antennas. These arrays build on a single element operating at X-band from 8.0 to 8.5 GHz. The single-element approach had to overcome issues like feeding loss and undesirable radiation. For RHCP generation, a novel SIW-based and cavity-backed ring-slot antenna was combined with a SIW and coaxial feeding network.

To design the single-element 2x2 antenna array, the team had to design a power divider providing equal amplitude at each output port in that array. That SIW-based, four-way power divider was designed and measured as a replacement for the microstrip structures. To further increase antenna gain and improve RHCP quality, a 2x4 antenna array with an eight-way power divider also was successfully designed and investigated.

A 2x4 antenna array was proposed to improve RHCP gain and enhance CP quality with a sequential feeding scheme. This antenna had eight radiating elements in the top layer, an eight-way power divider, and phase-delay lines in the bottom layer. The researchers reported notable improvements in electrical performance. See "SIW-Based Array Antennas with Sequential Feeding for X-band Satellite Communication," *IEEE Transactions On Antennas And Propagation*, Aug. 2012, p. 3632.

MM-WAVE RECEIVER Precisely Detects AOA

WHEN IT comes to automotive radar sensors, calibration is key. After all, mechanical misalignment of the radar sensor to the car body by only a few degrees will seriously degrade performance. A new calibration system based on the measurement of electromagnetic (EM) waves has been presented by Benjamin Laemmle, Gabor Vinci, Robert Weigel, and Alexander Koelpin from Germany's University of Erlangen-Nuremberg together with Linus Maurer from Austria's DICE GmbH.

Beyond automotive radar calibration, their six-port receiver front end can perform the angle-of-arrival (AOA) detection of 77-GHz signals for direction finding (DF) or high-precision industrial radar systems. The millimeter-wave integrated circuit (IC) leverages a measurement principle rooted in the passive superposition of two incident signals and power detection. Essentially, the magnitude of the four phase-shifted, superposed signals is downconverted to baseband by power detection. The phase difference—and thus the AOA of the two input signals—can be calculated from the four output voltages.

Included in this IC are the following: two input amplifiers; a broadband, passive six-port network; and four power detectors. The IC operates across a 3-dB bandwidth from 75 to 84 GHz. At 80 GHz, it boasts responsivity of 152 kV/W. The IC consumes 95 mW from a 5-V supply. It measures just 1028 x 1128 μm^2, having been fabricated in a 200-GHz f^T silicon-germanium (SiGe) bipolar process. See "A 77-GHz SiGe Integrated Six-Port Receiver Front-End for Angle-of-Arrival Detection," *IEEE Journal Of Solid-State Circuits*, Sept. 2012, p. 1966.

Synthesizer Consumes 400 μW To Support ISM

IN 2009, the Federal Communications Commission (FCC) debuted the Medical Device Radiocommunications Service (MedRadio) for transmitting data using implanted biomedical devices. As a result, wireless implantable biomedical devices gained 5 MHz of bandwidth from 401 to 406 MHz. To succeed, however, these devices had to overcome limited battery lifetime. In wireless transceivers, one of the most power-hungry components is the frequency synthesizer. At Purdue University, a low-power, low-voltage frequency synthesizer for implantable medical devices has been created by Wu-Hsin Chen, Wing-Fai Loke, and Byunghoo Jung.

Their 0.5-V medical-band frequency synthesizer consumes just 440 μW while exhibiting phase noise of –91.5 dBc/Hz at 1 MHz offset from the carrier. A number of design approaches were utilized to give this synthesizer its performance edge. To provide a high driving current with a low standby current, for example, the charge pump relies on dynamic threshold-voltage and switch-coupled techniques. In addition, a ring-based voltage-controlled oscillator (VCO) uses a dual resistor-varactor tuning method to compensate for process-voltage-temperature (PVT) variations and the exponential voltage-to-current curve. See "A 0.5-V, 440-μW Frequency Synthesizer for Implantable Medical Devices," *IEEE Journal Of Solid-State Circuits*, Aug. 2012, p. 1896.

FILTER SOLUTIONS

DC to 15 GHz

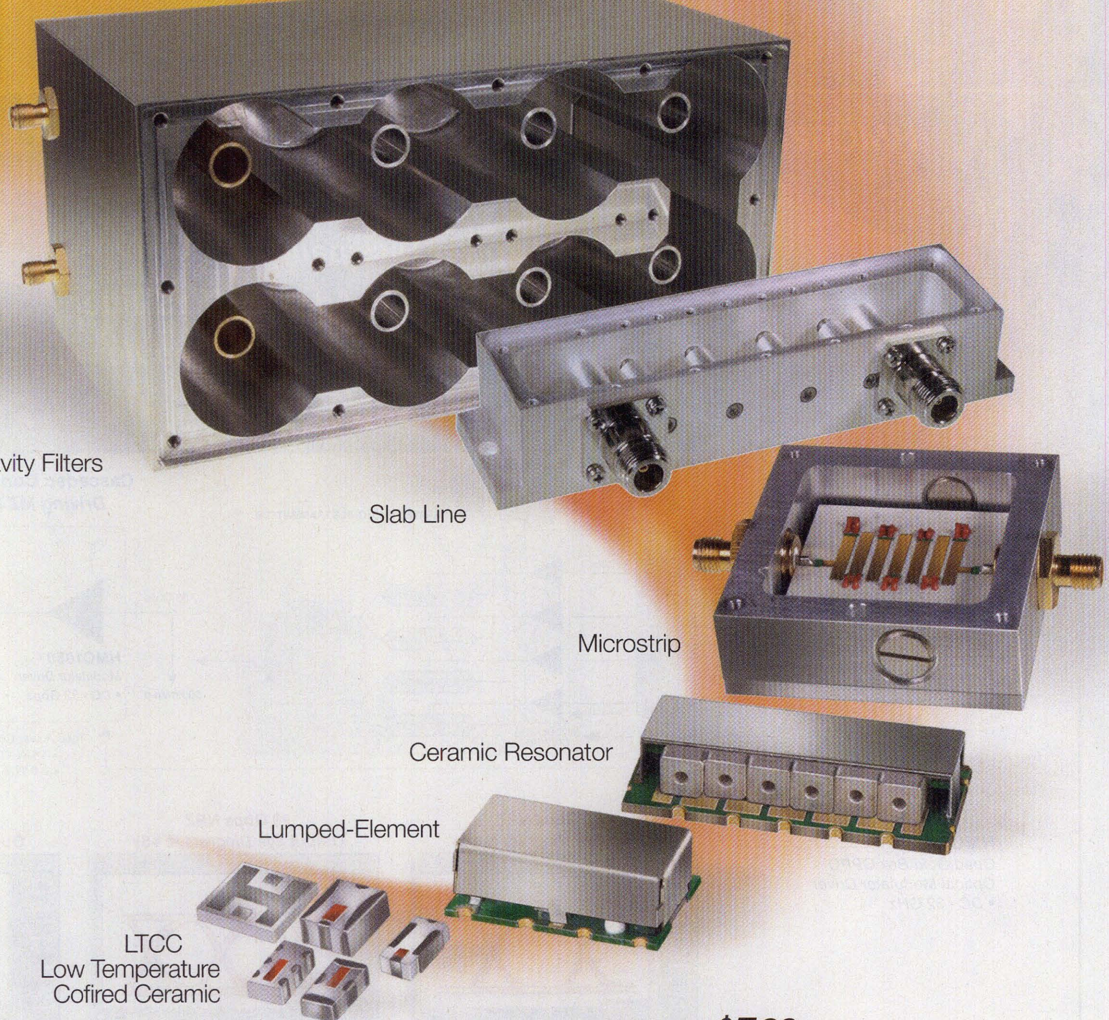

Over 300 Models IN STOCK ... Immediate Delivery! _from_ $1.99 ea. 10-49

Different needs demand different technologies, and the Mini-Circuits RF/microwave filter lineup delivers. Over 300 proven solutions, from DC to 15 GHz, are standing by, ready to ship. High-pass or low-pass, band-pass or band-stop, in coaxial, surface-mount, or plug-in packages. Across the board, our filters achieve low insertion loss and low VSWR in the passband and high attenuation in the rejection band. Just go to minicircuits.com for more information. If you need a specific performance and want to search our entire model database, including engineering models, click on Yoni2, our exclusive search engine.

In Yoni2, you can enter the response type, connection option, frequency, insertion loss, or any other specifications you have. If a model cannot be found, we understand the sense of urgency. So contact us, and our engineers will find a quick, cost-effective, custom solution and deliver simulation results within a few days.

Yoni2® U.S. Patent 7739260, 7761442 **The Design Engineers Search Engine...** _finds the model you need, Instantly._

Mini-Circuits...we're redefining what VALUE is all about!

Mini-Circuits®
ISO 9001 ISO 14001 AS9100

P.O. Box 350166, Brooklyn, New York 11235-0003 (718) 934-4500 Fax (718) 332-4661

Yoni2® U.S. Patents 7739260, 7761442 **_The Design Engineers Search Engine_** _finds the model you need, Instantly_ • For detailed performance specs & shopping online see minicircuits.com

IF/RF MICROWAVE COMPONENTS

484 Rev B

OPTICAL DRIVER SOLUTION

Ideal for Driving MZ Optical Modulator With Electrical NRZ Data

Analog, Digital & Mixed-Signal
ICs, Modules, Subsystems & Instrumentation

HMC6282A Quad Optical Modulator Driver Module, 32 Gbps

- *Operation Up to 32 Gbps*
- *5.3W Power Dissipation*
- *Less than 250 fs Additive RMS Jitter*
- *Fully Integrated Compact Module with GPPO Interface*
- *Hermetically Sealed Module*

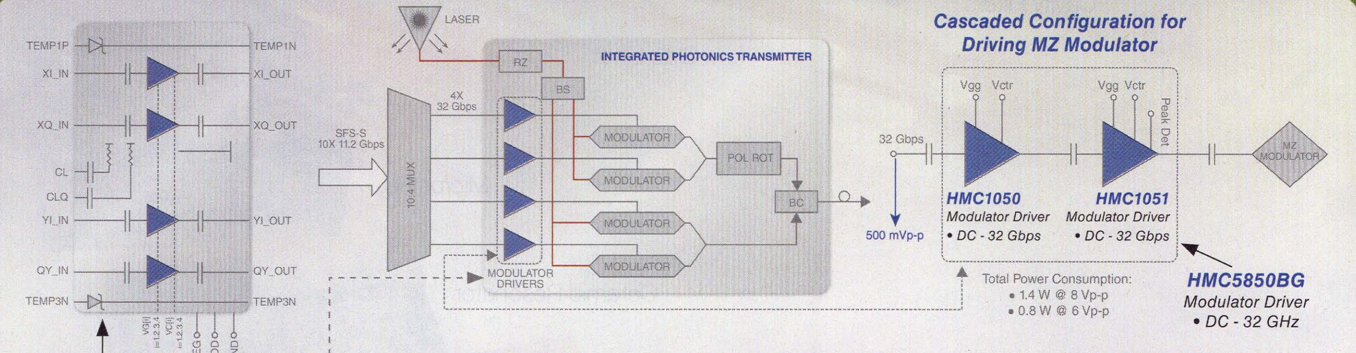

NEW! **HMC6282A**
Quad Gold Box GPPO Optical Modulator Driver
• DC - 32 GHz

21.5 Gbps NRZ Output Eye Diagram @ +6V

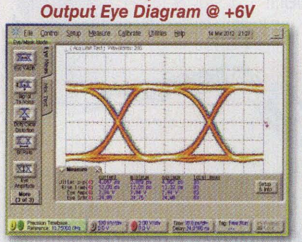

28 Gbps NRZ Output Eye Diagram @ +6V

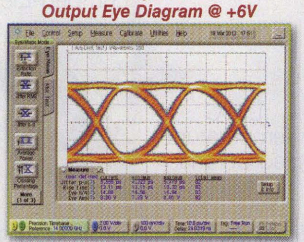

32 Gbps NRZ Output Eye Diagram @ +7V

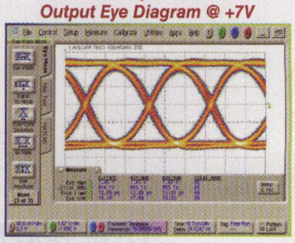

	Part Number	Data Rate Max. (Gbps)	Function	Gain (dB)	Group Variation Delay (ps)	Additive Jitter (ps)	P1dB (dBm)	Output Voltage Level (Vp-p)
	HMC870LC5	22.5	MZ Optical Modulator Driver	18	±15	0.3	22	2.5 - 8
	HMC871LC5	22.5	EA Optical Modulator Driver	15	±15	0.3	16.5	2.5 - 4
	HMC1050	32	3Vp-p Optical Modulator Driver / Wideband Amplifier	14	±5	0.3	14	3
	HMC1051	32	8Vp-p Optical Modulator Driver / Wideband Amplifier	16	±5	0.3	20	8
	HMC5850BG	32	Optical Modulator Driver	29	±7	0.23	22	8
NEW!	HMC6282A	32	Quad Optical Modulator Driver	26	±4	0.23	-	7.5

Ideal For Wideband Telecom Systems, Test & Measurement and NRZ Applications Up to 32 Gbps

JACK BROWNE | Technical Contributor

Software Integration Speeds Design Process

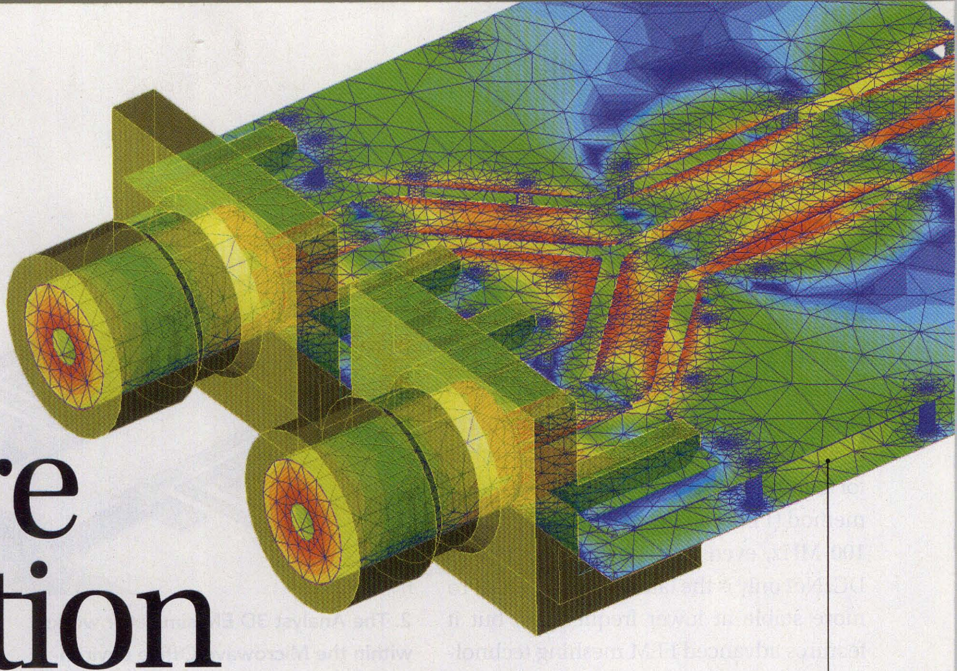

1. The EMPro 3D EM simulation software allows cosimulations at circuit levels as part of its integration with the ADS software. [Photo courtesy of Agilent Technologies (www.agilent.com).]

LEADING SUPPLIERS OF CAE SOFTWARE TOOLS ARE WORKING TOWARDS THE IMPROVED INTEGRATION OF THEIR SIMULATION AND ANALYSIS TOOLS, ALLOWING DESIGN ENGINEERS INCREASED FUNCTIONALITY FROM A SINGLE OPERATING ENVIRONMENT.

SOFTWARE IS VERY MUCH A PART OF HARDWARE IN THE RF/MICROWAVE INDUSTRY. Most designers now check their circuits or systems by mean of a favorite computer-aided-engineering (CAE) program, feeling a design validated when its simulated responses match closely with measurements on a prototype. For their part, developers of high-frequency simulation software have been responsive to the needs of their customers with constantly improving functionality, new device models, and intuitive graphical user interfaces (GUIs) that help simplify the operation of some reasonably complex programs. As most CAE software suppliers will offer, there is always room for improvement.

Simulation software within the RF/microwave industry has long been developing as separate projects, without much initial thought for integrating different functions, such as circuit simulation and electromagnetic (EM) simulation, together under one operating platform. But as high-frequency circuits themselves become more integrated, whether as discrete or monolithic circuits, with active and passive elements, transmission lines, and different circuit structures that must blend, the ways that engineers use simulation software must change as well. Optimizing a circuit usually requires looking at a design in different ways, which requires the use of different simulation programs for the same circuit or system design file. Because many simulation tools were initially developed as stand-alone programs, a current trend in RF/microwave simulation software is for the integration of different simulation and modeling functions under a single control platform.

At the recent European Microwave Week (Amsterdam, The Netherlands), Agilent Technologies (www.agilent.com) demonstrated their EMPro 2012 electromagnetic (EM) simulation software for modeling three-dimensional (3D) structures including antennas, connectors, and packages (**Fig. 1**). The software is highly integrated with the firm's flagship software platform, the Advanced Design System (ADS) program, allowing files of 3D modeled structures to be saved as data base "cells" for use within ADS. This allows a user to perform a circuit and EM cosimulation to be performed on a project to analyze not only the electrical circuit performance of the design but also its EM behavior and how the two are related.

The EMPro demonstration also showed some new features, including a new low-frequency analysis algorithm for improved accuracy for finite-element-method (FEM) analyses performed below 100 MHz, even at frequencies as low as DC. Not only is the latest version of EMPro more stable at lower frequencies, but it features advanced FEM meshing technology for increased processing speed. Interested parties can download a trial version of the software at the company's website: www.agilent.com/find/eesof-empro-downloads-and-trials.

Earlier this year, Sonnet Software (www.sonnetsoftware.com) released Version 13.56 of their Sonnet Suites 3D planar EM simulation software with support for Agilent's ADS 2011 software suite. This support allows users of ADS 2011 to operate Sonnet's EM simulation engine within the ADS 2011 layout and processing tools for truly efficient design and circuit optimization operations. The Sonnet functionality is installed as a Design Kit within ADS and can be automatically included in ADS 2011 Workspaces, allowing fully functional Sonnet EM extraction from within the ADS environment. This can simplify model development for radio-frequency integrated circuits (RFICs) and monolithic-microwave integrated circuits (MMICs) when working with commercial semiconductor foundries.

For most RF/microwave design engineers relying on simulation software, ADS is one of two main choices for simulation platform, with Microwave Office™ from AWR (www.awrcorp.com) being the other chief option. AWR was also in force in the European Microwave Week exhibition area with a demonstration of their Analyst™ 2012 3D EM FEM simulator, which is fully integrated within the AWR Microwave Office circuit simulation environment. This allows users working on a circuit design and simulation to perform a 3D EM simulation as needed, such as for interconnections and circuit junctions **(Fig. 2)**. The integration eliminates the need to open a third-party software tool when performing an EM simulation on part of a nominally planar design, such as an RF/microwave circuit. Having a 3D EM simulator as part of the circuit design flow can also simplify the adjustment of different settings required for the EM simulation to work with the circuit simulator, enabling the different tools to mesh together automatically **(Fig. 3)**.

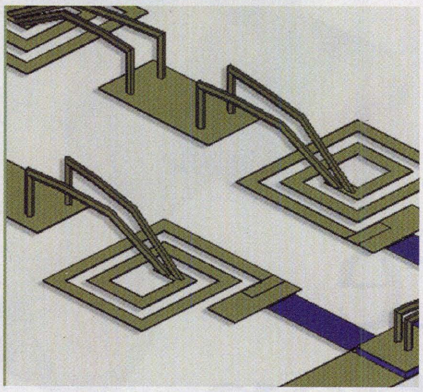

2. The Analyst 3D EM simulator works within the Microwave Office environment to perform analysis on discrete and monolithic circuit interconnections. [Photo courtesy of AWR (www.awrcorp.com).]

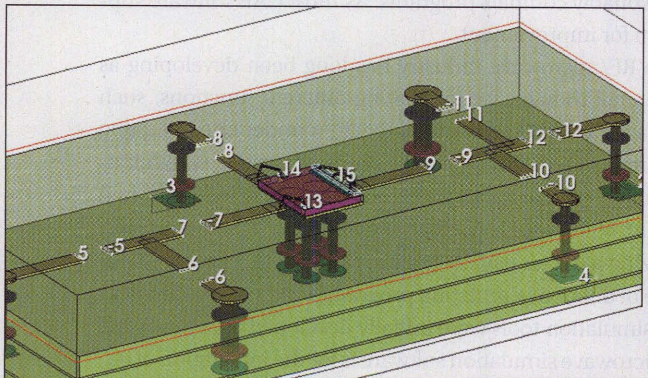

3. The Analyst 3D EM simulator and Microwave Office can combine for full circuit and EM cosimulation of complex circuit and package combinations. [Photo courtesy of AWR (www.awrcorp.com).]

This is not the first integration of EM simulation within the Microwave Office design flow, a process which has been evolving for years. However, this latest development makes EM simulation something less of an "esoteric" modeling tool for many designers, allowing them to automatically save a circuit layout (they are already working on) to an EM simulator within the Microwave Office for further analysis and model extraction. Rather than loading an EM simulator and creating an EM-specific design for analysis, the initial circuit design can also be analyzed in terms of EM behavior, with the results from the EM simulation automatically fed back to the circuit simulator for circuit tuning or optimization if necessary.

As an example of a commercial firm using this simulation integration, GreenPeak Technologies (Utrecht, The Netherlands) recently announced the development of a low-power communications controller integrated circuit (IC) for set-top video boxes and remote-control units. The fabless semiconductor company worked with AWR's AXIEM 3D planar EM software within the Microwave Office environment to perform RF circuit-board analysis, validation, and performance optimization while also minimizing design iterations. The firm developed 2.4-GHz radio circuits while also reducing their printed-circuit costs, integrating multiple components and performing EM simulations on single-layer and multilayer circuit boards.

In both ADS and Microwave Office, this growing trend of integration is enabling designers to more seamlessly use circuit and EM simulators together. The new features in Analyst, for example, allow layouts to be created according to EM variables and models with swept parameters. Layouts can make use of preconfigured layout cells with shapes that are controlled by EM parameters. Such cells, for example, can be used to place bond wires in MMIC designs. In support of Analyst, the Micro-

wave Office layout interface has been enhanced for working with the 3D structures commonly used in planar high-frequency circuit design.

Another leading supplier of simulation tools, Computer Simulation Technology (CST), has also enhanced the compatibility of their different simulation tools by integrating their CST BOARDCHECK™ EM simulator for checking electromagnetic-compatibility (EMC) and signal-integrity (SI) issues with circuit layouts. The CST BOARDCHECK software can work with a wide range of circuit layout formats, including CADENCE® ALLEGRO® and Mentor Graphics® Expedition® formats. The software allows engineers to import a layout file and then check the design according to selectable design rules to ensure proper EMC and SI performance for the circuit. CST BOARDCHECK generates a list of violations and enables an operator to highlight the problem sections of a circuit design. If necessary, the design file can be pulled into the CST MICROWAVE STUDIO® suite of simulation tools for a 3D full-wave EM simulation and analysis.

Even suppliers of somewhat dedicated simulation tools, such as MathWorks (www.mathworks.com) with their MATLAB® mathematical software, have worked towards a goal of making their programs easier to use, mainly through the development of highly focused "Toolboxes." MATLAB can be used with several of these toolboxes, including a Signal Processing Toolbox, a, RF Toolbox, and a Phased Array System Toolbox. The phased-array tools, for example, include algorithms for waveform generation, beamforming, target detection, and direction-of-arrival (DOA) estimations. Users can build a variety of different array geometries, including conformal arrays, uniform linear arrays (ULAs), and uniform rectangular arrays (URAs). The arrays can be based on stationary or moving platforms, and they can be simulated in terms of spatial, spectral, and temporal analysis.

For those still unwilling to invest in CAE software, the legacy AppCAD RF design software can be downloaded for free from www.hp.woodshot.com. It is written for personal computers with 32-b Windows operating systems and calculates S-parameters for circuit designs of interest and can show results in tabular form or as rectangular plots. It works with circuit files in .s2p form and analyzes S-parameter data for devices or circuits to obtain basic performance information, including gain, isolation, reflection loss, stability, and required matching impedances for a device. It can even load multiple .s2p files and make comparisons on different devices, or on one device under different sets or bias or temperature conditions. MWRF

JACK BROWNE | Technical Contributor

Measuring Power On RF/Microwave Signals

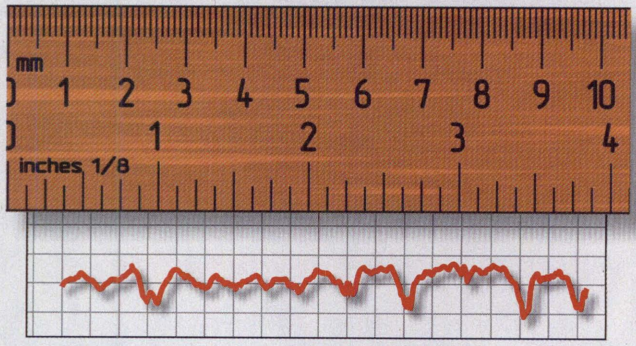

Accurate power measurements on RF/microwave signals require a thorough knowledge of the time-varying nature of the signals under test.

POWER MEASUREMENTS ARE not just for the laboratory; they are essential to the operation of many RF/microwave-based systems. Monitoring transmitted power from an antenna, for example, ensures that a communications system remains within its mandated power limits. Measuring received power in some systems can also help calibrate receiver sensitivity or identify the distance to a threat.

Fortunately, the various means of measuring power in RF/microwave systems have improved dramatically over the years, to a point where numerous semiconductor suppliers now offer integrated circuits (ICs) with power-measurement capability comparable to some benchtop instruments. To better appreciate current power-measurement solutions, it may help to review some fundamentals.

Power can be expensive to generate, and equally costly to maintain. Any power lost in a communications system can disrupt reception of a signal. Most systems have some means of measuring power to detect problems before they happen, and prevent operational interruptions.

From basic electricity, power is energy per unit time, defined in values of wattage, with 1 watt (W) equal to 1 Joule (J) per second. In terms of voltage, one volt (V) is equal to 1 W per ampere (A), or 1 V = 1 W/A. Power is often treated as the product of voltage and current, or P = V × I, although this quantity tends to vary in most systems as a function of time. Because power can change so much for some signals, measuring RF/microwave signal power requires test equipment suited to a specific type of signal.

In the lab, the trusted means of measuring the power levels of high-frequency signals is by means of a power meter and the appropriate power sensor. Three types of power sensors are used for RF/microwave power measurements: thermistor, thermocouple, and diode-based sensors. All three sensor types are appropriate for measuring the power levels of continuous-wave (CW) signals, but only diode sensors have the fast response times to accurately measure the time-varying power of pulsed and modulated signals.

Power sensors based on thermistors gauge the level of power from rises in temperature due to the heating effects of applied power on resistors. Thermistors are semiconductors with a negative temperature coefficient. They are a type of bolometer, a device in which resistance changes with temperature changes caused by applied RF/microwave power.

Because thermistors exhibit nonlinear resistance characteristics as a function of applied power, using them for power measurements is anything but straightforward. They are typically used with a bridge and some form of bias (AC or DC) to maintain a thermistor assembly or mount at a constant resistance with applied RF/microwave power. A power meter tuned to the sensor's changes in bias energy as a function of applied power is then used to calculate the RF/microwave power over a dynamic range enabled by the thermistor mount and its supporting electronics, including video amplifiers.

Thermocouple-based power sensors work on the principle that some dissimilar metals will produce a voltage due to temperature differences at the junctions of two of the metals. Known as the Peltier effect, a thermocouple formed of two appropriate metals can generate a small voltage in response to temperature rises. When current flows through a junction of a thermocouple formed of two of the proper metals, it induces a temperature rise in one of the metals in the junction, with heat absorbed by the other metal in the junction. The resulting flow of electrons or charge can be used as part of a power sensor. A power-sensor thermocouple is usually a loop or circuit made of two different metals, with two junctions. Heat is applied to one junction but not the other, with resulting electron flow towards the cold junction. Modern power sensors based on thermocouple

technology generally use thermocouples fabricated as semiconductor chips with the appropriate metal junctions.

Diode-based power sensors make use of a Schottky diode's capability of rectification, or converting an alternating current (AC) flowing alternately in two directions to a direct current (DC) signal flowing in only one direction. As diodes were fabricated on different materials, from early silicon devices to later gallium arsenide (GaAs) devices, the bandwidth and frequency capabilities of the devices increased, supporting power measurements through RF and microwave frequencies.

Of course, the rectification process has nonlinear voltage-current characteristics, so that various forms of linearization and temperature compensation are needed to perform accurate power measurements with diode-based sensors. But these correction factors can be measured for a specific diode type and stored in memory on board a sensor, such as electronically erasable programmable read-only memory (EEPROM).

Different types of RF/microwave power sensors are necessary because of differences in high-frequency signals. When measuring CW signals, all three types of power sensor would yield the same results. But that would not be the case for pulsed or modulated signals, especially signals with advanced digital modulation formats. The need for pulsed power measurements actually goes back as far as World War II, with the development of high-power radar systems and the magnetron and klystron vacuum electronic devices created for those radar systems. The wireless communications explosion that began in the early 1990s brought with it an expansion of complex modulation formats—notably those based on changing relationships of in-phase (I) and quadrature (Q) signal components, such as quadrature amplitude modulation (QAM). The crest factors for digital modulated signals can vary widely, requiring a power measurement solution with a very wide dynamic range.

Laboratory-grade power measurements have become possible sans power meters.

Many modern wireless communications systems transmit and receive signals that are noiselike or pseudorandom in nature, including Long-Term-Evolution (LTE) cellular communications systems, and making power measurements on such signals involves as much statistical analysis as signal capture. Because of the random nature of amplitude peaks for some of these signals, measuring power requires taking a large number of samples for a given communications channel. Next, statistical analysis must be performed to calculate the probability that power will be at or below a certain level in that channel during the sampled time period.

When measuring the peak envelope power (PEP) of the types of random or noiselike signals used in modern communications systems, a power-measurement solution must take on many of the traits of a digital sampling oscilloscope (DSO), such as sampling the input signal and making a large number of measurements in a short time in order to capture as many of the peak power levels as possible. Obviously, the greatest accuracy will come from a sensor capable of operating at fast sampling rates and performing as many measurements per second as possible.

Traditionally, power sensors have been one-half of a power-measurement solution, working with a compatible power meter. Power meters can be one of two types: a terminating power meter or a directional power meter. A terminating power meter is one in which the power sensor is used to measure the output power from a source but at the same time interrupting or terminating the flow of power. A directional power meter couples some of the power between a source and a load and can measure direct and reflected power levels with the aid of a directional coupler, without necessarily interrupting the power flow through the system under test.

The power meter can contribute to critical measurement linearity by providing a power reference signal for calibrating a connected power sensor. Standards organizations such as the National Institute of Standards and Technologies (NIST; www.nist.gov) in the United States specify traceable 0-dBm (1-mW) reference signal for calibrating power meter sensors. This reference is usually provided via a thermistor mount within the power-meter housing.

Modern power meters, especially when used with appropriate diode sensors for pulsed or PEP measurements on digitally modulated signals, can provide results in terms of detected power in addition to a host of other details about a signal. These include pulse width, pulse repetition frequency (PRF), and pulse repetition interval (PRI) for pulsed signals.

Traditions change, however, and laboratory-grade power measurements are now possible without the power meter, using a new breed of power sensor that uses a Universal-Serial-Bus (USB) connection to a personal computer and the computer for control and signal processing. These are available from a number of test-equipment manufacturers and even components suppliers, such as Mini-Circuits (www.minicircuits.com). A USB power sensor/meter typically incorporates a microprocessor-based controller in addition to the power-measurement circuitry, and uses a personal computer (PC) or laptop computer as the graphical user interface (GUI), computational capabilities, and memory storage. USB power sensors/meters are available for both CW and pulsed/modulated power measurements, over frequency ranges as wide as 10 MHz to 26.5 GHz.

One final note: This discussion has focused on laboratory power measurements. In many cases, power measurements may be part of the normal operation of an electronic device or system, and performed by an integrated circuit (IC) incorporating a diode detector, logarithmic-amplifier (logamp) detector, or root-mean-square (RMS) detector. Such ICs are often used for power monitoring and control in modern communications systems. They are capable of power measurements over wide dynamic ranges exceeding 60 dB at microwave frequencies. MWRF

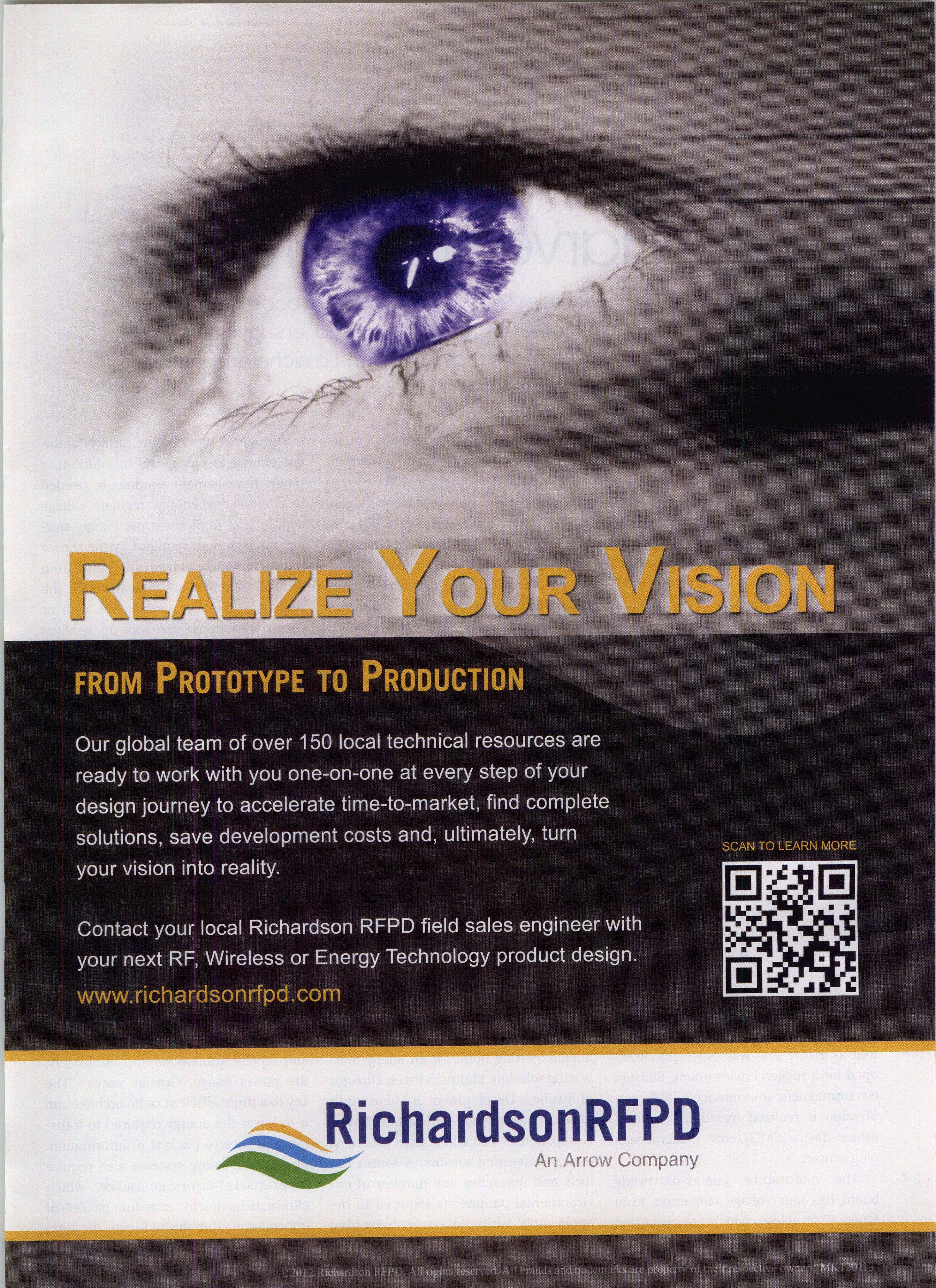
REALIZE YOUR VISION
FROM PROTOTYPE TO PRODUCTION
Our global team of over 150 local technical resources are ready to work with you one-on-one at every step of your design journey to accelerate time-to-market, find complete solutions, save development costs and, ultimately, turn your vision into reality.
Contact your local Richardson RFPD field sales engineer with your next RF, Wireless or Energy Technology product design.
www.richardsonrfpd.com
SCAN TO LEARN MORE
RichardsonRFPD
An Arrow Company
©2012 Richardson RFPD. All rights reserved. All brands and trademarks are property of their respective owners. MK120113

NANCY FRIEDRICH | Editor-in-Chief

Energy Harvesting Is Ready For The Big Time

As wireless-sensing components boost efficiency and other performance criteria, energy-harvesting solutions are moving beyond a niche and into everyday applications.

ENERGY IS ALL AROUND US—whether the sources are solar, electromagnetic, piezo-electric, or thermal. By "harvesting" even a fraction of this energy, engineering firms can deploy a growing number of sensing technologies for the greater good. Such sensing applications include wearable medical-monitoring devices, aircraft monitors, automotive monitors, and remote monitors for gas and energy sources. To help energy harvesting increase its global footprint, it is being applied to a growing number of solutions ranging from integrated circuits (ICs) to active and passive components.

Examples can be seen in the "Energy Harvesting Solution To Go" kit from Energy Micro (www.energymicro.com), Linear Technology (www.linear.com), and Würth Elektronik (www.we-online.com). The two basic parts of this kit are an energy-harvesting board and the Giant Gecko starter kit. Both elements contain passive components from Würth Elektronik. Würth's WE-EHPI power inductors derive their efficiency from the low ohmic resistance of each winding as well as a core that was especially developed for a rugged environment. Efficient electromagnetic-interference (EMI) suppression is realized by adding surface-mount-device (SMD) ferrite beads at each plug contact.

The multisource energy-harvesting board has four voltage converters from Linear Technology, which are optimized for the different energy sources. For instance, the LTC3588 is offered for alternating-current (AC) sources to 20 V, such as piezo-electric and inductive energy generators. The Giant Gecko Starter Kit contains the energy-friendly microcontroller, EFM32. (The EFM32GG990F1024 consumes only 200 μA/MHz in active mode.) It also includes an ARM Cortex M3 microcontroller unit (MCU) with 48-MHz speed, 1024-kByte Flash memory; 128-kByte random-access memory (RAM); Universal Serial Bus (USB), liquid-crystal-display (LCD) control, and more.

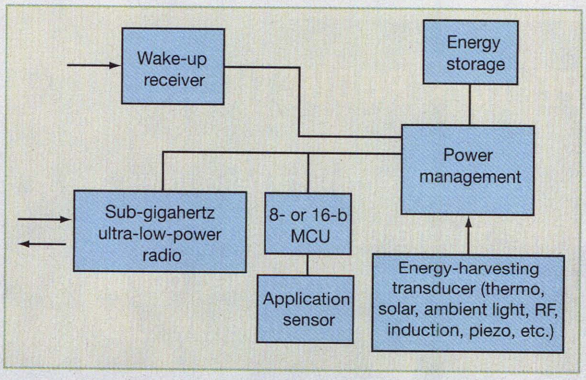

Shown is a basic energy-harvesting wireless sensor. (Courtesy of Microsemi)

With these components, this kit offers a solid starting point for an energy-harvesting solution. Mauricio Peres, Director of Business Development at Microsemi's (www.microsemi.com) Ultra Low Power Group, details the various aspects of most energy-harvesting sensors: A sensor detects and quantifies any number of environmental parameters required in the application, while an energy-harvesting transducer converts some form of ambient energy to electricity. In addition, a power-management module is needed to channel the energy, regulate voltage supply, and implement the energy-storage management required by the sensor node. An MCU manages the signal from the sensor and communicates with the radio link. Finally, a radio link with or without an RF wakeup receiver function is required at the sensor node **(see figure)**.

Energy-harvesting solutions place unique and stringent demands on all of their components—for example, by demanding very high power efficiency. Peres explains, "The microcontroller and radio must operate in low-power modes whenever possible in order to maximize the power-source lifetime."

There also is a need for microprocessors that can quickly move from deep sleep to idle and active modes, notes Mark Grazier, Low Power RF Product Marketing Manager, Wireless Connectivity Solutions at Texas Instruments (www.ti.com). This capability reduces current consumption between transmit and receive transitions and, ultimately, the power usage. Grazier states, "The key to a more efficient radio architecture is to lower the energy required to transmit and receive packets of information. Energy-harvesting systems also require lower packet-error-rate radios, which eliminate having to retransmit packets of information, thereby reducing the total

daily amount of energy provided by the energy harvester."

Issues also arise due to the makeup of most wireless-based sensor networks. For example, the majority of those networks rely on duty-cycling to conserve power and restrict the usage of radio space. This generates peaks in the sensor's current-consumption profile. Low peak current consumption in the radio transceiver reduces constraints on the wireless sensor's power supply.

Peres notes that these constraints are even more important for wireless sensors that run from harvested energy sources. "Often, energy-harvester transducers have higher output impedance than batteries," he explains. "The micro-power management layer between the energy transducer and the sensor converts the supply characteristics—including source impedance. Therefore, the low peak-current consumption in the radio transceiver reduces constraints on the power supply of the wireless sensor."

No matter their approach, the call for more efficiency is echoed by energy-harvesting systems of all types so that they can transmit data more often. Yet the extent to which each type of approach is actually harvesting energy varies greatly at this point. Solar harvesters are currently the most prevalent source of energy harvesting, as they operate between 25% to 50% efficiency per cm^2 **(see table)**. As they are more widely deployed, their cost will decrease per cm^2.

Energy-Harvesting Sources Today

Energy Source	Characteristics	Efficiency	Harvested Power
Light	Outdoor Indoor	10~24%	100 mW/cm^2 100 $\mu W/cm^2$
Thermal	Human Industrial	~0.1% ~3%	60 $\mu W/cm^2$ ~1-10 mW/cm^2
Vibration	~Hz–human ~kHz–machines	25~50%	~4 $\mu W/cm^3$ ~800 $\mu W/cm^3$
RF	GSM 900 MHz WiFi	~50%	0.1 $\mu W/cm^2$ 0.001 $\mu W/cm^2$

THE STATE OF RF ENERGY HARVESTING

For their part, RF energy-harvesting solutions are currently more a darling of the labs than a commonly used solution in their own right. A typical RF energy-harvesting system also looks quite different from its counterparts. John Bazinet, Product Line Manager, Power Products at Linear Technologies, provides a picture of a typical solution by dividing it into two parts: the receiver [tuned antenna, rectifier, storage element (capacitor), DC-DC converter] and transmitter [directed RF energy (PowerCast, for example) or ambient RF (WiFi, cellular, radio)]. Typically, he notes, RF energy systems have four components including a tuned antenna, an input storage element, power-management circuitry, and an output storage element.

Like their counterparts, RF energy-harvesting systems are in need of a number of performance enhancements. Bazinet explains that RF energy-harvesting solutions require or have required improvements to the following: directed RF energy source (not ambient), higher efficiency, ultra-low quiescent current, wider-input-range DC-DC, low-power MCUs, and RF transceivers. The microwave and RF industry in particular could better serve these systems by providing lower-power RF transceivers. Even if these demands are satisfied, however, Bazinet notes that directed RF energy systems are very niche. If they are using ambient RF, they have much less available energy compared to photovoltaic or thermal energy harvesters. RF energy harvesting also will have to overcome typical RF-centric issues, such as limited radio range due to building materials.

As RF energy harvesting finds its way, other energy-harvesting solutions are already broadening their reach. TI's Grazier summarizes, "Solar harvesters, over time, will continue to improve their efficiency so that they can expand their usage for both outdoor and indoor applications, where available lighting sources are available. Thermal harvesting solutions are also finding their way into building applications, where they can maximize the temperature differential between the outdoor and indoor temperature on a window. Thermal harvesting is also being used on body-worn devices. Overall, energy harvesting has a promising future as more and more products move from R&D development into mainstream products."

New solutions are starting to appear more steadily, reinforcing this point. The AS3953 NFiC (Near Field Communications interface Chip) from ams AG (www.ams.com) provides a high-data-rate interface between an NFC device, such as a smartphone, and any host microcontroller with a standard Serial Peripheral Interface (SPI). Because it operates on energy harvested from an NFC reader's RF emissions, the interface chip requires no external power source and a maximum of one external capacitor. The device can draw up to 5 mA of harvested energy from the external magnetic field. With an internal power-management circuit, it also can supply harvested energy to the application.

Another recent debut promises to solve the longstanding indoor-location-detection problem that has plagued emergency responders. ROHM (www.rohm.com), in collaboration with Ritsumeikan University and Information Services International - Dentsu, Ltd. (ISID), announced Guidepost Cell. Using the low-power IEEE 802.11-compliant wireless beacon protocol, this indoor location-detection infrastructure supplies precise positional data to smartphones and other mobile devices. The solution is powered by dye-sensitized solar cells (DSCs) that harvest energy from indoor lights. The DSCs promise to generate 48 $\mu W/cm^2$ under 1000 lux.

These are just two examples of myriad opportunities. The potential for these solutions knows no bounds—as long as they can achieve their efficiency goals and other performance metrics. Going forward, such solutions will increasingly be miniaturized to allow their use in more individual wellness and health applications. While ICs and active and passive components raise their performance while reining in efficiency, engineers will be taming the old demons of range, interference, and size. MWRF

IOANNIS PETROPOULOS
Research Assistant, PhD Candidate

STEVE M. R. JONES
Lecturer in Electronics and Telecommunications

KONSTANTINOS VOUDOURIS
Associate Professor on Wireless Telecommunications Systems

NIKOS ATHANASOPOULOS
Temporary Lecturer

RAED A. ABD-ALHAMEED
Professor of Electromagnetics and Radio Frequency Engineering

Phased Array Antenna Receives 4G Networks

Based on microstrip circuitry, commercial microwave components, and an advanced steering algorithm, this phased array helps connect 4G backhaul equipment.

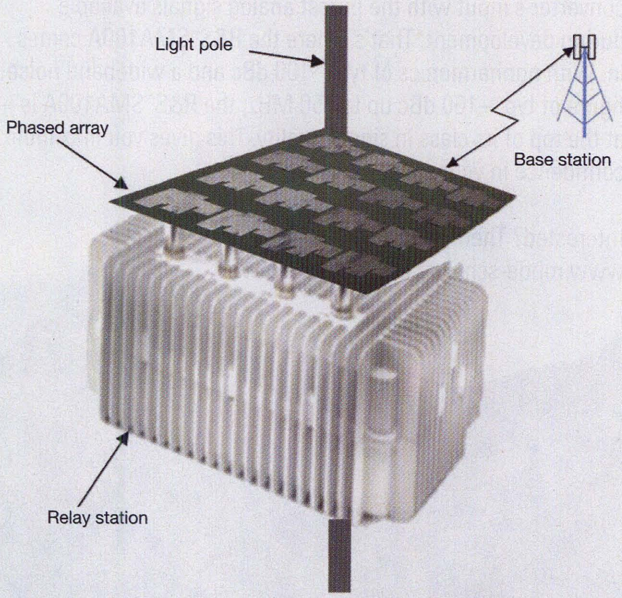

1. The proposed phased-array-antenna system can be used to connect cellular relay stations to 4G base stations.

FOURTH-GENERATION (4G) cellular networks rely on many key components to provide the bandwidth and coverage that wireless service providers and their customers expect. One of these components is a phased-array antenna system with beam-steering capabilities that supports communications between relay stations and base stations. The proposed antenna design operates at 3.42 GHz and features 21.17 dBi gain and 424 MHz bandwidth, employing a least-mean-square (LMS) algorithm to provide a steerable mainlobe response with desired nulls and sidelobe suppression.

Phased-array antennas have been used in a wide range of applications, from military systems to commercial cellular communications networks. They are often used in wireless systems to steer signals from base stations to desired destinations while creating nulls to suppress interference.[1,2] A number of algorithms have been developed and proposed for beam-steering purposes, including LMS, the constant modulus algorithm (CMA), and the recursive least-squares (RLS) algorithm.[3,4] These algorithms are characterized by different complexity levels and convergence times.[5,6] In addition, a wide range of antenna shapes and configurations have been proposed for use in phase-array systems for achieving bandwidth and gain enhancements.[7,8]

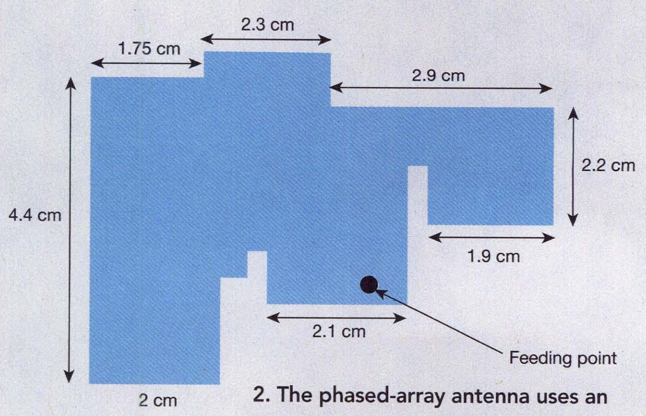

2. The phased-array antenna uses an E-shaped configuration to achieve high gain.

The proposed phased-array system was developed for use in a prototype WiMAX relay station[9] to establish a backhaul link between a relay station and base station. It includes a 4 x 4 microstrip-based modified E-shaped patch array[10] based on a

stacked geometry.[11] In addition, a beam-forming circuit was designed and fabricated for power division, signal processing, and array excitation. An LMS algorithm was used to properly assign phases and amplitudes to each radiating element and thus steer the radiation mainlobe to a base station.

Version 14 of the Mathcad simulation software from Parametric Technology Corp. (www.ptc.com) was used to generate the LMS algorithm. When the required element phases and amplitudes are obtained, they are applied to the array simulations as well as to the fabricated prototype to derive simulated and actual radiation patterns. **Figure 1** shows the application of the proposed phase-array antenna design.

Figure 2 shows the dimensions for the 4 x 4 antenna array. The modified E-shaped elements are placed on a foam substrate with relative dielectric constant ($\varepsilon_r = 1$) with height, h, of 0.5 cm. The foam substrate is then placed on RO3006 circuit-board material from Rogers Corp. (www.rogerscorp.com) with $\varepsilon_r = 6.15$ and h = 1.28 mm. Next, the RO3006 substrate is mounted on a ground plane of 35-µm-thick copper. **Figure 3** shows the structure of the array, in which the modified E-shaped elements are coaxial fed. The two circuit substrates are used for enhanced bandwidth and gain.[10] **Figure 4(a)** depicts the phased array for simulation purposes, while **Fig. 4(b)** shows the fabricated array.

Figure 5 denotes the edge-to-edge distance between elements. The center-to-center distance between two adjacent elements is $0.8\lambda_0$, where λ_0 is the free-space wavelength. This value was chosen to produce a radiation pattern with low sidelobe levels and to prevent grating lobes.[12] **Figure 6** provides the simulated and measured S_{11} response for element "1" in **Fig. 4(a)**. For the experimental S_{11} measurements of element 1, all other elements are terminated using 50-Ω impedance to eliminate mutual coupling effects.

The two S_{11} curves of **Fig. 6** are in close agreement, verifying that the proposed antenna array operates at 3.418 GHz with bandwidth of 424 MHz (S_{11} <–10 dB) or 12.4%. The S_{11} measurements were obtained using a model MS2036A vector network analyzer (VNA) from Anritsu Co. (www.anritsu.com).

Figure 7 offers simulated and measured radiation patterns [for the θ angle and XYZ planes denoted in **Fig. 4(a)**] for the 16-element array, with measurements performed in an anechoic cham-

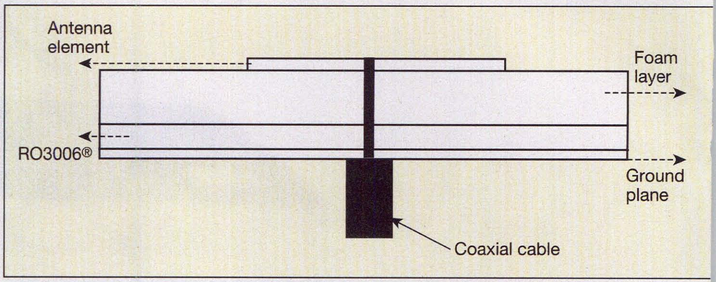

3. This cross-sectional view shows how a foam layer is used with a commercial circuit-board layer in the antenna design.

Comparing the proposed array with a commercial backhaul antenna

Antenna model	Gain (dBi)	HPBW for YZ plane (deg.)	HPBW for XZ plane (deg.)	Bandwidth (MHz)
4×4 phased array	21.17	14.44	14.25	424
Commercial backhaul antenna (ref.) (TSWL315177)	18	15	15	500

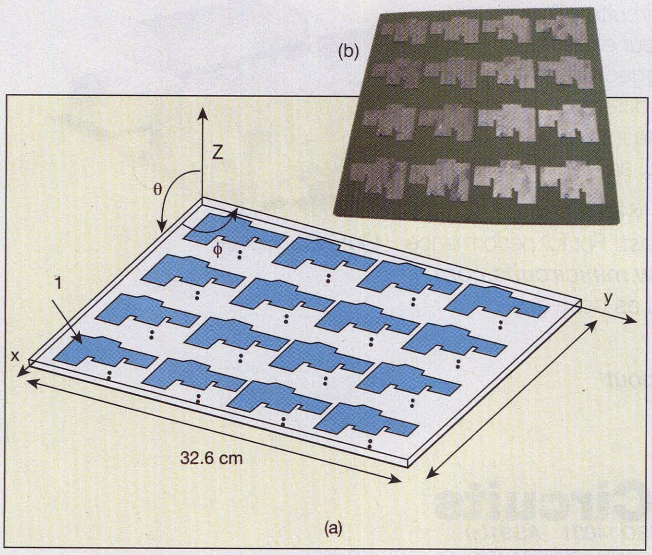

4. The phased-array antenna design was evaluated in terms of (a) software simulations and by means of measurements of a fabricated design (b) in an anechoic chamber.

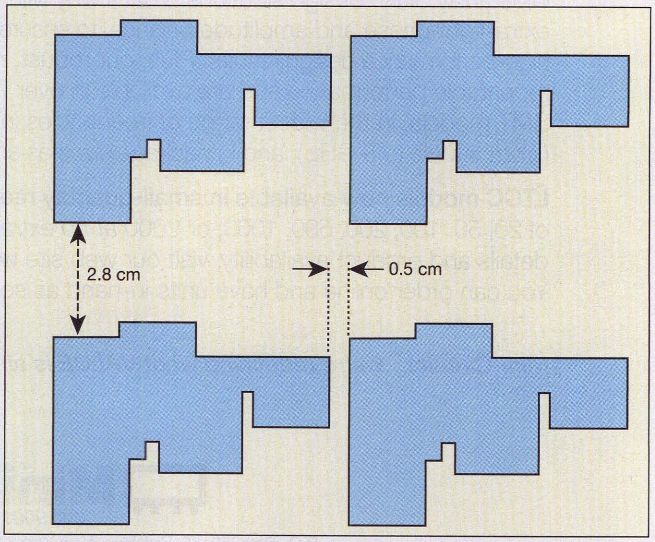

5. This diagram shows the inter-element spacing in the 4 x 4 antenna array.

6GHz Mixer Delivers 32dBm OIP3

LTC5544

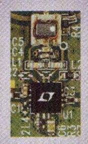

Excellent Performance at 5.8GHz

IIP3 = 25.8dBm
Conversion Gain = 6.4dB
NF = 12.8dB

OR

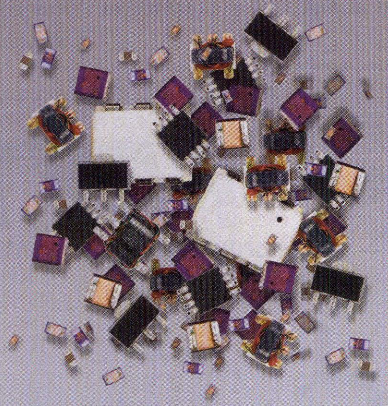

Take Your Chances

High Level Integration with LO Buffer, IF Amplifier and Balun Transformer

With its high level of integration, the LTC®5544 brings an unprecedented level of compactness, ease of use and outstanding performance that you can count on.

Features

- 4 to 6GHz Frequency Range
- 32.2dBm OIP3 at 5.8GHz
- 14.6dBm P1dB
- 2dBm LO Drive
- 50Ω Matched Single-Ended RF and LO Inputs
- Outstanding Blocking Performance
- IF Output up to 1GHz

Wideband Conversion Gain, IIP3, NF at 240MHz IF

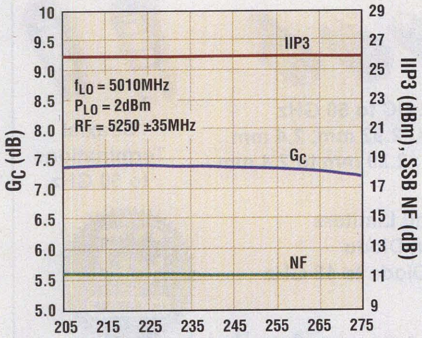

Info & Free Samples

www.linear.com/product/LTC5544
1-800-4-LINEAR

LINEAR TECHNOLOGY

ber. The currents that excite each radiation element have the same amplitude and phase. The radiation pattern that results has a mainlobe at θ = 0 deg. and sidelobe levels of less than 10 dBi. The radiation patterns depicted in **Fig. 7** were obtained at 3.418 GHz.

The **table** compares the proposed array with a commercial antenna at 3.5 GHz in terms of gain, bandwidth, and half-power beamwidth (HPBW) in the YZ and XZ planes. The array's enhanced gain and low HPBW are suitable for use in point-to-point communications applications.

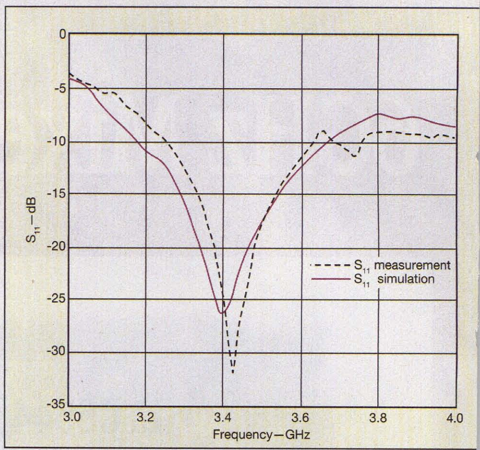

6. These plots compare the simulated and measured S_{11} responses for the E-shaped antenna.

The array satisfies the requirements of the IEEE 802.16j protocol for WiMAX, and can be used for achieving a backhaul link between a relay station and a base station.

The beam-forming module is a planar design with two substrates, including two eight-way power dividers. It was simulated and optimized with the help of the Advanced Design System (ADS2009) simulation software from Agilent Technologies (www.agilent.com) and then fabricated. It includes Wilkinson power dividers,[13] 100-Ω chip resistors, commercial digital attenuators [model HMC629LP4 from Hittite Microwave Corp. (www.hittite.com)], and

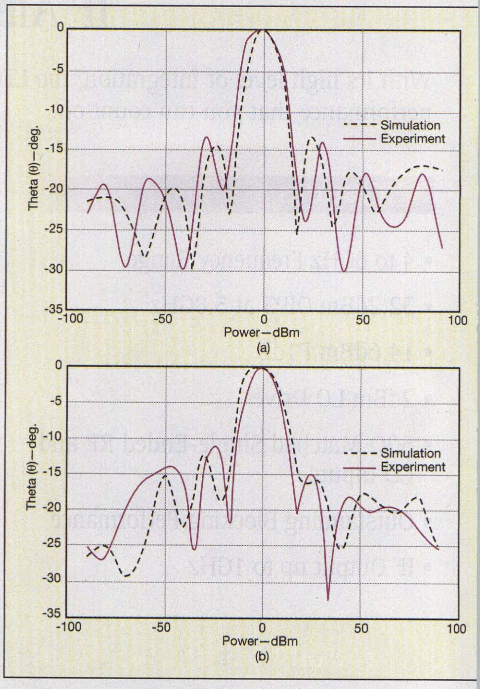

7. These radiation patterns are shown in terms of θ for (a) ϕ = 0 deg. (in the XZ plane) and (b) ϕ = 90 deg. (in the YZ plane).

HIGH POWER

5 - 500 WATTS PRODUCTS

POWER DIVIDERS

RoHS

Model #	Frequency (MHz)	Insertion Loss (dB) [Typ./Max.] ◊	Amplitude Unbalance (dB) [Typ./Max.]	Phase Unbalance (Deg.) [Typ./Max.]	Isolation (dB) [Typ./Min.]	VSWR (Typ)	Input Power (Watts) [Max.] ▫	Package
2-WAY								
CSBK260S	20 - 600	0.28 / 0.4	0.05 / 0.4	0.8 / 3	25 / 20	1.15:1	50	377
DSK-729S	800 - 2200	0.5 / 0.8	0.05 / 0.4	1 / 2	25 / 20	1.3:1	10	215
DSK-H3N	800 - 2400	0.5 / 0.8	0.25 / 0.5	1 / 4	23 / 18	1.5:1	30	220
P2D100800	1000 - 8000	0.6 / 1.1	0.05 / 0.2	1 / 2	28 / 22	1.2:1	5	329
DSK100800	1000 - 8000	0.6 / 1.1	0.05 / 0.2	1 / 2	28 / 22	1.2:1	20	330
DHK-H1N	1700 - 2200	0.3 / 0.4	0.1 / 0.3	1 / 3	20 / 18	1.3:1	100	220
P2D180900L	1800 - 9000	0.4 / 0.8	0.05 / 0.2	1 / 2	27 / 23	1.2:1	5	331
DSK180900	1800 - 9000	0.4 / 0.8	0.05 / 0.2	1 / 2	27 / 23	1.2:1	20	330
3-WAY								
S3D1723	1700 - 2300	0.2 / 0.35	0.3 / 0.6	2 / 3	22 / 16	1.3:1	5	316

◊ In excess of theoretical split loss of 3.0 dB
▫ With matched operating conditions

HYBRIDS

RoHS

Model #	Frequency (MHz)	Insertion Loss (dB) [Typ./Max.] ◊	Amplitude Unbalance (dB) [Typ./Max.]	Phase Unbalance (Deg.) [Typ./Max.]	Isolation (dB) [Typ./Min.]	VSWR (Typ)	Input Power (Watts) [Max.]	Package
90°								
DQS-30-90	30 - 90	0.3 / 0.6	0.8 / 1.2	1 / 3	23 / 18	1.35:1	25	102SLF
DQS-3-11-10	30 - 110	0.5 / 0.8	0.6 / 0.9	1 / 3	30 / 20	1.30:1	10	102SLF
DQS-30-450	30 - 450	1.2 / 1.7	1 / 1.5	4 / 6	23 / 18	1.40:1	5	102SLF
CSDK3100S	30 - 1000	0.8 / 1.2	0.05 / 0.2	0.2 / 3	25 / 18	1.15:1	50	378
DQS-118-174	118 - 174	0.3 / 0.6	0.4 / 1	1 / 3	23 / 18	1.35:1	25	102SLF
DQK80300	800 - 3000	0.2 / 0.4	0.5 / 0.8	2 / 5	20 / 18	1.30:1	40	113LF
MSQ80300	800 - 3000	0.2 / 0.4	0.5 / 0.8	2 / 5	20 / 18	1.30:1	40	325
DQK100800	1000 - 8000	0.8 / 1.6	1 / 1.6	1 / 4	22 / 20	1.20:1	40	326
MSQ100800	1000 - 8000	0.8 / 1.6	1 / 1.6	1 / 4	22 / 20	1.20:1	40	346
MSQ-8012	800 - 1200	0.2 / 0.3	0.2 / 0.4	2 / 3	22 / 18	1.20:1	50	226
180° (4-PORTS)								
DJS-345	30 - 450	0.75 / 1.2	0.3 / 0.8	2.5 / 4	23 / 18	1.25:1	5	301LF-1

◊ In excess of theoretical coupling loss of 3.0 dB

COUPLERS

RoHS

Model #	Frequency (MHz)	Coupling (dB) [Nom]	Coupling Flatness (dB)	Mainline Loss (dB) [Typ./Max.]	Directivity (dB) [Typ./Min.]	Input Power (Watts) [Max.] ▫	Package
KDS-30-30	30 - 512	27.5 ±0.8	±0.75	0.2 / 0.28	23 / 15	50	255 *
KFK-10-1200	10 - 1200	40 ±0.75	±1.0	0.4 / 0.5	22 / 15	150	376
KBS-10-225	225 - 400	10.5 ±1.0	±0.5	0.6 / 0.7	25 / 18	50	255 *
KDS-20-225	225 - 400	20 ±1.0	±0.5	0.2 / 0.4	25 / 18	50	255 *
KBK-10-225N	225 - 400	10.5 ±1.0	±0.5	0.6 / 0.7	25 / 18	50	110N *
KDK-20-225N	225 - 400	20 ±1.0	±0.5	0.2 / 0.4	25 / 18	50	110N *
KEK-704H	850 - 960	30 ±0.75	±0.25	0.08 / 0.2	38 / 30	500	207
SCS100800-10	1000 - 8000	10.5 ±1.5	±2.0	1.2 / 1.8	8 / 5	25	361
KBK100800-10	1000 - 8000	10.5 ±1.5	±2.0	1.2 / 1.8	8 / 5	25	322
SCS100800-16	1000 - 7800	16.8 ±1.5	±2.8	0.7 / 1	14 / 5	25	321
KDK100800-16	1000 - 7800	16.8 ±1.5	±2.8	0.7 / 1	14 / 5	25	322
SCS100800-20	1000 - 7800	20.5 ±2.0	±2.0	0.45 / 0.75	12 / 5	25	321
KDK100800-20	1000 - 7800	20.5 ±2.0	±2.0	0.45 / 0.75	14 / 5	25	322

* Add suffix - LF to the part number for RoHS compliant version.
▫ With matched operating conditions

Unless noted, products are RoHS compliant.

SYNERGY®
MICROWAVE CORPORATION

Phone: (973) 881-8800 | Fax: (973) 881-8361
E-mail: sales@synergymwave.com | Web: www.synergymwave.com
Mail: 201 McLean Boulevard, Paterson, NJ 07504

The Signal Source Noise Control & Signal Processing Experts.

digital phase shifters (model HMC648LP6 from Hittite). The microstrip circuit was fabricated on RO4003 circuit-board material from Rogers Corp. with relative permittivity of 3.55 and thickness of 0.508 mm. A second RO4003 board is placed beneath the first substrate, on the top of which the ground plane is positioned.

The amplitudes and phases of each radiating element are produced as a result of digital inputs; the resulting signal amplitudes and phases are assigned to specific attenuators and phase shifters, respectively. **Figure 8(c)** provides a cross-sectional view of the proposed beam-forming circuit, with the two substrates held together via holes. The length of the microstrip line on the top part of the circuit is an integer multiple of $\lambda_0(f_0 = 3.5$ GHz), while the width is defined using the formula in ref. 14. **Figure 9** shows the layout of the beam-forming circuit design. The simulated and measured S_{11} performance of the beam-forming circuit is shown in **Fig. 10**.

The S_{11} measurements on the circuit were performed with the Anritsu MS2036A VNA. The beam-forming circuit operates from 3.3 to 4.0 GHz, a 700-MHz bandwidth with S_{11} less than –10 dB. The minimum experimental value of S_{11} is –27.112 dB at 3.38 GHz. As **Fig. 10** shows, the measured and simulated responses are in good agreement, with differences resulting from ohmic, dielectric, and conductor losses in addition to microstrip line coupling. The beam-forming network thus covers the frequency range of the antenna array developed previously, making it a good match for the combined design. **Figure 11** shows the antenna array togeth-

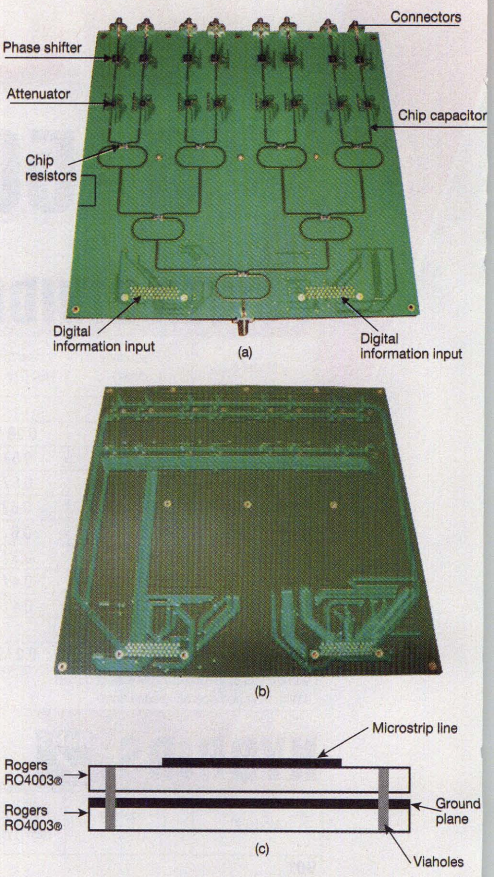

8. The two photographs shows the top view (a) and bottom view (b) of the beam-forming unit, while the cross-sectional diagram (c) shows the stacked circuit substrates.

er with the beam-forming circuit.

The test signals are generated by a model MXG N5182A commercial signal generator from Agilent Technologies. They are guided to a commercial two-way SMA power divider with frequency range of DC to 18 GHz, which splits the test signals into two equal outputs. These signals are then sent to the beam-forming module. Within the module, the test signals are further divided into 16 microstrip lines which feed each of the 16 antenna array elements. Commercial phase shifters and attenuators are incorporated to achieve the desired radiation pattern. The beam-forming circuit and the array are connected through SMA cables. In addition, the power divider is connected to the beam-forming circuit via SMA cables. All measurements are performed in an anechoic chamber.

The antenna array's radiation pattern can be shaped through the application of the LMS algorithm.[15] It is a gradient-based algorithm which performs iterative operations to minimize the mean square error between the array output and a reference signal. The algorithm was developed and operates according to Version 14 of the Mathcad software. A set of requirements is first defined regarding radiation pattern shape. The algorithm is then executed to yield the amplitude and phase for each patch element to create the required radiation pattern.

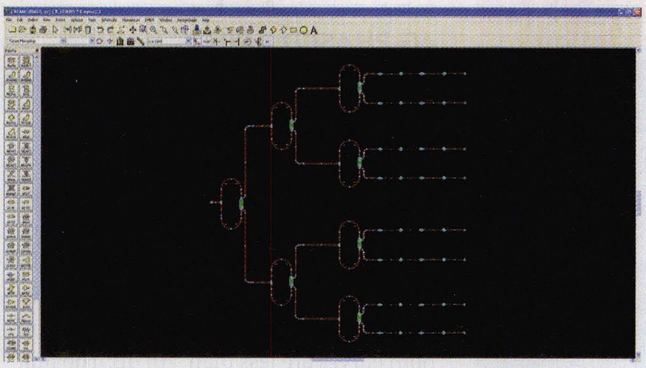

9. This layout shows the microstrip circuit pattern for the beam-forming module.

Three beam-forming scenarios were considered for the proposed design. In the first scenario, the conditions included a maximum level at (–18 deg., 0 deg.), a null at (34 deg., 0 deg.), and sidelobe level (SLL) of less than –10 dB. The specific quantized values of amplitude and phase[17,18] required for this scenario are:

α= [0, –3, –6, –9, –12, –15, –18, –21, –24, –27, –30, –33, –36, –39, –42, –45] in dB and
β = [0, 5.625, 11.250... 354.375] in deg. with step of 5.625 deg.

The algorithm gives the following results in terms of amplitude and phase:

See Eqs. 1(a) and (b), p. 61.

These results are assigned to each radiating element for the purpose of measurements and simulations, with the simulated and experimental radiation patterns for the phased array in this scenario shown in **Fig. 12**. The requirements of the scenario have been met. The sidelobe levels on both curves are less than –10 dB. The null angle is 34 deg., while the angle of maximum response is –18 deg. The deviations in the experimental results can be attributed to ohmic, dielectric, and conductor losses; line coupling; and imbalance phenomena of the attenuators and phase shifters. Imbalance phenomena are relevant to errors in attenuation and phase assignment to excitation currents due to circuit losses. In spite of these imbalances and losses, the radiation pattern exhibits the desired form.

In the second scenario, the maximum is at (22 deg., 0 deg.), the null is at (80 deg., 0 deg.), and the SLL is less than –10 dB. The procedure used in the first scenario is followed, with the LMS algorithm yielding the following results:

See Eqs. 2(a) and (b), p. 61.

The simulated and experimental response curves for this scenario are shown in **Fig. 13**. The simulation response meets the requirements except for the maximum of the mainlobe, where the simulation curve presents

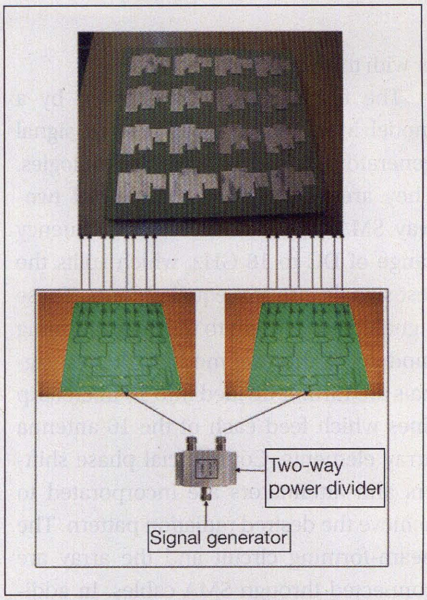

11. This diagram shows how test signals were created for evaluating the phased-array antenna system.

θ_{max} = 20 deg. The measured response shows the mainlobe maximum at θ_{max} = 18 deg. This deviation may be the result of power divider and cable losses in the experimental setup.

In the third scenario, the maximum is at (–24 deg., 0 deg.), the null is at (20 deg., 0 deg.), and the SLL is less than –10 dB. For this scenario, the LMS algorithm yields the following results:

See Eqs. 3(a) and (b), p. 61.

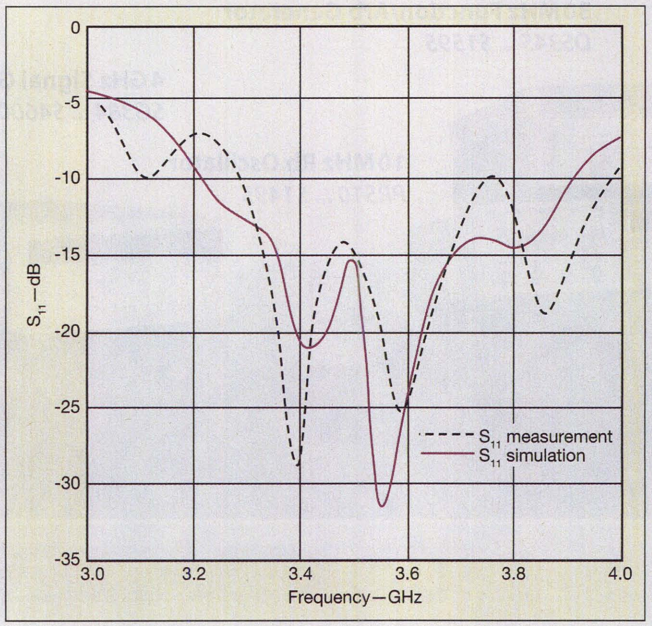

In this case the curves produced by simulation and experiment satisfy the requirements set by scenario (c). Blue and green lines coincide at high degree. The differences between simulation and experiment are probably caused by

10. This plot shows the simulated and measured S_{11} responses for the eight-way Wilkinson power divider.

power-distribution losses in the beam-forming circuit.

In summary, the simulated and measured results for the phased-array antenna system and its beam-forming network were in close agreement in most cases. The phased-array module—a compact 4 x 4 array with better than 21dBi gain across a 424MHz bandwidth at 3.5 GHz—was designed and simulated with the aid of the HFSS (Version 11) electromagnetic (EM) simulation software from Ansys (www.ansys.com). The proposed array was compared to a commercial array, revealing that it exhibits higher gain over a narrower beamwidth. MWRF

IOANNIS PETROPOULOS, Research Assistant, PhD Candidate, Wireless Communication and e-Applications Research Group, Department of Electronics, Technological Educational Institute of Athens, Athens, Greece; 00302105385367, FAX: 2105385304, e-mail: ipetro@teiath.gr. **NIKOS ATHANASOPOULOS**, Temporary Lecturer, Department of Electronics, Technological Educational Institute of Athens, Athens, Greece; 00302105385367, FAX: 2105385304, e-mail: nathan@teiath.gr. **KONSTANTINOS VOUDOURIS**, Associate Professor on Wireless Telecommunications Systems, Department of Electronics, Technological Educational Institute of Athens, Athens, Greece; 00302105385367, FAX: 2105385304, e-mail: kvoud@teiath.gr. **RAED A. ABD-ALHAMEED**, Professor of Electromagnetics and Radio Frequency Engineering, School of Engineering, Design, and Technology, University of Bradford, Richmond Road, Bradford, BD7 1DP, United Kingdom; (+44) (0) 1274 23 4542, e-mail: r.a.a.abd@bradford.ac.uk. **STEVE M.R. JONES**, Lecturer in Electronics and Telecommunications, School of Engineering, Design, and Technology, University of Bradford, Richmond Road, Bradford, BD7 1DP, United Kingdom; (+44) (0) 1274 23 4542, e-mail: s.m.r.jones@bradford.ac.uk.

REFERENCES

1. Lal C. Godara, "Application of Antenna Arrays to Mobile Communications," Proceeding of the IEEE, Vol. 85, No. 8, August 1997, pp. 1195-1234.
2. Salvatore Bellofiore, Jeffrey Foutz, Constantine A. Balanis, and Andreas S. Spanias, "Smart-Antenna System for Mobile Communication Networks Part 2: Beamforming and Network Throughput," IEEE Antennas and Propagation Magazine, Vol. 44, No. 4, August 2002.
3. S. Das, "Smart antenna design for wireless communication using adaptive beam-forming approach," TENCON 2008 - 2008 IEEE Region 10 Conference, November 19-21, 2008, pp. 1-5.
4. Reeta Gaokar and Dr. Alice Cheeran, "Performance Analysis of Beamforming Algorithms," International Journal of Electronics & Communication Technology, Vol 2, No. 1, 2011.
5. Y.H. Chen, Jun-Horng Chen, Peng Chia Hsien, Dau-Chyrh Chang, and Jung-Hao Huang, "Performance evaluation of mobile WiMAX beam forming network implemented by RF digital step attenuators," 14th European Wireless Conference, June 22-25, 2008, pp. 1-6.
6. J.M. Samhan, R.M. Shubair, and M.A. Al-Qutayri, "Design and Implementation of an Adaptive Smart Antenna System," Innovations in Information Technology, November 2006, pp. 1-4.
7. Kainan Zhao, Fei Liu, Wenhua Chen, and Zhenghe Feng, "Bandwidth-enhanced design of a planar

$$\alpha = \begin{bmatrix} -6 & 0 & 0 & 0 \\ -3 & -6 & -6 & -6 \\ -6 & -6 & -6 & -3 \\ 0 & 0 & 0 & -6 \end{bmatrix} \text{ in dB} \quad (1a)$$

$$\beta = \begin{bmatrix} 298.2 & 275.73 & 298.2 & 191.8 \\ 258.82 & 16.85 & 135 & 140.67 \\ 90 & 163.14 & 315.05 & 208.2 \\ 123.76 & 0 & 326.35 & 315.05 \end{bmatrix} \text{ in deg.} \quad (1b)$$

switched parasitic array antenna," 2010 International Conference on Microwave and Millimeter Wave Technology (ICMMT), May 8-11, 2010, pp. 1129-1131.
8. Qinjiang Rao and T.A. Denidini, "Electromagnetically coupling fed broadband low profile microstrip antenna array," 2007 IEEE Antennas and Propagation Society International Symposium, June 9-15, 2007, pp. 893-896.
9. V. Genc, S. Murphy, Y. Yu, and J. Murphy, "IEEE 802.16j Relay-based Wireless Access Networks: An Overview," IEEE Wireless Communications Magazine, Special Issue on Recent Advances and Evolution of WLAN and WMAN Standards, 2008.
10. A.C.O. Pedra, G. Bulla, P. Serafin, C.R. Fernandez, G. Monser, and A.A.A. de Salles, "Bandwidth and size optimization of a wide-band E-shaped patch antenna," SBMO/IEEE MTT-S International Microwave and Optoelectronics Conference, IMOC 2007., October 29 to November 1 2007, pp. 422-426.
11. D. Yoharaaj, D. Azmir, Raja Syamsul, and Ismail, Alyani, "A New Approach for Bandwidth Enhancement Technique in Microstrip Antenna for Wireless Applications," RF and Microwave Conference, September 2006, pp. 205-209.
12. R. Jedlicka, M. Poe, and K. Carver, "Measured mutual coupling between microstrip antennas," IEEE Transactions on Antennas & Propagation, Vol. 29, No. 1, January 1981, pp. 147-149.
13. E.J. Wilkinson, "An N-way hybrid power divider," IRE Transactions on Microwave Theory & Techniques, Vol. 8, January 1960, pp. 116-118.
14. E.O. Hammerstad, "Equations for microstrip circuit design," in Proceedings of the 5th European Microwave Conference, Hamburg, Germany, September

$$\alpha = \begin{bmatrix} -3 & 0 & 0 & 0 \\ -6 & -6 & -6 & -3 \\ -6 & -6 & -6 & -6 \\ 0 & 0 & 0 & -3 \end{bmatrix} \text{ in dB} \quad (2a)$$

$$\beta = \begin{bmatrix} 236.2 & 264.3 & 179.9 & 118.0 \\ 33.7 & 168.7 & 112.4 & 354.3 \\ 112.4 & 337.4 & 309.3 & 78.7 \\ 0 & 286.4 & 213.7 & 241.7 \end{bmatrix} \text{ in deg.} \quad (2b)$$

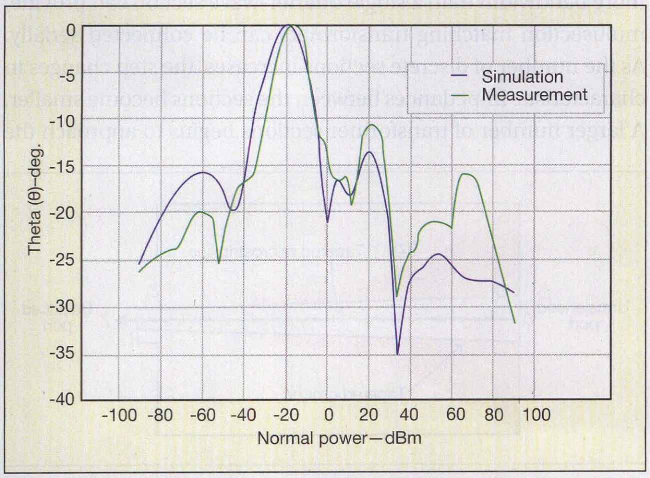

12. These curves show the simulated and measured radiation patterns for the phased-array antenna system in the first scenario.

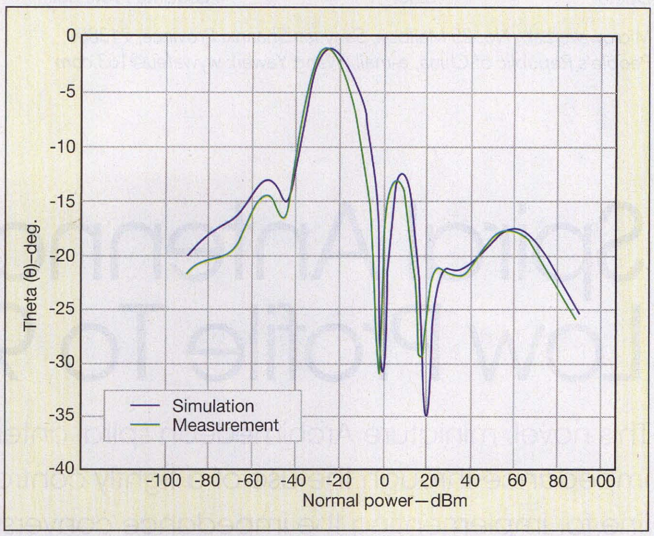

14. These curves show the simulated and measured radiation patterns for the phased-array antenna system in the third scenario.

1975, pp. 268-272.
15. Qun Yang, Xiang-yu Cao, Yao Xu, and Xiao-fei Xu, "Performance of LMS algorithm in smart antenna," 2010 International Conference on Microwave and Millimeter Wave Technology (ICMMT), May 8-11, 2010, pp. 1372-1375.
16. C.A. Balanis, Antenna Theory: Analysis and Design, Wiley, New York, 1997.
17. Data sheet for model HMC629LP4, Hittite Microwave Corp., Chelmsford, MA, 2008, www.hittite.com.
18. Data sheet for model HMC648LP6, Hittite Microwave Corp., Chelmsford, MA, 2008, www.hittite.com.

$$\alpha = \begin{bmatrix} -12 & 0 & 0 & 0 \\ -3 & 0 & 0 & 0 \\ 0 & 0 & 0 & -3 \\ 0 & 0 & 0 & -12 \end{bmatrix} \text{ in dB} \quad (3a)$$

$$\beta = \begin{bmatrix} 315.05 & 303.8 & 236.35 & 270.05 \\ 129.3 & 11.25 & 118.14 & 219.43 \\ 129.38 & 151.91 & 112.52 & 174.43 \\ 0 & 354.48 & 354.48 & 337.58 \end{bmatrix} \text{ in deg.} \quad (3b)$$

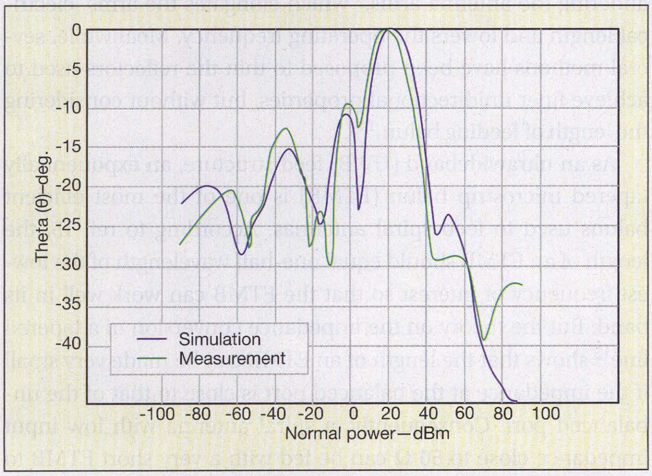

13. These curves show the simulated and measured radiation patterns for the phased-array antenna system in the second scenario.

WANG YAWEI Doctor
WANG GUANGMING Professor
LIANG JIANGANG Associate Professor

Microwave Lab, No. 25 Mailbox, Sanyuan Shaanxi Province, 713800, People's Republic of China, e-mail (Wang Yawei): wywafeu@163.com

Spiral Antenna Cuts Low Profile To 9.4 GHz

This novel, miniature Archimedean spiral antenna achieves a low input impedance through the use of a tightly controlled exponentially tapered spiral line for implementing the impedance conversion.

ARCHIMEDEAN SPIRAL antennas (ARSAs) are attractive for a variety of RF and microwave applications. They have been used for circularly polarized broadband communications and can be easily flush mounted in many systems. They are characterized by stable input impedance and radiation characteristics over several octaves. The size of these antennas is determined by the lowest operating frequency, the depth of the cavity, and the length of the feed balun. Many studies have been performed to overcome these size limitations by reducing the aperture[1-5] and/or by decreasing the profile.[6-14] This current report will show how the use of a very short exponentially tapered microstrip balun can lead to a low-profile antenna with impressive bandwidth of 0.8 to 9.4 GHz.

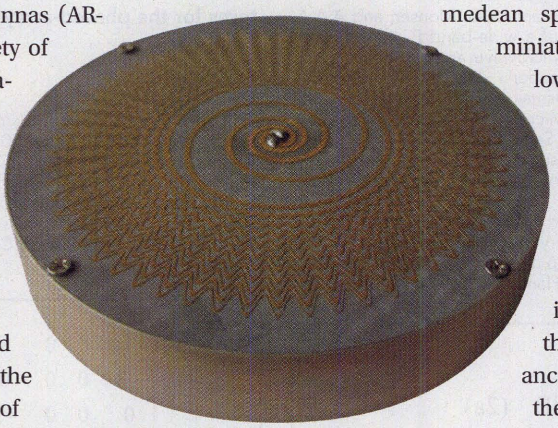

1. This photograph shows the exponential-Archimedean spiral antenna (EARSA) with highly miniaturized aperture.

An efficient way to miniaturize the antenna aperture is by meandering the antenna arms,[5] which elongates the arms' electrical length and lowers the operating frequency. Meanwhile, several methods have been proposed to thin the reflectors used to achieve finer unidirectional properties, but without considering the length of feeding balun.[14]

As an ultrawideband (UWB) feed structure, an exponentially tapered microstrip balun (ETMB) is one of the most efficient baluns used to feed spiral antennas. According to ref. 15, the length of an ETMB should equal one-half wavelength of the lowest frequency of interest so that the ETMB can work well in its band. But the theory on the impedance conversion of a tapered line[15] shows that the length of an ETMB can be made very small if the impedance at the balanced port is close to that of the unbalanced port. Consequently, a spiral antenna with low input impedance close to 50 Ω can be fed with a very short ETMB to achieve a very low profile.

To demonstrate this approach, an exponential Archimedean spiral antenna (EARSA) with highly miniaturized aperture and extremely low profile will be detailed in this report. The antenna is constructed in two parts: a sinuous meander Archimedean spiral line used to miniaturize the aperture and a controlled-width exponential spiral line that helps minimize the input impedance. Theoretically, when the ratio of the EARSA's input impedance to 50 Ω is equal to unity, the length of the ETMB can be arbitrarily small and its impedance conversion characteristic unchanged, making possible an EARSA with truly low profile.

By transmission-line theory,[15] a quarter-wavelength transformer offers a simple means of matching any real load impedance to any line impedance. A quarter-wave transformer provides a simple means of matching any real load impedance to any line impedance. For applications requiring more bandwidth than a single quarter-wave section can provide, multisection matching transformers can be connected serially. As the number of discrete sections increases, the step changes in characteristic impedances between the sections become smaller. A larger number of transformer sections begins to approach the

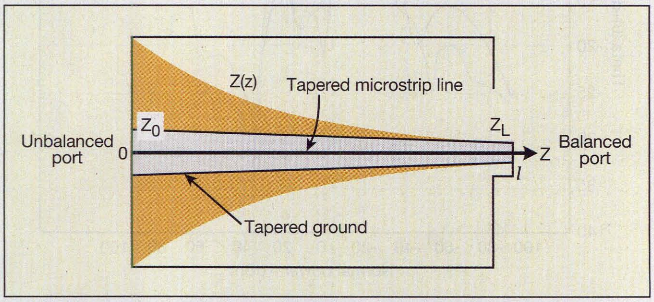

2. A tapered microstrip transmission line is the essential component of the impedance converter.

Smart
SYNTHESIZED SIGNAL GENERATORS 250-4000 MHz

WOW! only $1995.00 ea.

Rugged, portable, production test workhorses

Sweep or hop across wide frequency and power bands, use a pair for third-order intercept tests, or slip one into your laptop case and take it on the road! Our easy-to-use GUI will have you up and running in minutes. Compatible with most test software,* they add capabilities and increase efficiency, all without busting your budget!

*See data sheets for an extensive list of compatible software.

Accurate, reliable results at high speed

Signals within 1 ppm for frequency and 0.25 dBm for power, low harmonics, a resolution of 5 kHz, and 5-msec settling times help you get the data you need from complex, high-speed testing plans. Just go to minicircuits.com for specifications, performance data, and everything you need to make your choice — and get it in your hands as soon as tomorrow!

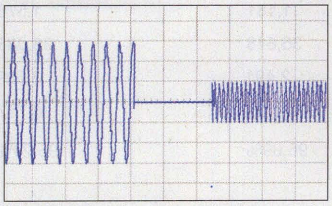

Frequency and power hopping.

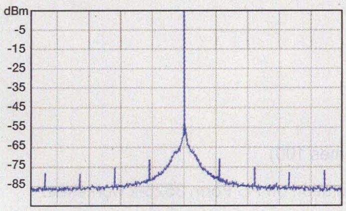

Low spurious.

Model	Frequency (MHz)	Power (dBm)	Harmonics (dBc typ.)	Price ($ ea.)
SSG-4000HP	250-4000	-50 to +20	-40	1995.00
SSG-4000LH	250-4000	-60 to +10	-66	2395.00

Mini-Circuits...we're redefining what VALUE is all about!

Mini-Circuits®
ISO 9001 ISO 14001 AS9100

P.O. Box 350166, Brooklyn, New York 11235-0003 (718) 934-4500 Fax (718) 332-4661

Yoni2® U.S. Patents 7739260, 7761442 **The Design Engineers Search Engine** *finds the model you need, Instantly* • For detailed performance specs & shopping online see **minicircuits.com**

IF/RF MICROWAVE COMPONENTS

499 rev C

United States Postal Service

Statement of Ownership, Management, and Circulation **(Requester Publications Only)**

1. Publication Title: MICROWAVES & RF
2. Publication Number: 797-680
3. Filing Date: 10/01/12
4. Issue of Frequency: Monthly except 2 issues in November
5. Number of Issues Published Annually: 13
6. Annual Subscription Price: Free to Qualified
7. Complete Mailing Address of Known Office of Publication (Not Printer): Penton Media, 9800 Metcalf Ave., Overland Park, Johnson County, KS 66212-2216 — Contact Person: Brenda Roode, Telephone: 913-967-1641
8. Complete Mailing Address of Headquarters or General Business Office of Publisher (Not Printer): Penton Media, Inc. 249 West 17th St, Fourth Floor, New York, NY 10011-5390
9. Full Names and Complete Mailing Addresses of Publisher, Editor, and Managing Editor - Publisher: Bill Baumann, Penton Media, Inc 249 West 17th St., Fourth Floor, New York, NY 10011-5390; Editor: Nancy Friedrich, Penton Media, Inc 249 West 17th St., Fourth Floor, New York, NY 10011-5390; Managing Editor: Jeremy Cohen, Penton Media, Inc 249 West 17th St., Fourth Floor, New York, NY 10011-5390
10. Owner - Full name and complete mailing address: Penton Media, Inc., 249 W 17th St, Fourth Floor, New York, NY 10011 - 5390; Penton Business Media Holdings, Inc. (owns 100% of the stock of Penton Media, Inc.), 249 W 17th St, Fourth Floor, New York, NY 10011 - 5390
11. Known Bondholders, Mortgagees, and Other Security Holders Owning or Holding 1 Percent or More of Total Amount of Bonds, Mortgages or Other Securities: None
12. Tax Status (For completion by nonprofit organizations authorized to mail at nonprofit rates) (Check one) The purpose, function, and nonprofit status of this organization and the exempt status for federal income tax purposes: N/A
13. Publication Title: MICROWAVES & RF

14. Issue Date for Circulation Data: September 2012 15. Extent and Nature of Circulation	Average No. Copies Each Issue During Preceding 12 Months	No. Copies of Single Issue Published Nearest to Filing Date
a. Total Number of Copies (Net press run)	38,139	36,717
b. Legitimate Paid and/or Requested Distribution (By Mail and Outside the Mail)		
(1) Outside County Paid/Requested Mail Subscriptions stated on PS Form 3541. (Include direct written request from recipient, telemarketing and Internet requests from recipient, paid subscriptions including nominal rate subscriptions, employer requests, advertiser's proof copies, and exchange copies.)	25,652	21,733
(2) In-County Paid/Requested Mail Subscriptions stated on PS Form 3541. (Include direct written request from recipient, telemarketing and Internet requests from recipient, paid subscriptions including nominal rate subscriptions, employer requests, advertiser's proof copies, and exchange copies.)	0	0
(3) Sales Through Dealers and Carriers, Street Vendors, Counter Sales, and Other Paid or Requested Distribution Outside USPS®	8,815	9,779
(4) Requested Copies Distributed by Other Mail Classes Through the USPS (e.g. First-Class Mail®)	0	0
c. Total Paid and/or Requested Distribution (Sum of 15b (1), (2), (3), and (4))	34,467	31,512
d. Nonrequested Distribution (By Mail and Outside the Mail)		
(1) Outside County Nonrequested Copies Stated on PS Form 3541 (include Sample copies, Requests Over 3 years old, Requests induced by a Premium, Bulk Sales and Requests including Association Requests, Names obtained from Business Directories, Lists, and other sources)	913	982
(2) In-County Nonrequested Copies Stated on PS Form 3541 (include Sample copies, Requests Over 3 years old, Requests induced by a Premium, Bulk Sales and Requests including Association Requests, Names obtained from Business Directories, Lists, and other sources)	0	0
(3) Nonrequested Copies Distributed Through the USPS by Other Classes of Mail (e.g. First-Class Mail, Nonrequestor Copies mailed in excess of 10% Limit mailed at Standard Mail® or Package Services Rates)	0	0
(4) Nonrequested Copies Distributed Outside the Mail (Include Pickup Stands, Trade Shows, Showrooms and Other Sources)	268	594
e. Total Nonrequested Distribution (Sum of 15d (1), (2), (3), and (4))	1,181	1,576
f. Total Distribution (Sum of 15c and 15e)	35,648	33,088
g. Copies not Distributed	2,491	3,629
h. Total (Sum of 15f and g)	38,139	36,717
i. Percent Paid and/or Requested Circulation (15c divided by 15f times 100)	96.69%	95.24%

16 ☐ Total circulation includes electronic copes. Report circulation on PS Form 3526-x worksheet

17. Publication of Statement of Ownership for a Requester Publication is required and will be printed in the November 2012 issue of this publication.

18 Brenda Roode, Audience Marketing Director — Date 10/1/12

I certify that all information furnished on this form is true and complete. I understand that anyone who furnishes false or misleading information on this form or who omits material or information requested on the form may be subject to criminal sanctions (including fines and imprisonment) and/or civil sanctions (including civil penalties).

structure of a continuously tapered line, such as the exponentially tapered line shown in **Fig. 2**.

According to the theory on the impedance conversion of an exponentially tapered line, the converter can work well at the smallest length, given that Z_L/Z_0 and reflection coefficient magnitude $|\Gamma_L|$. The smallest length, l_{min}, is found from the relationship:

$$l_{\min} = \frac{1}{4\beta|\Gamma_L|}\left|\ln\frac{Z_L}{Z_0}\right| \quad (1)$$

If the ETMB is designed on a substrate with relative permittivity of ε_r, then an empirical formula for calculating l_{min} can be found after substituting $2\pi\varepsilon_r/\lambda_0$ for β, as shown in Eq. 2:

$$l_{\min} = \frac{\lambda_0}{8\pi\varepsilon_r|\Gamma_L|}\left|\ln\frac{Z_L}{Z_0}\right| \quad (2)$$

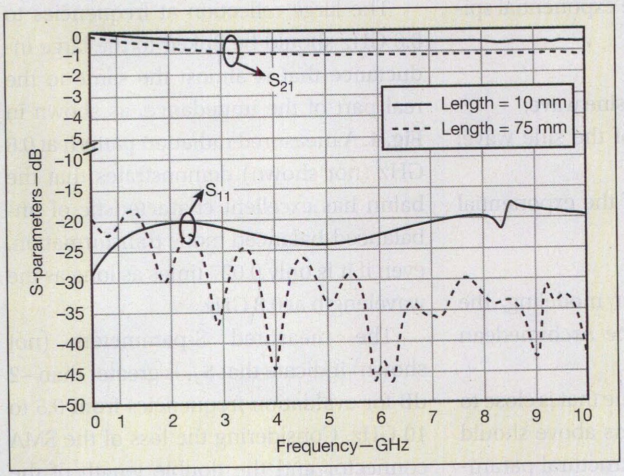

3. These simulations show S-parameters for the 10- and 75-mm ETMBs.

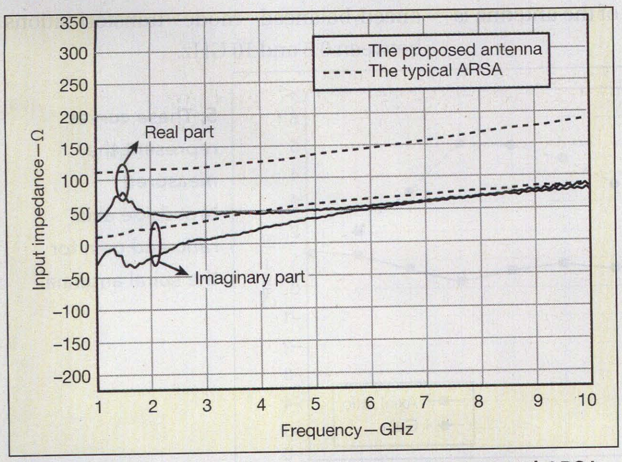

4. These plots show the input impedances for a typical ARSA and for the proposed antenna, from DC to 10 GHz.

where:

λ_0 = the free-space wavelength of the antenna's lowest operating frequency, and

β = the propagation constant of the substrate material.

Equation 2 indicates that an ETMB will work well for a wideband impedance conversion for any length and ratio combination of Z_L/Z_0 that equals 1. To evaluate the effectiveness of an ETMB, one was modeled on a 1-mm-thick circuit substrate with relative permittivity of 4.3 and loss tangent of 0.003. When an ETMB with microstrip line that is not tapered is simulated as part of a back-to-back structure, it is clear that shorter ETMBs result in less transmission loss, with respectable reflection coefficient. **Figure 3** shows simulated S-parameters for back-to-back ETMB structures with lengths of 10 and 75 mm, or almost one-half the wavelength at 1 GHz.

From ref. 16, it is known that "infinite balun" is one of the most effective ways to feed Equiangular spiral antennas. One prominent characteristic of infinite balun is its remarkable impedance conversion in ultrawideband, which is used in this paper to decrease the input impedance of ARSA and achieve a low value of Z_L/Z_0 for the ETMB. The EARSA antenna arm consists of two parts: an exponential spiral line and a sinuous meander Archimedean spiral line, both the lines are of the same width. The exponential spiral line is defined by Eq. 3:

Antenna structural parameters at a glance

Parameter	r_0	a_1	a_2	φ_1	m	n	φ_2
Value	1.5 mm	0.2 mm/rad	21π mm/rad	4π rad	3 mm	40 rad/s	12π rad

$$r = r_0 e^{a_1\varphi} \quad (3)$$

where:

r_0 = the original radius;
a_1 = the spiral constant; and
ϕ = the winding angle.

The sinuous meander Archimedean spiral line is given by Eq. 4:

$$r = a_2(\varphi - \varphi_1) + r_1 + m(1 + \sin(n\varphi)) \quad (4)$$

where:
r_1 = the final radius of the exponential spiral line;
a_2 = the spiral constant;
m = the amplitude of the sine wave;
n = angular frequency of the sine wave; and
ϕ_1 = the final winding of the exponential spiral line.

In terms of computer modeling, the final winding angle of the Archimedean spiral line is ϕ_2.

To achieve a Z_L/Z_0 value that is close to the ideal 1, the parameters above should be carefully tuned. The structural parameters of the antenna have been collected in the **table**. The antenna arm is 1 mm wide and the final radius of the antenna is 41.5 mm.

Figure 4 shows plots of input impedance for the EARSA and for a typical ARSA with the same initial radius, Archimedean spiral constant, and final radius, demonstrating the low impedance characteristic of the proposed structure. The input impedance and the characteristic impedance at the balanced port of the ETMB can be set to 50 Ω. As indicated by **Fig. 2**, it is reasonable to feed the antenna with a 10-mm-long ETMB; a plot of S_{11} for an integrated model of the EARSA (not shown) reveals that S_{11} is below −10 dB from 0.8 to 8.6 GHz.

The large reflection at frequencies to 8.6 GHz should be linked to the large inductance that is almost the same to the real part of the impedance, as shown in **Fig. 4**. A measured radiation pattern at 0.8 GHz (not shown) demonstrates that the balun has excellent characteristic of unbalanced-balanced mode transformation, even if it is only 0.027 times as long as the wavelength at 0.8 GHz.

The measured S-parameters (not shown) indicate that S_{21} is greater than −2 dB for evaluation frequencies from 0.5 to 10 GHz. Considering the loss of the SMA connector and the double length of the balun, the ETMB should perform well in any impedance conversions and unbalanced-balanced mode transformations between 0.5 and 10 GHz.

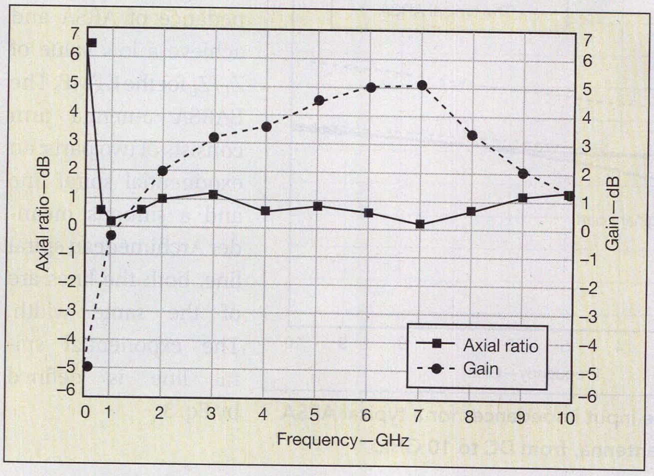

5. These curves represent the measured broadside axial ratio and gain for the spiral antenna.


i2S®
INTELLIGENT INTERACTIVE
SYNTHESIZERS
UP TO
18 GHZ
RF OUT
SYNERGY
MICROWAVE CORPORATION
Product Features
> Exceptional Phase Noise Performance
> Ultra Low RMS Jitter, As Low As 3.7 Femtosecond
> Fast Switching
> Selectable Or Standard Programming Interface
> Single Or Dual Supply Options
> Surface Mount Or Connectorized
PATENTED TECNOLOGY
RoHS
REL∞PRO®
For additional information, contact Synergy's sales and application team.
Phone: (973) 881-8800 | Fax: (973) 881-8361
E-mail: sales@synergymwave.com
Web: WWW.SYNERGYMWAVE.COM
SYNERGY®
MICROWAVE CORPORATION

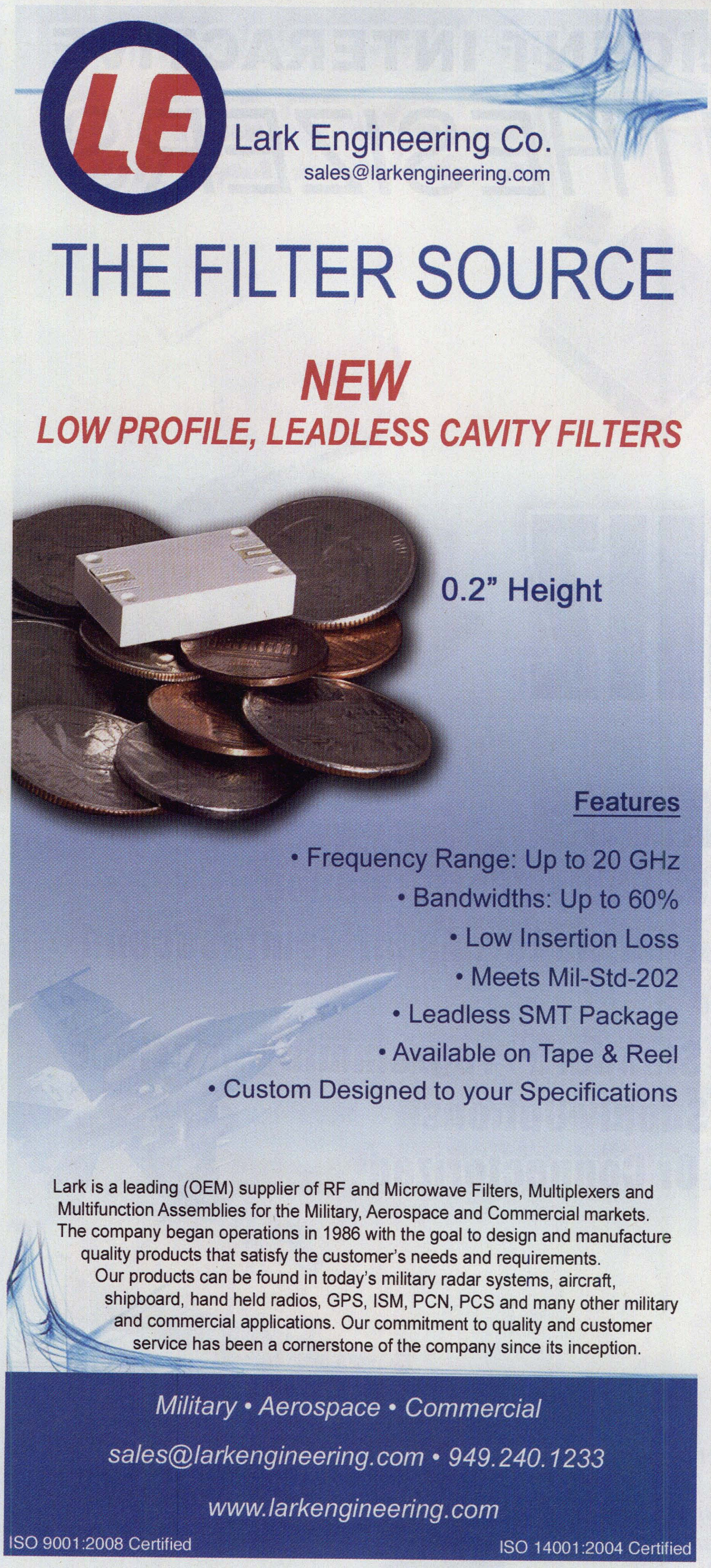

The EARSA was etched on a 1-mm-thick substrate with permittivity of 4.3. To achieve unidirectional radiation, a 10-mm-deep cavity filled with absorber material reinforces the back of the antenna **(Fig. 1)**. The radius of the packaged antenna is 50 mm, while the height is 10 mm.

The antenna's reflection coefficient was measured with a commercial microwave vector network analyzer (VNA). The results (not shown) indicate good performance between 0.8 and 9.4 GHz. The lowest measured operating frequency compares to the simulated results, with the measured reflection coefficient at the highest operating frequencies in excess of the simulation result due to the effects of the absorber material. **Figure 5** shows the gain and broadside axial ratio as measured at discrete frequencies in an anechoic chamber. **Figure 6** shows the radiation patterns in mutually perpendicular planes at several frequencies. The measured results indicate that the EARSA works well from 0.8 to 9.4 GHz, with reflection coefficient of less than −10 dB and broadside axial ratio of less than 3 dB. Compared with a typical ARSA working at the same lowest frequency, the EARSA offers a 78.62% reduction in area. It boasts a profile that is only 10 mm deep, or only about 0.027 times the physical wavelength at 0.8 GHz.

In summary, a new type of ARSA, the EARSA, was designed with low input impedance and a shallow cavity. The input impedance of a standard ARSA can be decreased by adding a controlled-width exponentially spiral line which is characterized by impedance conversion. Simulated and measured results show that this structure significantly reduces the input impedance of the ARSA. As a result, an EARSA developed with a short, 10-mm-long ETMB was fully capable of handling the impedance conversion and unbalanced-balanced mode transformation required.

The miniaturized EARSA works well from 0.8 to 9.4 GHz, with a profile only 0.027 times as long as the free-space wavelength of a 0.8-GHz signal. The antenna features a 78.62% reduction in area compared to a standard ARSA with the same

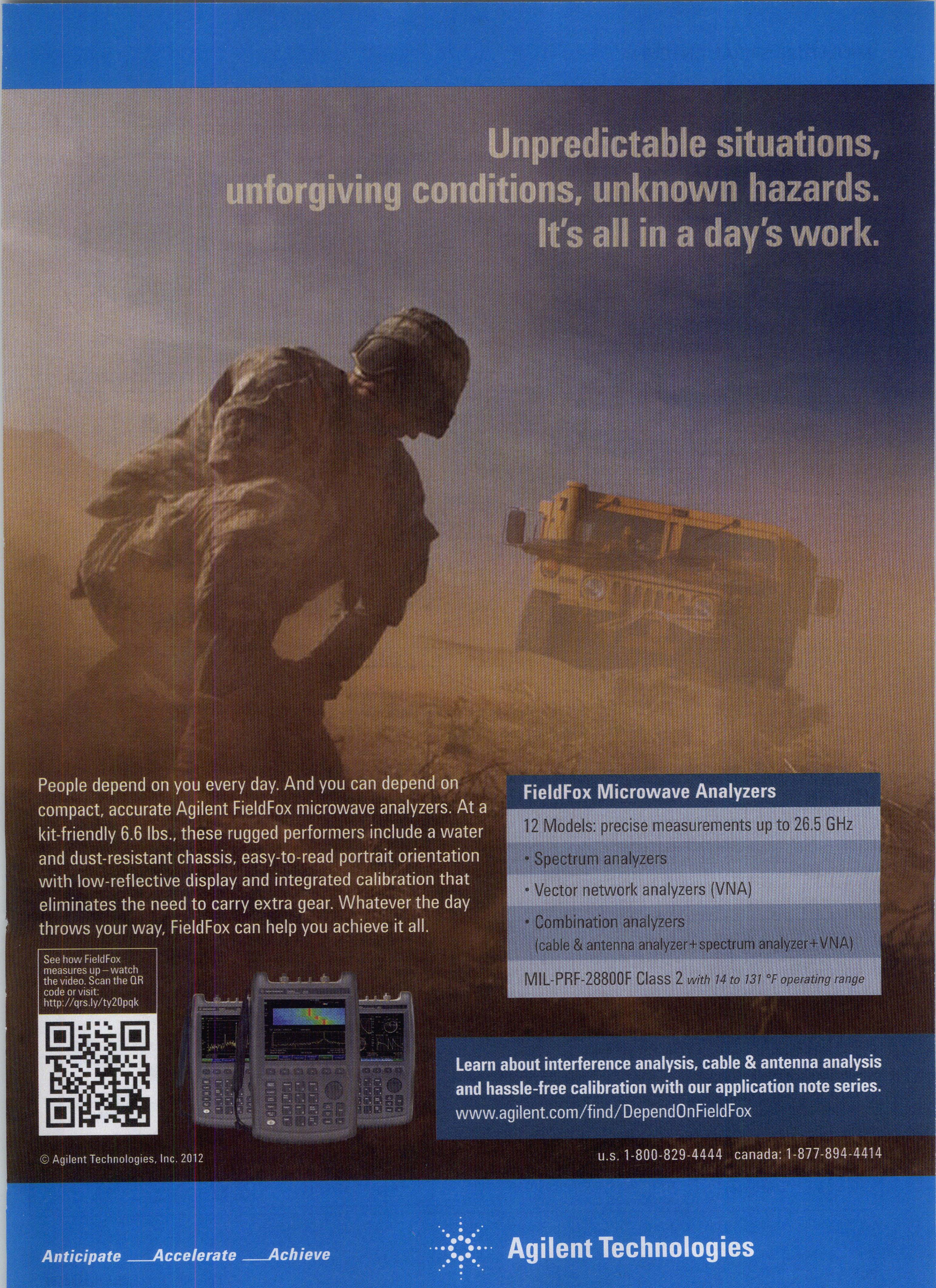
Unpredictable situations,
unforgiving conditions, unknown hazards.
It's all in a day's work.
People depend on you every day. And you can depend on compact, accurate Agilent FieldFox microwave analyzers. At a kit-friendly 6.6 lbs., these rugged performers include a water and dust-resistant chassis, easy-to-read portrait orientation with low-reflective display and integrated calibration that eliminates the need to carry extra gear. Whatever the day throws your way, FieldFox can help you achieve it all.
See how FieldFox measures up – watch the video. Scan the QR code or visit: http://qrs.ly/ty20pqk
FieldFox Microwave Analyzers
12 Models: precise measurements up to 26.5 GHz
• Spectrum analyzers
• Vector network analyzers (VNA)
• Combination analyzers (cable & antenna analyzer+spectrum analyzer+VNA)
MIL-PRF-28800F Class 2 with 14 to 131 °F operating range
Learn about interference analysis, cable & antenna analysis and hassle-free calibration with our application note series.
www.agilent.com/find/DependOnFieldFox
© Agilent Technologies, Inc. 2012
u.s. 1-800-829-4444 canada: 1-877-894-4414
Anticipate ___Accelerate ___Achieve
Agilent Technologies

low-end frequency, achieved by meandering the Archimedean spiral lines. MWRF

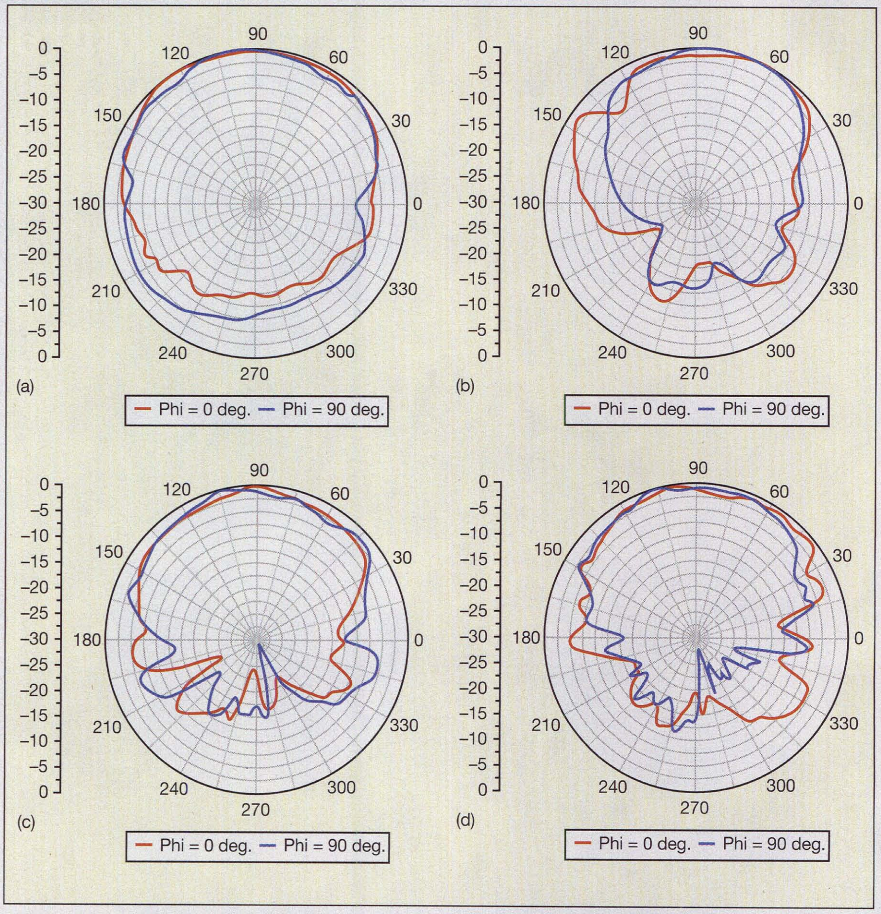

6. These radiation patterns were measured at (a) 0.8 GHz, (b) 3 GHz, (c) 6 GHz, and (d) 8 GHz.

REFERENCES

1. H. Nakano, "A Meander Spiral Antenna," IEEE Antennas and Propagation Society (AP-S) International Symposium Digest, 2004, pp. 2243-2246.
2. B.A. Kramer, C.-C. Chen, and J.L. Volakis, "Size Reduction of a Low-Profile Spiral Antenna Using Inductive and Dielectric Loading," IEEE Antennas and Wireless Propagation Letters, Vol. 7, 2008, pp. 22-25.
3. Zhu Yu-xiao, Zhong Shun-shi, and Xu Sai-qing, "Miniaturized Compound Spiral Slot Antenna," Microwave and Optical Technology Letters, Vol. 50, No. 11, 2008, pp. 2799-2801.
4. M.W. Numberger and J.L. Volakis, "New Termination for Ultra-Wideband Slot Spirals," IEEE Transactions on Antennas and Propagation, Vol. 50, No. 1, 2002, pp. 82-85.
5. Ya-Wei Wang, Guang-Ming Wang, and Hui-Yong Zeng, "Design of a New Meander Archimedean Spiral Antenna," Microwave and Optical Technology Letters, Vol. 52, No. 10, 2010, pp. 2384-2387.
6. H. Nakano, S. Sasaki, H. Oyanagi, et al., "Cavity-backed Archimedean Spiral Antenna with Strip Absorber," IET Microwaves Antennas & Propagation, Vol. 2, No. 7, 2008, pp. 725-730.
7. H. Nakano, K. Kikkawa, Y. Iitsuka, et al., "Equiangular Spiral Antenna Backed by a Shallow Cavity with Absorbing Strips," IEEE Transactions on Antennas and Propagation, Vol. 56, No. 8, 2008, pp. 2742-2747.
8. Hisamatsu Nakano, Tatsuya Igarashi, Hiroshi Oyanagi, et al., "Unbalanced-Mode Spiral Antenna Backed by an Extremely Shallow Cavity," IEEE Transactions on Antennas and Propagation, Vol. 57, No. 6, 2009, pp. 1625-1633.
9. Brad A. Kramer, Stavros Koulouridis, Chi-Chih Chen, et al., "A Novel Reflective Surface for an UHF Spiral Antenna," IEEE Antennas and Wireless Propagation Letters, Vol. 5, 2006, pp. 32-24.
10. Hisamatsu Nakano, Kazuo Hitosugi, Naoki Tatsuzawa, et al., "Effects on the Radiation Characteristics of Using a Corrugated Reflector with a Helical Antenna and an Electromagnetic Band-Gap Reflector with a Spiral Antenna," IEEE Transactions on Antennas and Propagation, Vol. 53, No. 1, 2005, pp. 191-199.
11. L. Schreider, X. Begaud, M. Soiron, et al., "Broadband Archimedean Spiral Antenna Above a Loaded Electromagnetic Band Gap Substrate," IET Microwaves & Antenna Propagation, Vol. 1, No. 1 2007, pp. 212-216.
12. Hisamatsu Nakano, Katsuki Kikkawa, Morihiro Kondo, et al., "Low-Profile Equiangular Spiral Antenna Backed by an EBG Reflector," IEEE Transactions on Antennas and Propagation, Vol. 57, No. 5, 2009, pp. 1309-1318.
13. Hisamatsu Nakano, Ryohei Satake, and Junji Yamauchi, "Extremely Low-Profile Single-Arm Wideband Spiral Antenna Radiating a Circularly Polarized Wave," IEEE Transactions on Antennas and Propagation, Vol. 58, No. 5, 2010, pp. 1511-1520.
14. Chunheng Liu, Yueguang Lu, Chunlei Du, et al., "The Broadband Spiral Antenna Design Based on Hybrid Backed-Cavity," IEEE Transactions on Antennas and Propagation, Vol. 58, No. 6, 2010, pp. 1876-1882.
15. David M. Pozar, Microwave Engineering, 3rd ed., Wiley, New York, 2006, p. 257.
16. John D. Dyson, "The Equiangular Spiral Antenna," IRE Transactions on Antennas and Propagation, Vol. 7, No. 2, 1959, pp. 181-187.

WANG WEI
Professor

ZHAO YING GONG
Graduate Student

College of Electronics Engineering, Chongqing University of Posts and Telecommunications, Chongqing 400065, People's Republic of China

CMOS LNA Serves Flat Gain To 5 GHz

Fabricated in a commercial semiconductor process, this low-noise amplifier uses current-reuse techniques to achieve high gain from 3 to 5 GHz for UWB applications.

AMPLIFICATION IS an important part of any communications system, and particularly challenging to achieve in broadband and ultrawideband (UWB) communications. To serve those applications, the authors designed a broadband amplifier capable of flat gain from 3 to 5 GHz using a commercial 0.18-μm silicon CMOS semiconductor process. A shunt inductor was used for flat gain and wideband impedance matching, along with a common-gate structure for the input match and a source follower for the output match. Current-reuse helped boost gain while minimizing power dissipation.

The proposed low-noise amplifier (LNA) operates from a +1.8-VDC supply and delivers 21.83-dB power gain with only 0.15-dB variation. The average noise figure is 5.4 dB while the input-referred output power at 1-dB compression is –19 dBm. The LNA achieves input and output reflection coefficients of –13.3 and –19.5 dB, respectively.

The drive for increased data is encouraging the spread of UWB communications systems across the 3.1-to-10.6-GHz range, with a low band from 3.1 to 5.0 GHz and a high band from 6.0 to 10.6 GHz.[1] An LNA is a key component in these systems, and must provide flat gain across these wide frequency ranges with good linearity and low noise figure. Silicon CMOS technology provides one avenue for achieving these LNA attributes—in this instance, utilizing the commercial foundry of Taiwan Semiconductor Manufacturing Company Ltd. (TSMC; www.tsmc.com).

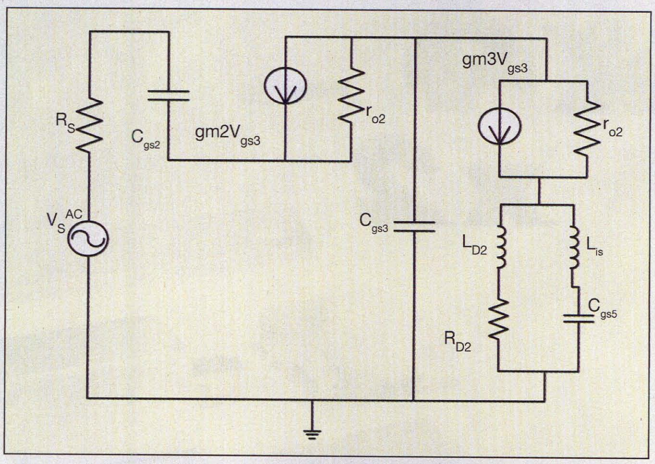

2. This is a small-signal equivalent-circuit version of the LNA, which incorporates loaded parastics over device M2 for the amplifier stage.

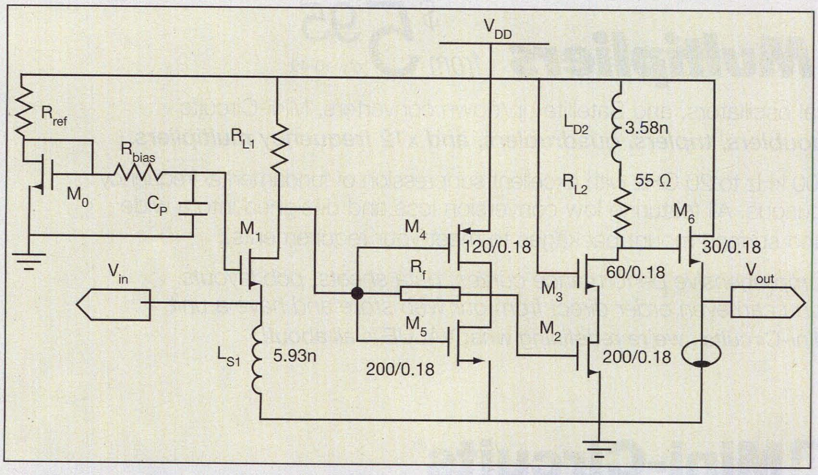

1. This block diagram shows the components used in the UWB LNA circuit.

The proposed LNA incorporates a common-gate input matching circuit, common-source amplifier stage with shunt inductor, and current-reuse topology **(Fig. 1)**. The combination of structures and its biasing circuit contribute to its high, flat gain. The circuit was designed and simulated based on TSMC's 0.18-μm RF CMOS process.

The cascade structure helps provide high gain, even with the lower gain of the common-gate first stage. As shown in **Fig. 1**, transistor M_2 provides high gain, while transistor M_3 helps reduce the Miller effect induced by gate-drain capacitor C_{gd} on M_2. This decreases interactions between the output and input ports and contribute to higher gain and better frequency response. **Figure 2** provides a small-signal equivalent circuit with loaded parasitic circuit elements for M_2.

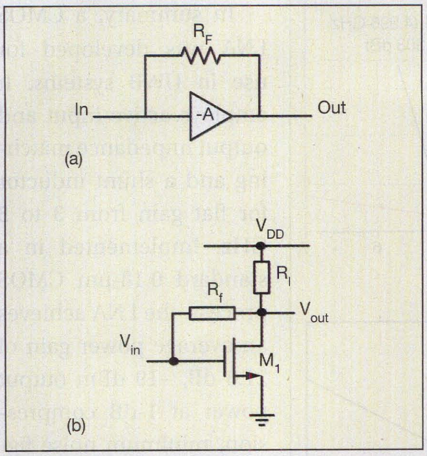

3. These diagrams show (a) the basic LNA and (b) a resistor shunt feedback structure.

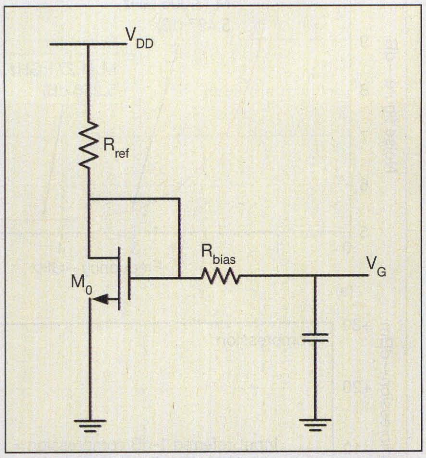

5. This is the bias circuit used with the LNA.

The cascade stage contributes to inductive shunt peaking to enhance LNA bandwidth.[2] The shunt peaking inductance and parasitic capacitance C_{D3} in the drain of transistor M_3 work at a harmonic frequency of 4 GHz, according to the relationship:

$\omega = 1/(L_{D2}C_{D3})$

From **Fig. 2**, the transfer function of this stage can be presented as follows:

$$\frac{V_{D2}}{V_{D1}} = g_{m2} \times \left[(g_{m3} \cdot r_{o3} \cdot r_{o2}) // \frac{R_{L2}\left(\frac{L_{D2}}{sR_{L2}} + \frac{1}{S^2}\right)}{L_{D2}C_{D3} + \frac{R_{L2}C_{D3}}{s} + \frac{1}{s^2}} \right]$$

To reduce the parasitic capacitance, the size of device M_3 can be reduced. The low resistance, R_{L2}, at about 55 Ω, can result in flat gain over the full band from 3 to 5 GHz.

Earlier work[3] detailed a relationship between transistors M_2 and M_3 capable of reducing the noise figure. In this relationship, the width of the cascoding transistor, M_3, is chosen to be three times less (this ratio may vary slightly during computer simulations) than that of input transistor M_2. In the current report, the width of transistor M_2 is 200 μm while the width of M_3 is 60 μm.

An increase in amplifier gain usually comes at a cost of higher dissipated power. But the current-reuse technique can increase gain without an increase in power dissipation. As **Fig. 1** indicates, a type of current-reuse approach was adopted for this LNA design. The configuration is based on the resistor shunt-feedback structure shown in **Fig. 3(b)**, with an elementary diagram of the resistor shunt-feedback structure shown in **Fig. 3(a)**. According to that diagram, the input impedance can be expressed as:

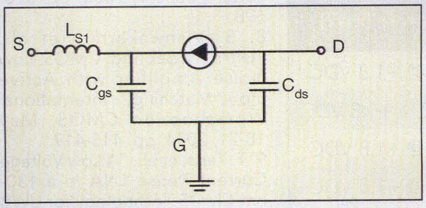

4. This is a small-signal equivalent circuit of the LNA.

$Z_{in} = R_F/(1 + A)$

From **Fig. 3(b)**, transistor M_1 and lead resistor R_L account for the forward gain, A. In addition, the input impedance (Z_{in}), the voltage gain (A_V), the noise factor (F), and the –3-dB bandwidth (BW_{-3dB}) in **Fig. 3(b)** can be approximated by:

$$Z_{in} = \frac{R_f + r_{ds}//R_l}{1 + g_m(r_{ds}//R_l)}$$

$$A_V \approx -g_m(R_f//R_l//r_{ds})$$

$$F \approx 1 + \frac{\gamma}{R_s g_m} + \frac{1}{R_s R_l g_m} + \frac{4R_s}{R_f}\left(1 + \frac{R_f + R_s}{(1 + g_m R_l)R_l}\right)^{-2}$$

$$BW_{-3dB} \approx \frac{1}{R_f C_{gs1}} + \frac{g_m(R_l//r_{ds})}{(R_f + R_l//r_{ds})C_{gs1}}$$

For increased voltage gain and improved noise factor, feedback resistor R_f should be increased, which will decrease the bandwidth. In such a case, the current-reuse configuration is used to achieve improved gain and noise factor. By stacking both NMOS and PMOS transistors—that is, by employing the current-reuse method shown in **Fig. 1**—the overall equivalent transconductance of the circuit is changed from simply g_{mN} to the combination of the two devices, $g_{mN} + g_{mP}$. This increases the voltage gain and results in wider bandwidth for the LNA.[4]

For maximum power transfer and minimal reflections, the input impedance of the first-stage cascade amplifier should be impedance matched with the source impedance, R_S = 50 Ω. The most common matching circuits for this purpose are inductance-capacitive (LC) network matching and common-gate-stage matching. For good power matching and wideband noise characteristics, broadband input impedance matching can be accomplished by an input common-gate stage or $1/g_m$ termination.

The noise performance of an LNA is dependent on the quality of its input impedance matching, so optimized noise characteristics for the amplifier should be calculated. This involves adopting an optimal relaxation factor, W_{optP} in the power consumption limit. Parameter W_{optP} can be approximated by:

$$W_{optP} = \frac{1}{3\omega L C_{OX} R_S} = 165\mu m$$

where $C_{OX} = \varepsilon_{OX}/T_{OX}$; $R_S = 50\ \Omega$; $\omega = 4$ GHz; and COX can be calculated based on TSMC's 0.18-μm CMOS process.

An approximation of W_{optP} with effective results is 165 μm. A small-signal equivalent circuit for a common-gate stage with an input inductor, L_{S1}, is shown in **Fig. 4.** After neglecting the loading effects of the other amplifier stages, the input impedance can be simplified as:

$$Z_{in} = \frac{1}{\dfrac{1}{sL_{S1}} + \left(g_{m1} + sC_{gs1}\right)}$$

where:

g_{m1} = the transconductance of M_1, and
C_{gs1} = gate-to-source capacitance of M_1.

As the frequency increases, the input impedance is close to $1/g_{m1}$, which dominates the magnitude of input impedance Z_{in} during operation at gigahertz frequencies. The input inductor (L_{S1}) matches with the source impedance of 50 Ω, while the load resistance (R_{L1}) supplies the bias voltage to the second stage of the LNA.

Neglecting induced gate noise, the noise factor of the basic LNA is given by:

$$F = 1 + (\gamma/\alpha)$$

where γ and α represent empirical process- and bias-dependent parameters, respectively. The noise figure, which is higher when induced gate noise is taken into account, is above 4.8 dB for short-channel devices and will be significantly worse at higher frequencies.[5]

The biasing circuits for the LNA are shown in **Fig. 5.** The bias voltage can be calculated by the following relationship:

$$V_{bias} = R_{on}/(R_{on} + R_{ref})$$

where $R_{on} = 1/g_m$.

The proposed 3-to-5-GHz CMOS LNA was simulated with Spectre RF from Cadence Design Systems (www.cadence.com) based on parameters for TSMC's 0.18-μm CMOS technology. The amplifier's input and output impedance matching are good: less than −13.3 and −19.5 dB, respectively, with power gain (S_{21}) from 21.67 to 21.97 dB from 3 to 5 GHz.

Figure 6 shows the layout for the proposed LNA circuit, which occupies an area of 0.473 mm^2.

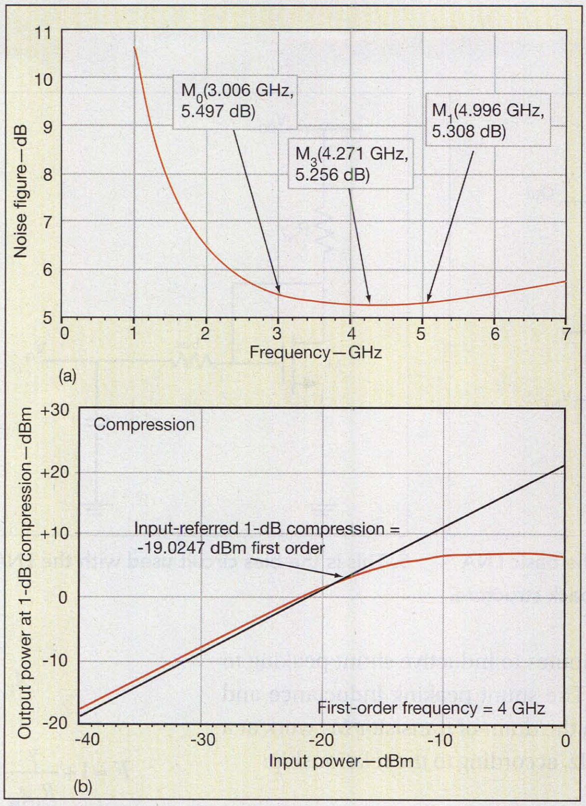

6. This is a layout of the proposed LNA.

In summary, a CMOS LNA was developed for use in UWB systems. It employs active input and output impedance matching and a shunt inductor for flat gain from 3 to 5 GHz. Implemented in a standard 0.18-μm CMOS process, the LNA achieves an average power gain of 21.8 dB, −19 dBm output power at 1-dB compression, minimum noise figure of 5.26 dB, with input and output impedance matching of −13.3 and −19.5 dB, respectively. While its noise figure is high, the amplifier provides advantages of good input/output impedance matching and broadband gain flatness. MWRF

Comparing the LNA with other results

Reference	Process (μm)	S_{11} (dB)	S_{22} (dB)	S_{21} (dB)	P_{1dB} (dBm)	Noise figure (dB)	Power (mW)
This work	0.18	<-13.39	<-19.46	21.67 - 21.97	-19.04	5.26 - 5.50	47 @ +1.8 VDC
6	0.18	<-6.5	<-20	20[a]	-9.57	5.2 - 6.1	26.2 @ +1.8 VDC
7	0.18	<-12.19	<-10.1	13.53 - 15.91	-14	4.7 - 6.7	60 @ +1.8 VDC
8[b]	0.18	<-15.1	N/A	16.4 - 16.98	N/A	3.9 - 4.3	21 @ +1.8 VDC
9	0.13	<-10	<-10	10.5 - 12.5	N/A	4.45 - 9.00	28 @ +1.4 VDC

[a]Shown as voltage gain. [b]In a 3.1-to-4.8-GHz band.

REFERENCES

1. United States Federal Communications Commission (FCC), "Final Rule of the Federal Communications Commission," 47 CFR Part 15, Sec. 503," Federal Register, Vol. 67, No. 95, May 2002.
2. T.H. Lee, The Design of CMOS Radio-Frequency Integrated Circuits, 2nd ed., Cambridge University Press, Cambridge, UK, 2006.
3. M. Reja, et al., "A New CMOS 3.1-11.7-GHz Low Power LNA for Ultra-Wideband Wireless Applications," IEEE International Symposium, May 27-30, 2007, pp. 1453-1456.
4. T. Taris, et al., "A Low Voltage Current Reuse LNA in a 130-nm CMOS Technology for UWB Applications," Proceedings of the European Microwave Conference, October 9-12, 2007, pp. 1105-1108.
5. T.H. Lee, The Design of CMOS Radio-Frequency Integrated Circuits, 1st ed., Cambridge University Press, New York, NY, 1998.
6. C. Garuda, et al., "A 3-5-GHz Fully Differential CMOS LNA with Dual-Gain Mode for Wireless UWB Applications," 48th Midwest Circuits and Systems Symposium, August 7-10, 2005, Vol. 1, pp. 790-793.
7. C-P. Chang, et al., "0.18 μm 3–6 GHz CMOS broadband LNA for UWB radio," Electronics Letters, June 9, 2005, pp. 696-698.
8. S. Vishwakarma, et al., "Ultra Wideband CMOS Low Noise Amplifier with Active Input Matching," International Workshop on CMOS, May 18-21, 2004, pp. 415-419.
9. T. Taris, et al., "A Low Voltage Current Reuse LNA in a 130-nm CMOS Technology for UWB Applications," Proceedings of the European Microwave Conference, October 9-12, 2007, pp. 1105-1108.

photo courtesy of the U.S. Military & NASA

OPTIMIZE TESTING OF MULTI-STANDARD RADIO DEVICES

BASE STATIONS HAVE faithfully evolved as cellular telecommunications networks migrated from second- to third-generation (2G to 3G) technologies. As cellular networks migrate to 3.9G or even fourth-generation (4G) technologies, however, base-transceiver-station (BTS) transmitters must be reinvented. From what was originally a single-carrier, narrowband design for 2G GSM/TDMA networks, they evolved into multi-carrier wideband designs (3/3.5G) and now will have to transition to a software-defined-radio (SDR) architecture. In a five-page application note, Agilent Technologies provides guidance on how multi-standard-radio (MSR) base-station transmitter devices can be tested quickly, accurately, and efficiently.

Titled "Solutions for Testing Multi-Standard Radio Base Stations," the note explains that next-generation base-station transmitters and receivers will support wider bandwidths. In addition, they will include multiple carriers (MCs) of a single radio format as well as multiple formats in one transmitter path. For example, the MSR base station can simultaneously transmit different radio-access technologies (RATs) from a single unit. While such capabilities will drive down base-station cost and size, they also invite a challenge: the conformance testing of MSR base stations in accordance with the 3GPP Release 9 (TS37 series) standard.

Agilent Technologies, Inc., 5301 Stevens Creek Blvd., Santa Clara, CA 95051; (877) 424-4536, www.agilent.com

The TS37 document covers the MSR MC combinations of 3GPP frequency-division-duplexing (FDD) and time-division-duplexing (TDD) formats. Transmitter conformance tests have to be performed under MSR MC allocating scenarios. The document defines MSR RF test requirements by specifying measurement of the following when testing MSR MC-active configurations: channel power, error vector magnitude (EVM), frequency error, spurious emissions, and spectrum emission mask (SEM).

To provide a realistic use scenario, base-station manufacturers may also want to test each single-format single carrier. Such testing calls for measurement of the adjacent-channel leakage ratio (ACLR), occupied bandwidth, and time alignment between transmitter branches. The note provides details of how all of this testing can be done in an optimized manner using signal analyzers and vector-signal-analyzer (VSA) software. With the accurate and efficient testing of MSR base-station transmitter devices, the note emphasizes that it is possible to ensure their successful deployment.

EXPECT AN UPSURGE IN AUTOMOTIVE ASSISTANCE AND SAFETY FEATURES

AUTOMOTIVES INCLUDE AN increasing number of safety features. Like the airbags based on microelectromechanical systems (MEMS), most of these safety features are electronic in nature. And an increasing amount of these safety innovations are rooted in RF and microwave engineering. Freescale Semiconductor looks at where the market for automotive safety features currently stands and the technologies that are currently shaping them in a five-page white paper dubbed, "Automotive Safety Innovations: When Will Zero Fatalities Become a Reality?"

The paper begins by explaining the need for such features. Road deaths are currently the number-one cause of death for young people worldwide. With the economic cost of automotive deaths estimated at close to $100 billion per year for developing countries, the document points out that making vehicles safer is an economic imperative as well as a moral one. Electronic systems are the optimal way to improve vehicle safety. In developed countries, fatalities have already been greatly reduced by airbags and active safety systems like electronic stability control and radar.

Freescale Semiconductor, Inc., 6501 William Cannon Dr. West, Austin, TX 78735; www.freescale.com.

One of the fastest-growing safety application areas is advanced driver assistant systems (ADASs). They require state-of-the-art, cost-effective RF technology that can be embedded in the vehicle. To make the system efficient and reliable for the driver, great computation power also is needed. This document provides a very helpful overview of ADASs and where they currently stand.

ADAS features can be divided into comfort and active categories. Among the comfort ADASs are applications that provide warnings or information for the driver, but do not adhere to ISO 26262 safety requirements. They include blind-spot detection using short-range radar; lane detection; and parking assistance using multiple cameras with a panoramic view and potentially ultrasonic technologies.

In contrast, active ADASs are standalone, autonomous systems that actively influence the car. They have high functional safety requirements on a system—not a sensor—level. Among these applications are adaptive cruise control using long-range radar and lane keeping, which performs active steering using a front-view camera. In addition, collision-avoidance systems provide full-stop emergency braking using a fusion of long-range radar and a front-view or stereo camera.

In the collision-warning system from Freescale, for example, a 77-GHz silicon-germanium (SiGe) chipset transmitter emits signals that are reflected from objects ahead of the vehicle—as well as to the side and rear of it. These signal reflections are captured by multiple receivers integrated throughout the vehicle. The radar system can detect and track objects in the frequency domain, warn the driver of an imminent collision, and initiate electronic-stability-control intervention. The document closes by sharing Freescale's vision of automotive safety: each car being its own small network, with systems exchanging information about everything from road conditions to tire pressure. These in-car networks will become elements of a larger network of vehicles.

HITTITE MICROWAVE CORP.
2 Elizabeth Dr., Chelmsford, MA 01824; (978) 250-3333, FAX: (978) 250-3373, www.hittite.com

Transceiver ICs Energize Wideband Infrastructure

These dual-channel downconverter and direct-quadrature-modulator devices both feature flexible integrated frequency-synthesizer and oscillator circuitry and broad bandwidths.

1. Model HMC1190LP6GE is a dual frequency downconverter with integrated VCO and synthesizer circuitry, while model HMC1197LP7FE is a direct modulator also with synthesizer and VCO circuitry.

WIRELESS SERVICE PROVIDERS face an ever-increasing demand for capacity on their networks, due to handheld devices that can process voice, data, and video. Not only must wireless infrastructure architects implement versatile systems using multiple data standards and frequency bands, but they must do so while occupying as little space and power as possible. To keep pace with the needs of infrastructure designers, Hittite Microwave Corp. (www.hittite.com) has developed a new receiver and transmitter integrated-circuit (IC) chipset suitable for a wide range of cellular applications, from femtocells to macro base stations. The chipset features the model HMC1190LP6GE dual-channel downconverter, with integrated fractional-N phase-lock loop (PLL) synthesizer and voltage-controlled oscillator (VCO), for use with receivers. Also included is the model HMC1197LP7FE direct quadrature modulator, with fractional-N PLL frequency-synthesizer circuitry and VCO, for use with transmitters.

The two new ICs **(Fig. 1)** combine for efficient low-power operation over wide bandwidths, supporting a wide range of wireless communications standards. The HMC1190LP6GE downconverter IC, for example, covers an RF range of 700 to 3500 MHz, with typical power dissipation of only 2.34 W. But power consumption can be reduced further by means of external bias control pins, which allow high-speed optimization of power consumption under changing operating environments. This externally controlled enable/disable feature—combined with RF and external LO ports matched to 50 Ω—make it possible to dynamically reduce power consumption as conditions allow.

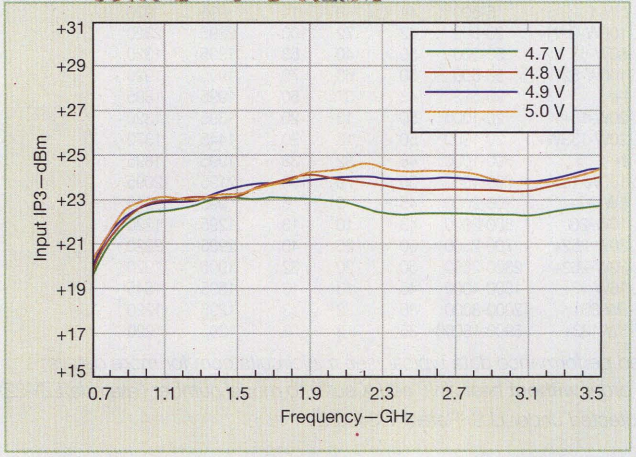

2. This plot shows input IP3 performance as a function of frequency for the HMC1190LP6GE dual downconverter.

With its integrated VCO and frequency-synthesizer circuitry, the HMC1190LP6GE is designed to provide excellent third-order-intercept (IP3) performance, as well as outstanding control of 2 x 2 spurious products. The HMC1190LP6GE supports both high- and low-side LO frequency conversion plans across its full bandwidth.

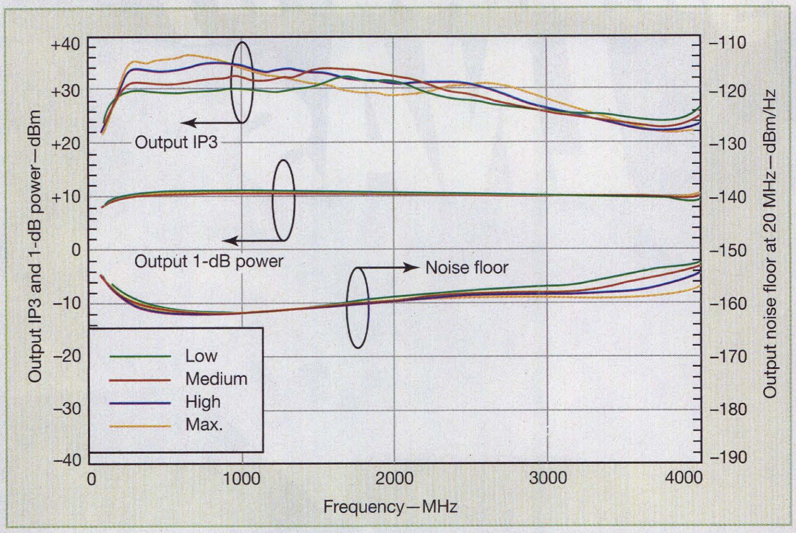

3. The HMC1197LP7FE direct modulator IC features excellent dynamic range performance across its frequency range.

It incorporates a single-ended input port, with inputs converted to differential signals by means of an on-chip RF balanced-unbalanced (balun) circuit.

This approach allows for a variety of LO input/output (I/O) configurations, including a differential LO input for use with an external VCO and a differential LO output port. The latter allows a user to drive multiple receiver and transmitter frequency converters using just a single HMC1190LP6GE dual downconverter IC. The HMC1190LP6GE's RF input port and external LO input port are both impedance matched to 50 Ω.

The HMC1190LP6GE incorporates a passive mixer core with high linearity and high-linearity intermediate-frequency (IF) amplifiers to achieve its excellent frequency-downconversion performance. It boasts RF-to-IF isolation of typically better than 45 dB, with LO leakage at the RF port of typically only –55 to –60 dBm. The 2 x 2 spurious products are controlled to –70 dBm, while channel-to-channel isolation of 50 dB on the downconverter help simplify filtering requirements. The dual downconverter delivers a wide dynamic range for a wide range of wireless standards. High input IP3 (IIP3) performance reaches +24 dBm for frequencies to 3500 MHz **(Fig. 2)**. At the other end of the dynamic range, low noise figure of 9 dB enables the HMC1190LP6GE to contribute to excellent receiver sensitivity, meeting the most demanding wireless receiver applications.

Additionally, the HMC1190LP-6GE dual downconverter provides conversion gain that ranges from 6.2 dB at 2700 MHz to 8.4 dB at 900 MHz. It exhibits input 1-dB compression at power levels of +12 dBm at 2700 MHz and typically +10.7 dBm at 900 MHz. A summary of its performance can be found in **Table 1**.

The HMC1190LP6GE downconverter IC is ideal for diversity receivers in third-generation (3G) and fourth-generation (4G) cellular systems, as well as in multiple-input, multiple-output (MIMO) receiver architectures. Although it includes an internal VCO, its external VCO input port allows it to lock to external sources, enabling cascaded LO architectures for MIMO applications. Two separate charge-pump outputs enable separate loop filters optimized for both the integrated or external VCOs, with seamless switching possible between external and internal VCOs during operation for dynamically optimized performance. In addition, programmable RF output phase control makes possible phase adjustments and synchronization of multiple HMC1190LP-6GE ICs in MIMO and phased-array beam-forming systems.

Table 1: The HMC1190LP6GE downconverter IC at a glance

Parameter	At RF = 900 MHz	At RF = 2700 MHz
Conversion gain (dB)	8.4	6.2
Noise figure (dB)	8.5	10.0
Input 1-dB compression (dBm)	+10.7	+12
Input IP3 (dBm)	+24.5	+23.5
LO leakage (dB)	–67	–58
RF-to-IF isolation (dB)	40	52
Channel-channel isolation	–53	–48 dBc

Table 2: The HMC1197LP7FE direct quadrature modulator IC at a glance

Parameter	450-960 MHz	3400-4000 MHz
Output power (at 1-dB comp.) (dBm)	+0.4	–0.6
Output IP3 (dBm)	+10.5	+10.0
RF port return loss (dB)	12	12
Output noise floor (dBm)	–162	–158
Carrier feedthrough (dBm)	–45	–33

The HMC1190LP6GE downconverter provides a configurable LO output mute function and an "exact frequency mode" in which the IC's fractional-N frequency synthesizer circuitry can be programmed to generate fractional frequencies with 0-Hz frequency error. Another powerful function is the capability to change frequencies without changing the phase of the output signal, which can greatly boost the efficiency of digital-predistortion (DPD) loops. The multifunction HMC1190LP6GE IC is housed in a RoHS compliant 6 x 6 mm leadless QFN package.

On the transmitter side, the model HMC1197LP7FE direct quadrature modulator also covers a broad frequency range, suitable for delivering digital modulation to wireless systems from 0.1 to 4.0 GHz [including 3G and 4G cellular, broadband wireless access (BWA), and Industrial-Scientific-Medical (ISM)-band applications]. **Table 2** provides a sample of its performance.

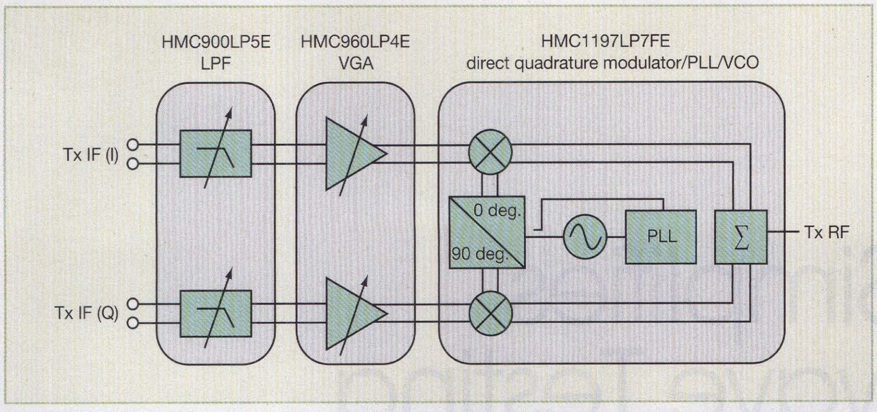

4. This is an example of a wideband direct-conversion transmitter based on the HMC1197LP7FE direct modulator IC.

The low-noise direct modulator requires minimal external components and serves as a low-cost alternative to more complicated double-upconversion modulation approaches. **Figure 3** highlights the wideband, high linearity performance of the HMC1197LP7FE. The highly integrated modulator/PLL/VCO delivers +10 dBm and better than +30 dBm output IP3 across all cellular infrastructure frequency bands from 400 to 4000 MHz. In addition, the low output noise floor (as low as –160 dBm/Hz) helps to maintain excellent signal-to-noise ratio for modulated signals.

The single-ended RF output port is matched to 50 Ω with no external components, while the auxiliary LO output enables the HMC1197LP7FE to distribute identical frequency and phase signals to multiple destinations within a transmitter or receiver. An integrated programmable-bandwidth lowpass filter (LPF) in the LO path ensures little or no LO contribution to modulator sideband rejection. Sixteen programmable LPF bands enable true wideband operation, eliminating the need for band-specific harmonic filtering hardware and allowing agile LO frequency filtering for different band plans during and after deployment.

Figure 4 offers an example of how the HMC1197LP7FE direct modulator and various other ICs can be used to assemble a complete transmitter for cellular communications applications. Differential in-phase (I) and quadrature (Q) input signals are applied to the model HMC900LP5E baseband tunable lowpass filter and model HMC960LP4E digital variable gain amplifier (VGA) (both also from Hittite) to remove unwanted harmonic content, as well as to set I and Q signal strength. These differential signals are then fed to the HMC1197LP7E direct modulator, which requires only a power supply and crystal reference oscillator to then generate virtually any modulation format in any cellular frequency band.

Figure 5 shows the PLL section common to both the HMC1190LP6GE downconverter and the HMC1197LP7FE modulator. The PLL section features a low figure-of-merit (FOM) noise floor of –227 dBm/Hz in fractional-frequency mode and –230 dBm/Hz in integer-frequency mode. The integrated root-mean-square (RMS) jitter is less than 150 fs. The modulator's internal VCO circuitry can generate frequencies from 50 to 4100 MHz, while the PLL circuitry also accepts external VCO signals. This allows both the HMC1190LP6GE and the HMC1197LP7FE ICs to lock to external VCOs and enables cascaded LO architectures for MIMO radio applications.

The PLL section's integrated phase detector and delta-sigma modulator can operate to 100 MHz, permitting frequency synthesis with wide loop bandwidths and excellent spurious performance. In the HMC1197LP7FE modulator—as well as the HMC1190LP6GE downconverter—two separate charge-pump outputs enable separate loop filters for both the integrated and external VCOs, with seamless switching between internal and external VCOs. Also, the HMC1197LP7FE modulator, like the HMC1190LP6GE, can phase-adjust and synchronize multiple transmit and receiver ICs from Hittite for scalable MIMO and beam-forming architectures.

The PLL/VCO section in the HMC1197LP7FE shares the other features of the HMC1190LP6GE's PLL/VCO section, including VCO mute control, synchronously changing frequency without changing phase, and the capability to generate fractional frequencies with 0-Hz frequency error. The HMC1197LP7FE direct modulator is housed in a compact 7 x 7 mm (LP7) surface mount QFN package.

The HMC1190LP6GE and the HMC1197LP7FE ICs feature stable performance over a wide temperature range, from –40 to +85°C. Their high levels of integration help simplify many wireless and cellular receiver and transmitter system designs at the infrastructure level, and their programmable power-consumption control helps "modulate" operating expenses for wireless base stations. In addition, with the broad frequency ranges covered by both of these ICs, one device can be used for a wide variety of different communications standards. MWRF

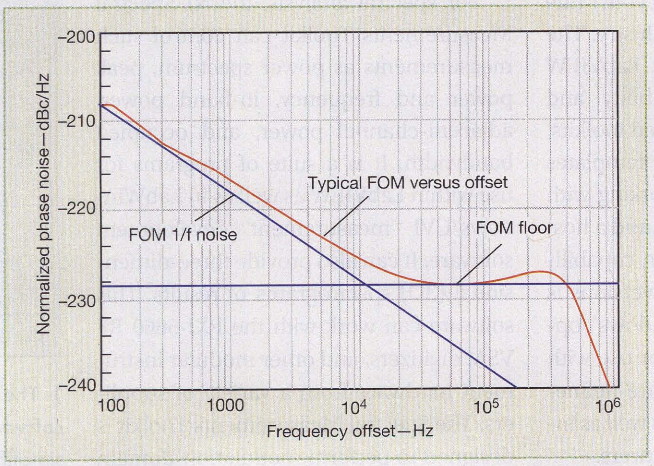

5. This is a figure of merit versus frequency for the PLL/VCO section integrated into the HMC1190LP6GE and HMC1197LP7FE devices.

HITTITE MICROWAVE CORP., 2 Elizabeth Dr., Chelmsford, MA 01824; (978) 250-3333, FAX: (978) 250-3373, *www.hittite.com*.

JACK BROWNE | Technical Contributor

Software Simplifies RF/Microwave Testing

Software and computer programming are playing larger roles in RF/microwave measurements, with electronic devices and systems moving to more complex signal and modulation formats.

MAKING A high-frequency measurement once involved a rack full of instruments and the knowledge to use it. It still involves the rack, although the shapes and the sizes of the instruments are changing. And some of the knowledge can now be found in the form of software, written to guide engineers through tests ranging from the conventional to the esoteric.

Measurement software for RF/microwave applications comes in many forms and for many applications—including for performing measurements according to communications protocols, such as IEEE 802.11 for wireless local area networks (WLANs), for electromagnetic-compatibility (EMC) analysis, and for spectral analysis of operating environments.

Any review of measurement software should probably start with LabVIEW from National Instruments (www.ni.com) due to its widespread use in the industry. The latest version of the software, LabVIEW 2012, features improved stability and analysis power, numerous added toolkits, including a biomedical toolkit, templates to help users get started by working with a proven system configuration, and a host of new analysis and simulation capabilities. The software in its many versions is written for the Microsoft Windows® operating system and designed for use with the firm's many modular software-define-radio (SDR) test instruments, as well as instruments from other manufacturers.

For engineers working in specific areas, LabVIEW offers numerous toolkits and measurement suites devoted to test products in a particular technology—such as the NI WLAN generation toolkit, analysis toolkit, and measurement suite—for physical-layer measurements on IEEE 802.11a/b/g wireless-local-area-network (WLAN) designs. When teamed with National Instruments' models NI PXIe-5663 vector signal analyzer (VSA) and NI PXIe-5673 vector signal generator (VSG), the software can perform a wide range of measurements on both WLAN semiconductors and fully integrated devices and systems. These include error vector magnitude (EVM); frequency offset; in-phase/quadrature (I/Q) gain imbalance; quadrature skew; carrier suppression; spectral flatness; and gated power levels. The measurement suite includes the NI WLAN Analysis Toolkit for RF VSAs and the NI WLAN Generation Toolkit for RF VSGs.

For spectral analysis, the NI Spectral Measurements Toolkit can control such measurements as power spectrum, peak power and frequency, in-band power, adjacent-channel power, and occupied bandwidth. It is a suite of programs for use within LabVIEW as well as in LabWindows/CVI measurement development software. It can also provide three-dimensional (3D) spectrograms of results. This software can work with the PXI-5660 RF VSA, digitizers, and other modular instrument hardware from a variety of suppliers. The Spectral Measurements Toolkit is designed to perform modulation-domain functions such as converting digitally modulated in-phase (I) and quadrature (Q) signals to intermediate frequencies (IFs), as well as generating and analyzing analog modulated signals.

Agilent Technologies (www.agilent.com) recently announced that it had enhanced its model N7609B Signal Studio for Global Navigation Satellite Systems (GNSS) software, intended for simulation of Galileo signals for receiver testing. The software can now coordinate real-time, multiple-satellite simulations for the European Galileo satellite system, a navigation constellation similar to the US Global Positioning System (GPS).

The Signal Studio software for Galileo testing can generate signals that simulate signals from Galileo satellites, or else a combination of Galileo, GPS, or even Russian GLONASS navigation satellites. Us-

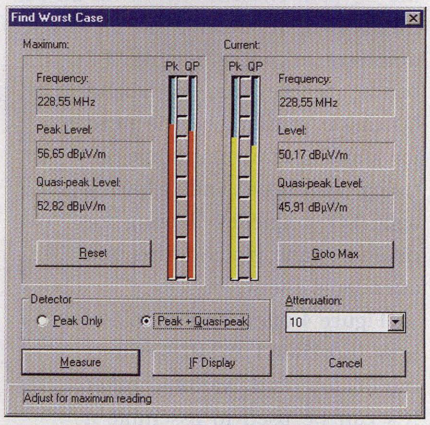

1. The R&S ESxS-K1 EMI measurement software provides numerous features that simplify the capture of peak power levels during testing. [Photo courtesy of Rohde & Schwarz (www.rohde-schwarz.com).]

ers can create different signal scenarios based on the locations of satellite at different dates and times, for the purposes of evaluating satellite-positioning chipsets and other products. Chipsets and other hardware are being introduced for this system, which is expected to be completed in 2019.

Signal Studio is a Windows/Windows NT program that works with the firm's modular test hardware to produce a wide array of test and simulation signals—including for fixed and mobile WiMAX; WLANs; Bluetooth; cellular communications; and detection, positioning, and tracking applications. For example, the software simplifies pulse building. This allows users to precisely define all pulse parameters, such as frequency, phase, pulse repetition interval (PRI), pulse width, and even with chirp and other intra-pulse modulation.

The company also offers more specialized test programs, such as the Agilent PDQ-WLR™ test and analysis software for wafer-level-reliability (WLR) testing and analysis on Windows NT and HPUX computer platforms. The test software has more than 30 WLR algorithms and can evaluate all major semiconductor reliability failure mechanisms. The software can also coordinate post-test statistical and physical analysis of the data taken during testing.

Rohde & Schwarz (www.rohde-schwarz.com) also offers some specialized test software packages, including its R&S ESxS-K1 electromagnetic-interference (EMI) measurement software. The software is written for the company's wide range of measurement receivers; it helps simplify measurement setup, data capture and display, and test data analysis. On-screen color displays can include limit lines, while using automatic data reduction to remove unneeded results. The software includes many helpful functions, including a zoom feature for closer looks at displays, automatic peak search, and a worst-case function to find the maximum hold level **(Fig. 1)**.

In tune with emerging needs, the firm also has created the R&S FS-K112PC near-field-communications (NFC) measurement software to characterize the RF parameters of signals from devices equipped with NFC capabilities. The software is written for use with the firm's FSV/FSL series spectrum analyzers and its RTO family of digital oscilloscopes. The software provides automatic detection of NFC-A, NFC-B, and NFC-F transmission methods or can be preset for testing any one of the configurations.

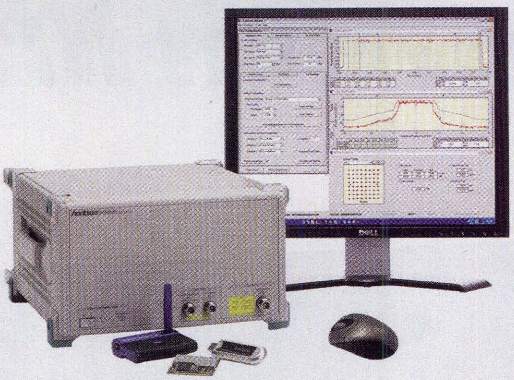

2. The MT8860C WLAN test set combines hardware and software for production-line testing of WLAN transmitters and receivers. [Photo courtesy of Anritsu Co. (www.anritsu.com).]

The latest version (Version 5) Automated Tuner System Software from Maury Microwave (www.maurymw.com) is easy-to-use device characterization software in spite of its functional power. Written for Windows XP and Windows 7 operating systems, the software works with the firm's impedance tuners and additional commercial signal generation and analysis test hardware to measure an extensive list of device parameters. These include gain, noise figure, power, efficiency, intermodulation distortion, adjacent-channel power ratio, error vector magnitude, and harmonics. It can also export test results into the Advanced Design System (ADS) simulation software suite from Agilent Technologies for modeling and simulation. This latest version simplifies impedance-tuner control with a new graphical user interface (GUI). It also provides a new means of performing cascaded load-pull measurements without need of diplexers or triplexers.

Teseq (www.teseq.com), which specializes in EMC compliance emission and immunity software, has created its Compliance 5 software based on expertise and experience. With an extensive driver data base available on the firm's website, the software supports more than 350 test instruments for EMC testing. The software even includes a driver editing tool so that users can create their own instrument drivers. Compliance 5 is supplied with a dedicated package for making compliant measurements to a wide range of commercial standards, including EN 55011 and EN 55022 for emissions and IEC 61000-4-3 and IEC 61000-4-6 for immunity testing.

AR RF/Microwave Instrumentation (www.ar-worldwide.com) now makes its SW1007 electromagnetic-compatibility (EMC) test software available free of charge. It automatically performs both calibration and immunity testing and is available as a download from the company's website. It features military standard (MIL STD) emissions capabilities (such as MIL-STD-461/462), along with its legacy radiated susceptibility and conducted immunity measurement capabilities.

Many instrument suppliers support their hardware with complementary software packages, such as the Tektronix Application Developer Toolkit from Tektronix (www.tek.com) for integrating the analysis capabilities of the MATLAB mathematical software from MathWorks (www.mathworks.com) directly with one of their digital oscilloscopes. The combination allows users to create custom math functions and provides fast, efficient access to captured waveform data, with the ease of a computer GUI tailored for the tasks. Similarly, the MT8860C WLAN test solution combines dedicated test hardware with a PC software program **(Fig. 2)** for full IEEE 802.11b/g/a/n transmitter and receiver testing. The hardware has a built-in reference receiver and transmitter analyzer and the software builds on the firm's CombiTest measurement software to simplify testing in production environments. MWRF

Editor's Note: To read an expanded version of this article, visit http://mwrf.com/software/software-simplifies-rfmicrowave-testing.

**Domestic Edition only **International Edition only This index is provided as an additional service by the publisher, who assumes no responsibility for errors or omissions.*

MARKETING & ADVERTISING STAFF

VICE PRESIDENT & MARKET LEADER
BILL BAUMANN
T: (201) 845-2403 F: (201)845-2484
bill.baumann@penton.com

BRAND DIRECTOR, e|DESIGN
CENTRAL U.S.
TRACY SMITH
T: (913) 967.1324 F: (913) 514.6881
E: tracy.smith@penton.com

BRAND CHAMPION
NORTHEAST
DAVID MADONIA
T: (212)-204-4331
E: dave.madonia@penton.com

SOUTH
BILL YARBOROUGH
T: (713) 636-3809 T: (713) 523-8384
E: bill.yarborough@penton.com

NORTHERN CALIFORNIA, NEVADA, NORTHWEST
JAMIE ALLEN
T: (415) 608-1959 F: (913) 514-3667
E: jamie.allen@penton.com

ONLINE SALES DEVELOPMENT DIRECTOR
STEPHANIE CAMPANA
T: (312) 840-2403-8437
stephanie.campana@penton.com

EUROPEAN SALES REP
MARK DURHAM
T: +44 (0)7958 564137
E:mark.durham@penton.com

TAIWAN, R.O.C.
CHARLES C.Y. LIU
T: (886)-2-2727-7799 F: (886)-2-2728-3686

JAPAN
HIRO MORITA
T: 81-3-3261-4591 F: 81-3-3261-6126

KOREA
JO YOUNG SANG
T: 011-82-2-739-7840
F: 011-82-732-3662

CUSTOMER SERVICE - SUBSCRIPTIONS
New/Renew/Cancel/Change Address/Missing and Back Issues
T: 866-505-7173 F: 847-763-9673
E: microwaves&rf@halldata.com

Penton Design Engineering & Sourcing Group

Subscription Assistance and Information: Microwaves & RF (ISSN 0745-2993) is published monthly, except semi-monthly in December. **Microwaves & RF** is sent free to individuals actively engaged in high-frequency electronics engineering. In addition, paid subscriptions are available. Subscription rates for U.S. are $95 for 1 year ($120 in Canada, $150 for International). Published by Penton Media, Inc., 9800 Metcalfe Ave., Overland Park, KS 66212-2216. Periodicals Postage Paid at Shawnee Mission, KS and at additional mailing offices.

POSTMASTER: Send change of address to Microwaves & RF, Penton Media Inc., P.O. Box 2095, Skokie, IL 60076-7995. For paid subscription requests, please contact: Penton Media Inc., P.O. Box 2100, Skokie, IL 60076-7800. Canadian Post Publications Mail agreement No. 40612608. Canadian GST# R126431964. Canada return address: Bleuchip International, P.O Box 25542,London, ON N6C6B2.

Back issues of **MicroWaves** and **Microwaves & RF** are available on microfilm and can be purchased from National Archive Publishing Company (NAPC). For more information, call NAPC at 734-302-6500 or 800-420-NAPC (6272) x 6578.

Microwaves & RF Direct Connection Ads

TO ADVERTISE, CONTACT A SALES REPRESENTATIVE at http://mwrf.com/advertising

DECEMBER 2012 ISSUE PREVIEW

Ad Close 11/15/2012 • Ad Materials due 11/28/2012

Theme: Technology Assessment
Industry Insight: Wireless Standards Update
Product Trends: Top Products of 2012
RF Essentials: Phase Noise

TO ADVERTISE, CONTACT:

Brand Director, S. California
Tracy Smith: tracy.smith@penton.com

Brand Champion, Northeast/Eastern Canada
David Madonia: dave.madonia@penton.com

Northwest/Northern CA/Western Canada
Jamie Allen: jamie.allen@penton.com

South
Bill Yarborough: bill.yarborough@penton.com

Mid-Atlantic/Midwest
Stephanie Campana: stephanie.campana@penton.com

Europe
Mark Durham: mark.durham@penton.com

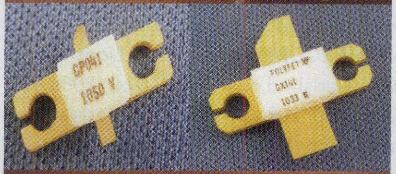

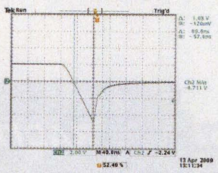

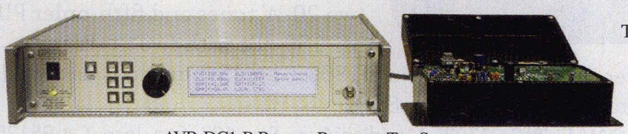

Coupler Channels High Power To 4 GHz

A high-power coupler developed by VidaRF operates from 2 to 4 GHz with a coupling value of 30 dB (other coupling values are available). It can handle 500 W average power on its primary and secondary lines, with peak values as high as 8 kW. The insertion loss (excluding coupling losses) is a low 0.25 dB, while the VSWR is 1.30:1. The high-power coupler, which is supplied with Type N female connectors, features directivity of 18 dB. It is a high-power version of the firm's popular model VDC-2040-30 30-dB coupler for 2 to 4 GHz, with coupling flatness of ±1.25 dB and 20-dB directivity. This lower-power model, with 0.2-dB insertion loss (excluding coupling losses) and 1.15:1 maximum VSWR on primary and secondary lines, handles 50 W average and reflected power and 3 kW on peaks. It boasts frequency sensitivity of ±0.75 dB.

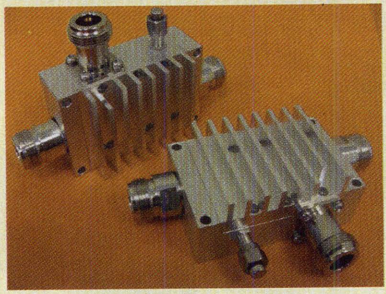

VIDARF, 11330 Vanstory Dr., Huntersville, NC 28078; (704) 897-0558, FAX: (704) 897-0559, e-mail: sales@vidarf.com, ***www.vidarf.com***

Base-Station Coupler Links 800 to 2500 MHz

A line of high-power base-station couplers with 7/16-DIN connectors has been announced by Raditek. As an example, model RCPL-800-2500M-7/16f-500W operates from 800 to 2500 MHz with better than 1.25:1 VSWR and better than 30-dB isolation between ports. It is available with coupling factors from 5 to 40 dB and achieves third-order passive-intermodulation (PIM) distortion of –140 dBc with two 20-W tones and fifth-order PIM of –150 dBc with two 20-W test tones. The high-power coupler measures just 180 x 61 x 45 mm and is designed for operating temperatures from –25 to +85°C.

RADITEK INTERNATIONAL, INC., 1702L Meridian Ave., Ste. 127, San Jose, CA 95125; (408) 266-7404, FAX: (408) 266-4483, e-mail: sales@Raditek.com, ***www.Raditek.com***

Signal Generators Switch To 20 GHz

A line of high-performance signal generators from Berkeley Nucleonics includes models capable of operating to 20 GHz and beyond. A number of configurations are available, including benchtop units and portable models able to operate on battery power. As an example, model 845 is a compact signal generator with a frequency range extending from 10 MHz to beyond 20 GHz. It can be tuned with 0.001-Hz frequency resolution and offers output levels from –90 to +13 dBm, adjustable with 0.01-dB resolution. The phase noise is typically –108 dBc/Hz offset 20 kHz from a 10-GHz carrier. Model 845 features better than 200 μs switching speed and can generate a wide range of modulation formats; these include amplitude modulation (AM), frequency modulation (FM), phase modulation, and fast pulse modulation. The broadband signal generator weighs only 2.5 kg and consumes a mere 18 W power. A two-year warranty is standard with all instruments.

BERKELEY NUCLEONICS CORP., 2955 Kerner Blvd., San Rafael, CA 94901; (800) 234-7858, (415) 453-9955, FAX: (415) 453-4496, ***www.berkeleynucleonics.com***

Power Amplifier Drives 2.9 To 3.1 GHz

Model SSPA 2.9-3.1-300 is a high power gallium-nitride (GaN) amplifier that can be used for pulsed or continuous-wave (CW) applications from 2.9 to 3.1 GHz, also usable from 2.7 to 2.9 GHz and from 2.7 to 3.5 GHz. The amplifier is rated for typical peak output power of 300 to 400 W at room temperature with typical noise figure of about 10 dB. The output power across the band is flat within ±0.25 dB. The input/output VSWR is typically 2.0:1. The amplifier is designed for use with a +5-VDC supply. It measures 5.00 x 8.00 x 1.94 in.; weighs about 2.5 lbs with SMA input and output connectors; and has an operating temperature range of –40 to +85°C. The amplifier includes an external DC blanking command that enables and disables the module in typically 5.0 μs. Standard features include over/under voltage protection and reverse polarity protection.

AETHERCOMM, INC., 3205 Lionshead Ave., Carlsbad, CA 92010; (760) 208-6002, FAX: (760) 208-6059, e-mail: sales@aethercomm.com, ***www.aethercomm.com.***

Low-PIM Cables Jump DC To 3 GHz

A line of low-passive-intermodulation (PIM) jumper cables from Microlab has been extended for applications from DC to 3 GHz. The firm's JP/JR/JS series jumper cables are suitable for telecommunications applications in frequency bands from 380 to 2700 MHz. The cable assemblies are based on 0.141-in.-diameter cables with silver-plated copper conductors and PTFE dielectric material. The cables feature better than 90-dB shielding. The jumper cables are available with straight and right-angle Type N and 7/16 DIN connectors. The cables feature trimetal plated connectors made to MIL-C-39012 specifications. The PIM performance is better than –150 dBc when tested with two +43-dBm tones and guaranteed to –145 dBc at 1800 MHz. Cable lengths of 0.5 and 1.0 m are available from stock.

MICROLAB, a Wireless Telecom Group, Inc., 25 Eastmans Rd., Parsippany, NJ 07054; (973) 386-9696, FAX: (973) 386-9191, ***www.wtcom.com***


The sweetest & largest
assortment of
Miniatures
in the world . . .
from ARRA, of course!
For your "sweet tooth"...
Miniature
Variable Attenuators
Bands from DC−18GHz
Some models feature:
♥ Extremely flat attenuation vs. frequency response
♥ Constant phase with △ attenuation.
The ultimate in reliability, and wear-free performance ... achieved with ARRA's non-contacting method of attenuating.
Most units incorporate ARRA's proprietary attenuating elements which give excellent stability over a wide temperature range.
Customerized to your requirements.
Call us, write or Fax your specs to 631-434-1116
ARRA
...the last word in variable attenuators
ARRA INC.
Visit our website at www.arra.com
15 Harold Court, Bay Shore, N.Y. 11706 • 631-231-8400

BLUETOOTH® RF MODULES

www.panasonic.com/Bluetooth

Bluetooth, which is based on IEEE 802.15.1, was developed for the purpose of sending larger amounts of data quickly from computers to portable handheld devices. Key features include high data rate, frequency hopping, very small form factor and modest power consumption.

Panasonic offers a new *Bluetooth* RF module product line that makes connectivity between mobile devices easily implemented, creating a seamless data chain from sensors to the Web.

New Series featuring:

Bluetooth® Classic
Bluetooth Dual Mode
Bluetooth ANT™
Bluetooth Low Energy

POWERED BY Panasonic Electronic Components

Just another way we're engineering a better world for you.

- Capacitors
- Resistors
- Inductors and Filters
- Circuit Protection
- Electromechanical
- RF Modules
- Semiconductors

Visit us online at **www.panasonic.com/industrial/electronic-components**
email **industrial@us.panasonic.com**
or call **1-800-344-2112**

Panasonic
ideas for life

New! PAN1323ETU Triple Mode *Bluetooth* Development Module

One Development Module, Three Standards: *Bluetooth* Classic, *Bluetooth* Low Energy and ANT™

This unique triple mode ETU - that's ETU for "Easy-To-Use" - module plugs directly into Panasonic development kits, Texas Instruments MSP430 and Stellaris experimentor boards with the added benefit of header connectors that simplify prototype wiring and field trials.

ANT

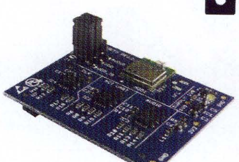

New! PAN1720 Series *Bluetooth* Low Energy

A Complete *Bluetooth* 4.0 Low Energy Solution

Bluetooth® SMART

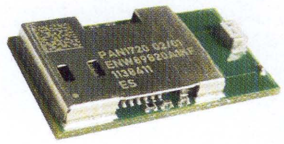

The **New PAN1720 Series** is a cost-effective, low-power, true system-on-chip (SoC) for *Bluetooth* Low Energy applications. The module includes an eight channel, twelve bit analog-to-digital converter, 19 GPIOs plus battery and temperature sensors.

New! PAN1321i Series

Wireless *Bluetooth* Connectivity Compatible with Apple® and Android™ Devices

The **New PAN1321i Series** Bluetooth RF Module is compatible with Apple devices such as the iPod®, iPhone® and iPad®. The PAN1321i Series interfaces with the Apple authentication coprocessor and supports iPod Accessory Protocol (iAP) to enable *Bluetooth* Serial Port data communication with Bluetooth enabled Apple Devices.

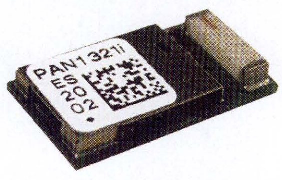

Apple, iPod, iPhone and iPad are registered trademarks of Apple Inc.
Android is trademark of Google Inc.